"DESIGN OF NOVEL ANTI-CANCER AGENTS: PHARMACOPHORE MODELING, VIRTUAL SCREENING, MOLECULAR DOCKING, SYNTHESIS, 3D QSAR STUDIES, PHARMACOLOGICAL EVALUATION AND *IN-SILICO* ADMET STUDIES"

A THESIS SUBMITTED TO

NIRMA UNIVERSITY

IN PARTIAL FULFILLMENT OF THE REQUIREMENTS FOR

THE DEGREE OF

MASTER OF PHARMACY

IN

DRUG DISCOVERY

BY

BINOY SHAH (11MPH603)
B. PHARM

UNDER THE GUIDANCE OF

Dr. Hardik G. Bhatt – GUIDE
Associate Professor, Department Of Pharmaceutical Chemistry

DEPARTMENT OF PHARMACEUTICAL CHEMISTRY
INSTITUTE OF PHARMACY
NIRMA UNIVERSITY
AHMEDABAD-382481
GUJARAT, INDIA

MAY 2013

CERTIFICATE

This is to certify that the dissertation work entitled *"Design Of Novel Anti-Cancer Agents: Pharmacophore Modeling, Virtual Screening, Molecular Docking, Synthesis, 3D Qsar Studies, Pharmacological Evaluation And In-Silico Admet Studies"* in partial fulfillment for the award of Master of Pharmacy in *"Drug Discovery"* is a bonafide research work carried out by the candidate at the Department of Pharmaceutical Chemistry, Institute of Pharmacy, Nirma University under our guidance. This work is original and has not been submitted in part or full for any other degree or diploma to this or any other university or institution.

Guide

Dr. Hardik G. Bhatt
M. Pharm., Ph.D.,
Associate Professor,
Department of Pharmaceutical
Chemistry,
Institute of Pharmacy,
Nirma University.

Forwarded Through:

Dr. Manjunath D. Ghate,
M. Pharm., Ph.D.,
Director & Head,
Department of Pharmaceutical Chemistry,
Institute of Pharmacy,
Nirma University.

Date: 24th MAY, 2013

DECLARATION

I hereby declare that the dissertation entitled *"Design Of Novel Anti-Cancer Agents: Pharmacophore Modeling, Virtual Screening, Molecular Docking, Synthesis, 3D Qsar Studies, Pharmacological Evaluation And In-Silico Admet Studies"* is based on the original work carried out by me under the guidance of Dr. Hardik G. Bhatt, Associate Professor, Department of Pharmaceutical Chemistry, Institute of Pharmacy, Nirma University. I also affirm that this work is original and has not been submitted in part or full for any other degree or diploma to this or any other university or institution.

Bm shah

MS. BINOY SHAH (11MPH603)
Department of Pharmaceutical Chemistry,
Institute of Pharmacy
Nirma University
Sarkhej - Gandhinagar Highway
Ahmedabad-382481
Gujarat, India

Date: 24th MAY, 2013

DEDICATED TO MY FAMILY

ACKNOWLEDGEMENT

"Effort only fully releases its reward after a person refuses to quit."

The joyness, satisfaction and euphoria that comes along with successful completion of any work would be incomplete unless we mention the name of those people who made it possible, whose constant guidance and encouragement served as a beam of light and crowed out efforts.

First of all, I am thankful to **Almighty (the supreme soul)** for always being with me and blessing me with good family, friends, teachers and well wishers and extend his helping hands to complete this project successfully.

But, I was not alone in this praiseworthy journey of success: with deep gratitude and humbleness I would like to express my indebtedness and reverence to **Dr. Hardik G. Bhatt**, Associate Professor, Department of Pharmaceutical Chemistry, Institute of Pharmacy, Nirma University whose priceless guidance and supervision led me to carry out this work successfully.

I am highly thankful to **Dr. Manjunath Ghate** (Director, Institute of Pharmacy, Nirma University, Ahmedabad) for providing all necessary help and facility for my work and also for his constant support and encouragement.

I would like to express my humble and whole hearted thanks to **Mr. Vivek Vyas, Dr. Jignasa Savjani, Ms. Bhoomika Patel**, Assistant professor for their back-up, active shore up and able direction at every step. I am thankful to **Dr. Appaji Mandhare**, Senior Scientist, Torrent Research Centre (Bhat) for providing guidance regarding softwares and other computational techniques necessary for my project.

I am also thankful to **Dr. Anuradha Gajjar**, Professor, Department of Pharmaceutical Chemistry for her guidance during project.

My jovial gratitude is to **Mr. Jignesh bhai** and **Rohitbhai** (lab assistants) for being immeasurably considerate, non-formal and open in offering priceless and timely own advices during my dissertation work.

I sincerely thanks to **Dr. P. Lalitha**, for library facilities and constant encouragement during my work.

I owe special thanks to **Nitinbhai** for helping me in maximum utilization of computer lab. I also wish to acknowledge **Satejbhai, Shreyashbhai and Mukeshbhai** for providing me all the materials required in my work

 A special word of gratitude to my friends **Dhruvi, Bhoomi, Setu, Kwisha, Mruganki, Suhani, Pooja and Atisha,** who were always there besides me with the hand of support and encouragement.

Thank to my batchmates **Keyur, Nikum, Ashutosh, Nirzari, Pritam** and **Chirag** as well as my juniors **Udit, Abhishek** and **Harshal** for their support.

Last but not least I am indebted infinitely to love, care and trust being showered on me by my Family without their consistent prayers, affectionate blessings, selfless care and endless confidence in me, I would have never come to the stage of writing this acknowledge. It is strength of my parents who had scarified their present to secure future for us. Thank you **Mom, Dad** and my brother **Dhruven** for believing in me and making me what I am today.

In the end, No words of thanks are enough to express my gratefulness to my fiancée, **KUSH** for his love, care, worthwhile support and faith in me. You have always proved to be my strength.

Finally, I express my gratitude and apologize to anybody whose contributions, I could not mention in this page.

Date: **Binoy Shah**

Place: **Institute of Pharmacy,
Nirma University,
Ahmedabad.**

CONTENTS

CONTENTS

A. List of Tables

Table No	Table Title	Page No
1	Training set molecules used to develop Pharmacophore Hypothesis for Aurora Kinase-A inhibitors	60
2	Result of Pharmacophore Hypothesis Generated by GALAHAD	64
3	Chemical Structures of Pyrolo Triazene derivatives	77
4	Experimental and Predicted pIC50 of the Training and Test Sets Using CoMFA and CoMSIA Models	87
5	Summary of CoMFA and CoMSIA Results	88
6	Docking Results of 10 Compounds using Surflex	96
7	Amino-acids involved in Docking-Interactions	97
8	Chemicals required for synthesis	100
9	List of Products synthesized	102
10	List of Synthesized compounds with IUPAC Name	109
11 (a)	Synthesis Data	110
11 (b)	Summary of the Physical Data of Synthesized compounds	90
12	*In-vitro* cytotoxicity assays and theirs principle	127
13	Stock Solution of Compounds	132
14	(1:3) dilution of test compound used in the assay	133
15	Results for Characterization of cell lines	145
16	Concentration of compounds and % cell inhibition MCF-7 cell line (Breast Cancer)	147
17	Show concentration of compounds and % cell inhibition of A-375 cell line (Human Melanoma, Skin cancer)	148
18	Concentration of compounds and % cell inhibition of HCT-15 cell line (Human Colon cancer)	149
19	Compounds and IC_{50} value	150
20	*In silico* Pharmacokinetic and Toxicity Study of Synthesized Compounds	153

B.List of Figures

C. Abbreviations

Short Name	Abbreviation
AURKA	Aurora Kinase- A
GALAHAD	Genetic Algorithm with Linear Assignment for Hypermolecular Alignment of Datasets
GASP	GASP Genetic Algorithm Similarity Programme
DS	DS Donor Site
AA	AA Acceptor Atom
HY	Hydrophobic Region
QSAR	QSAR Quantitative Structure Activity Relationship
CoMFA	CoMFA Comparative Molecular field analysis
CoMSIA	CoMSIA Comparative Molecular Similarity Indices Analysis
ADMET	ADMET Absorption, Distribution, Metabolism, Excretion and Toxicity
HBD	HBD Hydrogen Bond Donor
HBA	HBA Hydrogen Bond Acceptor

Abstract:

Cancer can strike people at any age, although they can be diagnosed and can be treated successfully in their early ages. The major problem with cancer therapy is the frequent relapses seen in patients. In order to reduce such relapses it is necessary to develop various therapies that target the cancer site. The molecular analysis of the cancer genomes have shown a remarkable complexity and pointed to key genomic and epigenomic alterations in cancer. The Aurora kinase family members (A,B and C) are a collection of highly related and conserved serine/threonine kinases that fulfill these criteria, being key regulators of mitosis and multiple signaling pathways. Alterations in Aurora kinase signaling are associated with mitotic errors and have been closely liked to chromosomal aneuploidy in cancer cells. In course of my research to discover novel Aurora kinase-A inhibitors, both computational and synthetic approaches were used to design and synthesis of newer agents. Pharmacophore mapping was performed on 11 chemically diverse molecules using GALAHAD. Twenty pharmacophore models were generated and model 5 was considered the best model as it had higher specificity compared to all other models. The best pharmacophore hypothesis contained 5 features including 2 donor sites, 1 acceptor atom and 2 hydrophobic region. Model 6 was used as a query in NCI and Maybridge hit finder databases. A total number of 16829 molecules were obtained after Lipinski filtering. 3D-QSAR studies (CoMFA and CoMSIA) were conducted on a series of 48 compounds . The best prediction were obtained with a CoMFA ($q^2 = 0.491$, $r^2 = 0.963$) and with CoMSIA ($q^2 = 0.500$, $r^2 = 0.961$). Both models were validated by a test set of 10 compounds producing good predictive r^2 values of 0.607 and 0.519 respectively. On the basis of pharmacophore modeling, virtual screening and 3D QSAR studies, various molecules were desgined having mercaptopurine ring system as the common core structure and were docked on co-crystal structure of Aurora kinase A (PDB ID: 3K5U) to predict the binding orientation of drug candidates to their protein target. From this, 10 different substituted mercapto-purine derivatives were synthesized and characterized by FTIR, ^{1}HNMR and Mass. Anti-cancer activity was carried out using various cell lines like MCF-7, MCF-7, A-375, DU-145. In-silico ADMET studies were carried out using admetSAR . The designed compounds showed good potential to be anti-cancer agents.

CHAPTER-1

INTRODUCTION

1. INTRODUCTION

Cancer is one of the leading killers in the world. Currently, one in four deaths is due to cancer. Nearly half of all men and a little over one third of all women in the world do develop cancer during their lifetimes. Cancer can strike people at any age, although they can be diagnosed and can be treated successfully in their early stages. Cancer begins when there is a change in the DNA, or a mutation. Most of the time when DNA is damaged, the body is able to repair it by a process called apoptosis. In cancer, the damaged DNA cannot be repaired. Such a damaged DNA can be inherited by a person. More often, a person's DNA becomes damaged by exposure to certain agents in the environment like smoking, alcohol and some toxic chemicals which are termed as carcinogens. Cancer usually forms a tumor. Often, not all tumors are cancerous. Cancer develops when cells in a part of the body begin to grow out of control. Normally, the cells in the body divide and grow in a controlled and orderly manner. Cancer occurs when cells grow in an uncontrolled manner. Instead of dying, they outlive normal cells and continue to form new abnormal cells.[1]

Inspite of impressive progress, surgery and therapy, since sixties, the overall cancer mortality , declined in late nineties in most of the countries, is still very high, with some exceptions for some specific tumor types. The classical 5-year survival rate for the average of more common cancers is about 60% but is as low as 14% for lung cancer. In general, the 5-year survival rate is increasing which reflects the progress made in early diagnosis of cancer through mammography, PSA and PAP test than the real capability of therapeutic control[2]. In spite of the large number of available chemotherapeutic agents, the medical need is still largely unmet. The main reasons are: the lack of selectivity of conventional drugs, leading to toxicity; the metastatic spreading, implying early tumor growth in organs other than primary site; heterogeneity of the disease, comprising about 100 types of cancer; the intrinsic or acquired resistance to chemotherapy developed after few therapeutic cycles (multi-drug resistance). A number of innovative strategies are in development, aimed to target the malignant abnormalities of tumor cells arising from the activation of tumor promoter genes or inhibition of tumor suppressor genes. Some focused molecular targets are oncogene encoded proteins acting as signal transducer like RAS, cell cycle targets as Aurora kinases,

cyclin dependent kinases. Alternatively, angiogenesis inhibition may prevent the formation of tumor blood vessels, thus limiting the tumor ability to grow and metastasize. However, it will likely take some years to fully define the role of innovative agents in preventing disease progression. Therefore, cytotoxic drugs will continue to represent a chief part of the therapy in the near future, and this implies a need for new agents with better activity and safety profile. [3]

The terms cancer, malignant neoplasm (neoplasm simply means 'new growth') and malignant tumor are synonymous. Both benign and malignant tumors manifest uncontrolled proliferation, but the latter are distinguished by their capacity for dedifferentiation, their invasiveness and their ability to metastasise (spread to other parts of the body). The appearance of these abnormal characteristics reflects altered patterns of gene expression in the cancer cells, resulting from genetic mutations. There are three main approaches to treat cancer-surgical excision, irradiation and chemotherapy and the relative value of each of these approaches depends on the type of tumor and development stage. Chemotherapy may be used on its own or as an adjunct to other forms of therapy. [4]

1.1 Cell cycle in relation to Mitosis

FIGURE 1.1: Cell cycle and its phases[5]
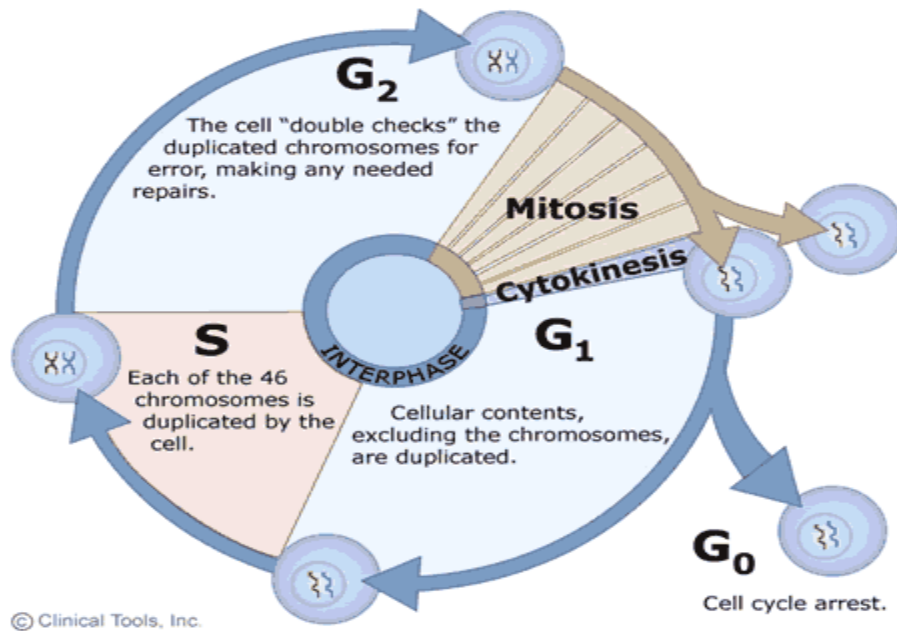
Mitosis — the process by which a complete copy of the duplicated genome is precisely segregated by the MICROTUBULE spindle apparatus into two daughter cells — is an extraordinarily complex biological process. Given that the survival of a cell depends on the accuracy of mitosis, multiple fidelity-monitoring CHECKPOINT systems have evolved to ensure correct temporal and spatial coordination of this process. Errors in these mechanisms can lead to genomic instability, an important aspect of tumorigenesis and so it is not surprising that these regulatory systems are frequently found to be abnormal in tumour cells compared with normal cells.[6]

1.2 Development of cancer

Cancer cells manifest, to varying degrees, four characteristics that distinguish them from normal cells. These are:

- Uncontrolled proliferation
- Dedifferentiation and loss of function
- Invasiveness
- Metastasis

- Cells do not themselves produce cancer but they increase the likelihood that the genetic mutation(s) will result eventually in cancer

    There are two main categories of genetic change that are important.

    ☐ The activation of proto-oncogenes to oncogenes. Proto-oncogenes are genes that normally control cell division, apoptosis and differentiation, which can be converted to oncogenes that induce malignant change by viral or carcinogen action.

    ☐ The inactivation of tumor suppressor genes. Normal cells contain genes that have the ability to suppress malignant change-termed tumor suppressor genes (antioncogenes)-and there is now evidence that mutations of these genes are involved in many different cancers. The loss of function of tumor suppressor genes can be the critical event in carcinogenesis.

About 30 tumor suppressor genes and 100 dominant oncogenes have been identified. The changes those lead to malignancy are result of point mutations, gene amplification or chromosomal translocation, often caused by viruses or chemical carcinogens.

1.2.1 Special Characteristics of Cancer Cells

1. Uncontrolled proliferation.

Some healthy cells (such as neurons) have little or no capacity to divide and proliferate, whereas others, in the bone marrow and the epithelium of the gastrointestinal tract, have the property of continuous rapid division. Some cancer cells multiply slowly (e.g. those in plasma cell tumors) and some much more rapidly (e.g. the cells of Burkitt's lymphoma). It is therefore not generally true that cancer cells proliferate faster than normal cells. The significant issue is that cancer cells have escaped from the mechanisms that normally regulate cell division and tissue growth. It is this, rather than their rate of proliferation, that distinguishes them from normal cells.

Inactivation of tumor suppressor genes or transformation of proto-oncogenes into oncogenes can confer autonomy of growth on a cell and thus result in uncontrolled proliferation by producing changes in several cellular systems including:

☐Growth factors, their receptors and signaling pathways

☐ The cell cycle transducers, for example cyclins, cyclin-dependent kinases (cdks) or the cdk inhibitors

☐ The apoptotic machinery that normally disposes of abnormal cells

☐Telomerase expression

☐Local blood vessels, resulting from tumor-directed angiogenesis.

Potentially all the genes coding for the above components could be regarded as oncogenes or tumor suppressor genes Fig. 1.2, although not all are equally prone to malignant transformation. Malignant transformation of several components is needed for the development of cancer.

1.2.1   Dedifferentiation and loss of function

One of the main characteristics of cancer cells is that they dedifferentiate to varying degrees. In general, poorly differentiated cancers multiply faster and carry a worse prognosis than well-differentiated cancers.

1.1.3 Invasiveness

Normal cells are not found outside their 'designated' tissue of origin; for example, liver cells are not found in the bladder and pancreatic cells are not found in the testis. This is because, during differentiation and tissue or organ growth, normal cells develop certain spatial relationships with respect to each other. These relationships are maintained by various tissue-specific survival factors that prevent apoptosis. In this way, any cells that escape accidentally lose these survival signals and die. Consequently, although the cells of the normal mucosal epithelium of the rectum proliferate continuously as the lining is shed, they remain as a lining epithelium. A cancer of the rectal mucosa, by comparison, invades other tissues forming the rectum and may even invade the tissues of other pelvic organs. Cancer cells have not only lost, through mutation, the restraints that act on normal cells, but they also secrete enzymes (e.g. metalloproteinases) that break down the extracellular matrix, enabling them to move around.

1.1.4 Metastases

Metastases are secondary tumors formed by cells that have been released from the initial or primary tumor and have reached other sites through blood vessels or lymphatics, or as a result of being shed into body cavities. Metastases are the principal cause of mortality and morbidity in most cancers and constitute a major problem for cancer therapy.
Hence, dislodgment or aberrant migration of normal cells would lead to programmed cell

death as a result of withdrawal of the necessary antiapoptotic factors. Cancer cells that metastasize have undergone a series of genetic changes that alter their responses to the regulatory factors that control the cellular architecture of normal tissues, enabling them to establish themselves 'extraterritorially'. Tumor-induced growth of new blood vessels locally makes metastasis easier and more likely.

FIGURE 1.2 : Development of Cancer [6]
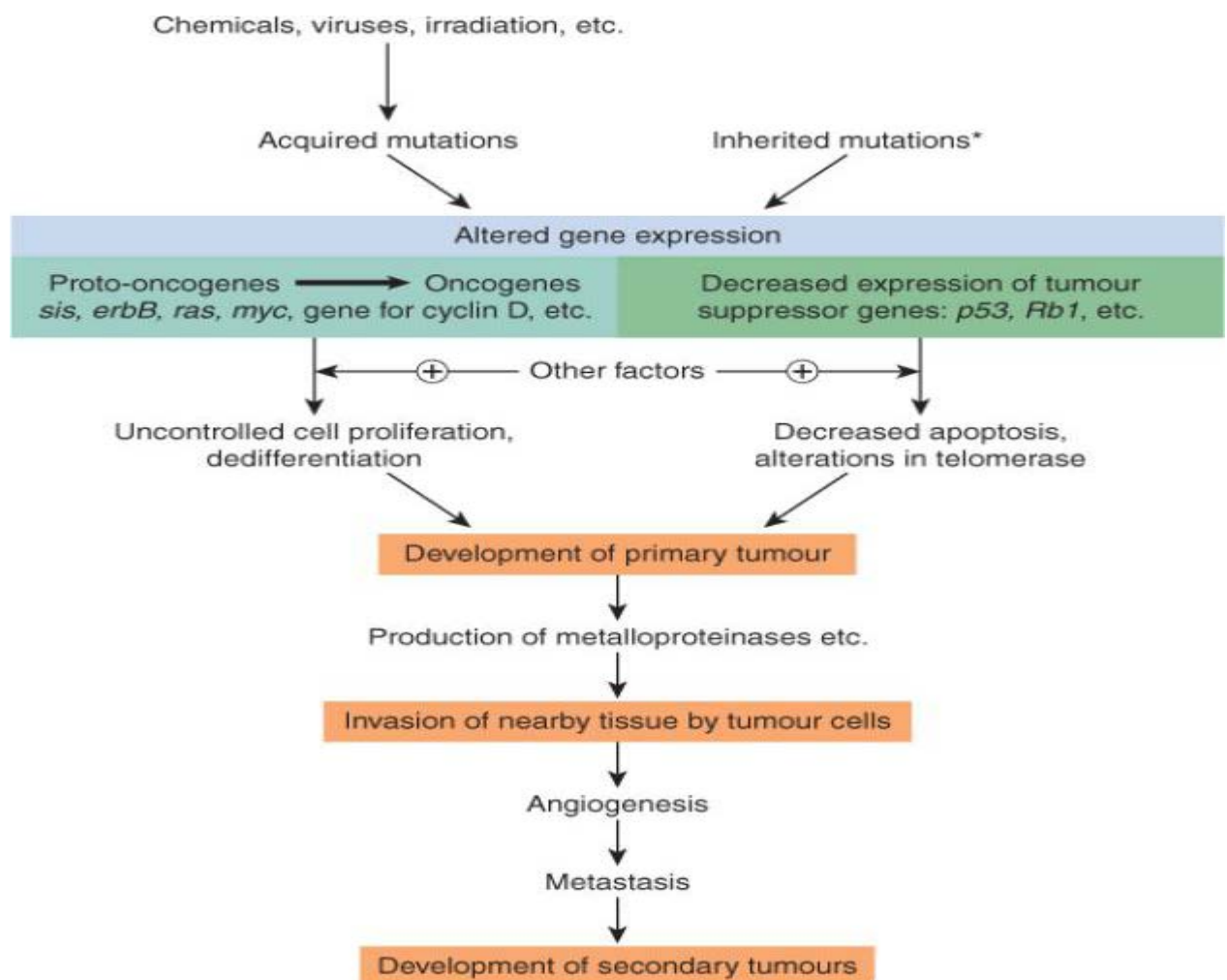
1.3 Treatment of cancer

FIGURE 1.3 : Treatment of cancer[7]
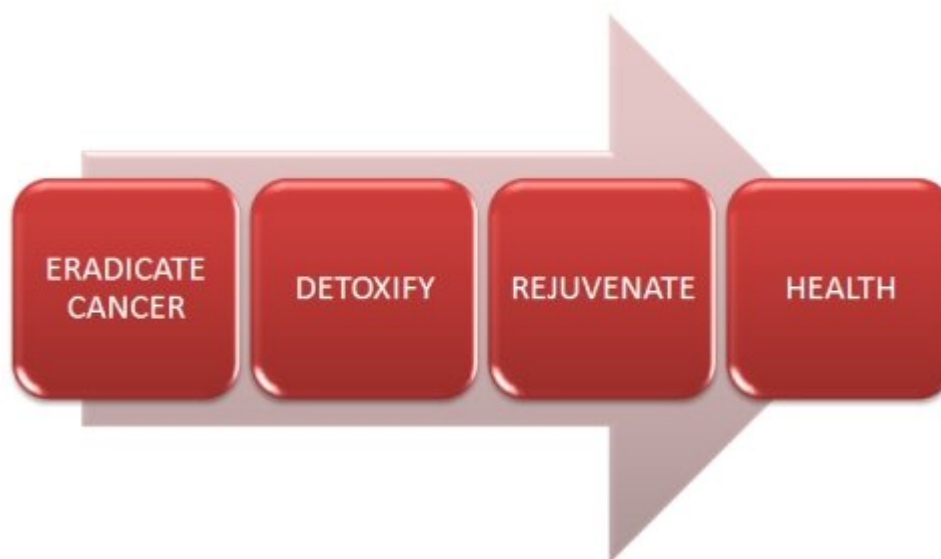
1.3.1 Classification of drugs used as anti-cancer agents:

❖ **ALKYLATING AGENTS:**

The nitrogen at position 7 (N7) of guanine, being strongly nucleophilic, is probably the main molecular target for alkylation in DNA , although N1 and N3 of adenine and N3 of cytosine may also be affected. A bifunctional agent, being able to react with two groups, can cause intra- or interchain cross-linking . This interferes not only with transcription but also with replication, which is probably the critical effect of anticancer alkylating agents. Other effects of alkylation at guanine N7 are excision of the guanine base with main chain scission, or pairing of the alkylated guanine with thymine instead of cytosine, and eventual substitution of the GC pair by an AT pair. Their main impact is seen during replication (S phase), when some zones of the DNA are unpaired and more susceptible to alkylation. This results in a block at G2 and subsequent apoptotic cell death. All alkylating agents depress bone marrow function and cause gastrointestinal disturbances. With prolonged use, two further unwanted

effects occur: depression of gametogenesis (particularly in men), leading to sterility, and an increased risk of acute non-lymphocytic leukemia and other malignancies. Alkylating agents are among the most commonly employed of all anticancer drugs. A large number are available for use in cancer chemotherapy . Only a few commonly used ones will be dealt with here.

- **Nitrogen Mustards:**
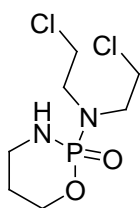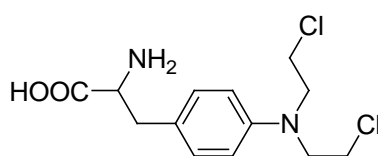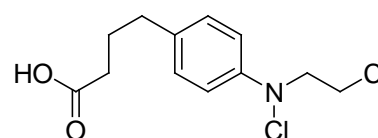
Cyclophosphamide	Melphalan	Chorambucile
(1)	(2)	(3)

- **Nitrosoureas**
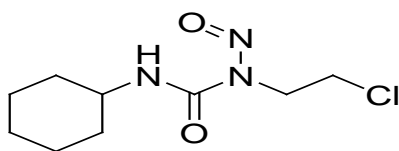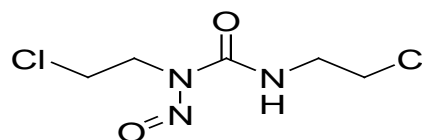
Lomustine	Carmustine
(4)	(5)
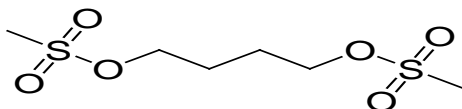
- **Busulfan**

Busulfan

(6)
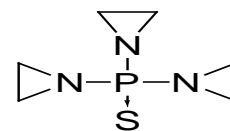
Thiotepa

(7)

- **Platinum Compounds**
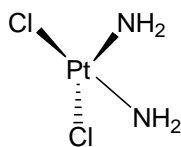
Cisplatin

(8)
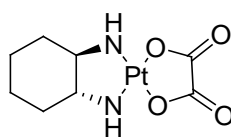
Carboplatin

(9)
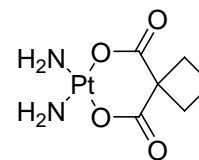
Oxaliplatin

(10)
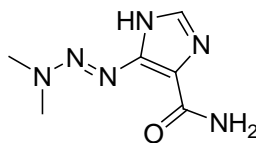
Dacarbazine

(11)

❖ **Anti-metabolites**

Folate antagonists

The main folate antagonist is **methotrexate (13)**, one of the most widely used antimetabolites in cancer chemotherapy. Folates are essential for the synthesis of purine nucleotides and thymidylate, which in turn are essential for DNA synthesis and cell division. The main action of the folate antagonists is to interfere with thymidylate synthesis.

Pyrimidine analogues

Fluorouracil (14) , an analogue of uracil, also interferes with DTMP synthesis. It is converted into a 'fraudulent' nucleotide, *fluorodeoxyuridine monophosphate* (FDUMP). This interacts with thymidylate synthetase but cannot be converted into DTMP. The result is inhibition of DNA but not RNA or protein synthesis.

Fluorouracil is usually given parenterally. The main *unwanted effects* are gastrointestinal epithelial damage and myelotoxicity. Cerebellar disturbances can also occur. Another drug, capecitabine , is metabolised to fluorouracil .
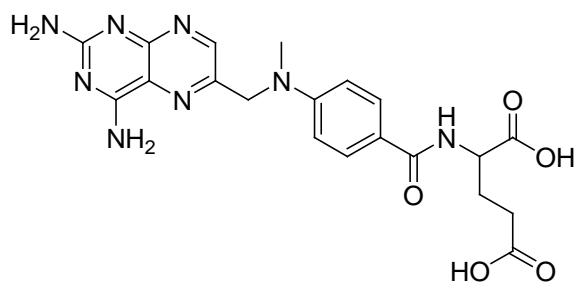
Methotrexate   Fluorouracil
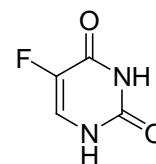
(13)   (14)
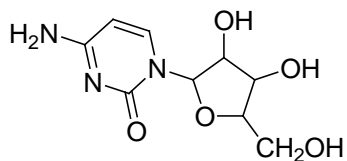
Cytarabine

(15)
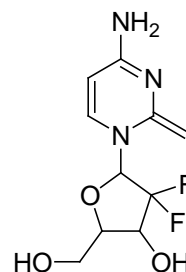
Gemcitabine

(16)

❖ **Purine Analogues**

Mercaptopurine is converted into fraudulent nucleotide. Fludarabine in its trisphosphate form inhibits DNA polymerase and is myelosuppressive. Pentostatin inhibits adenosine deaminase-a critical pathway in purine metabolism.
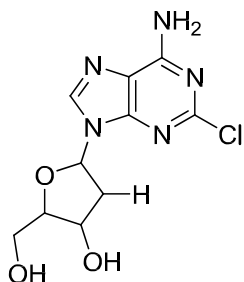
Fludarabine

(17)
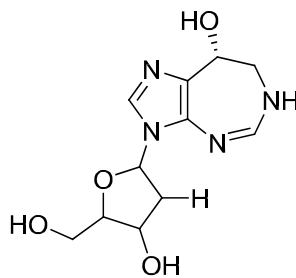
Pentostatin

(18)
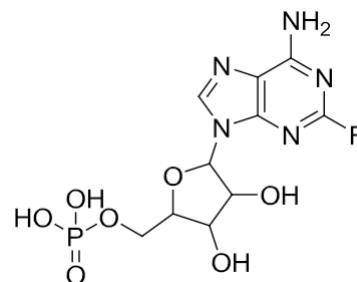
Cladribine

(19)

❖ **Cytotoxic Antibiotics**
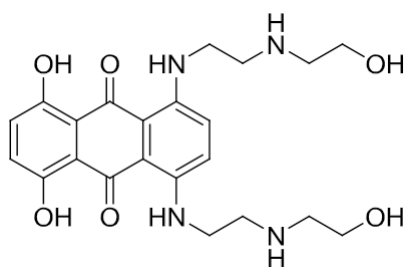
Mitoxantrone   Dactinomycin
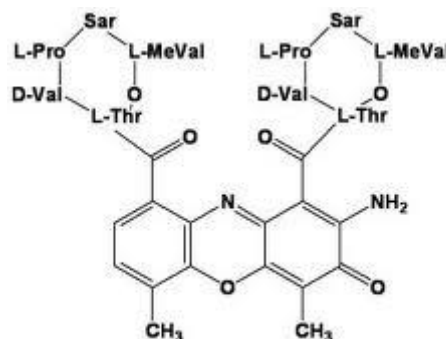
(20)   (21)

❖ **Plant Derivatives**

Several naturally occurring substances exert potent cytotoxic effects and have earned a place in the arsenal of anticancer drugs on that basis.

➢ **Vinca Alkaloids**

The vinca alkaloids are derived from the Madagascar periwinkle. The principal members of the group are **Vincristine(22) , Vinblastine (23)** and **Vindesine (24). Vinorelbine** (25) is a semi synthetic vinca alkaloid with similar properties that is mainly used in breast cancer. The drugs bind to tubulin and inhibit its polymerization into microtubules, preventing spindle formation in dividing cells and causing arrest at metaphase. Their effects become manifest only during mitosis. They also inhibit other cellular activities that involve the microtubules, such as leucocyte phagocytosis and chemotaxis, as well as axonal transport in neurons.

The vinca alkaloids are relatively non-toxic. Vincristine has very mild myelosuppressive activity but causes paraesthesias (sensory changes), abdominal pain and muscle weakness fairly frequently. Vinblastine is less neurotoxic but causes leucopenia, while vindesine has both moderate myelotoxicity and neurotoxicity.
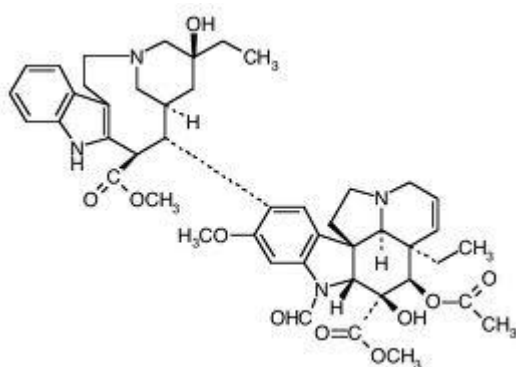
(22)
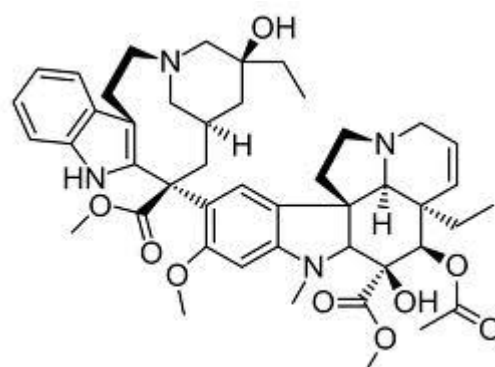
(23)
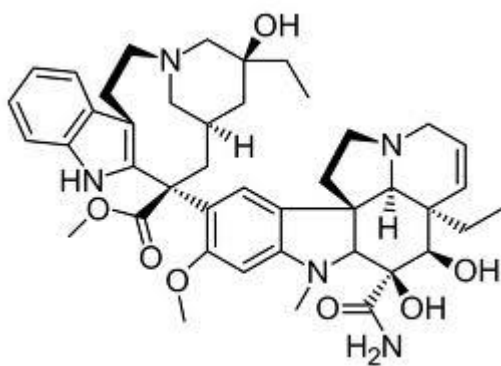
(24)
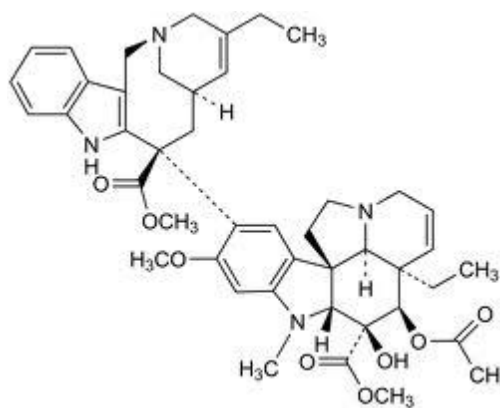
(25)

➢ **Taxanes**

Paclitaxel (26) and **Docetaxel (27)** are derived from a naturally occurring compound found in the bark of the yew tree. They act on microtubules, stabilising them (in effect 'freezing' them) in the polymerised state, achieving a similar effect to that of the vinca alkaloids. Paclitaxel is given by intravenous infusion and docetaxel by mouth. Both have a place in the treatment of breast cancer, and paclitaxel, given with carboplatin, is the treatment of choice for ovarian cancer.
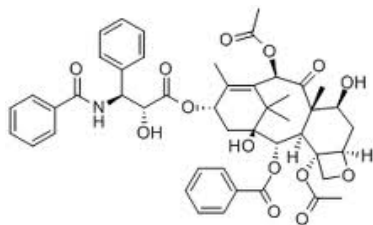
(26)
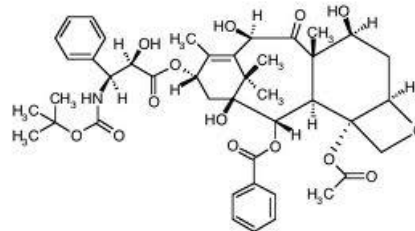
(27)

Unwanted effects, which can be serious, include bone marrow suppression and cumulative neurotoxicity. Resistant fluid retention (particularly oedema of the legs) can occur with docetaxel. Hypersensitivity to both compounds is liable to occur and requires pretreatment with corticosteroids and antihistamines.

Etoposide

Etoposide is derived from mandrake root. Its mode of action is not clearly known, but it may act by inhibiting mitochondrial function and nucleoside transport, as well as having an effect on topoisomerase II similar to that seen with doxorubicin. Unwanted effects include nausea and vomiting, myelosuppression and hair loss.

Campothecins

The campothecins irinotecan and topotecan, isolated from the stem of the tree Camptotheca acuminata, bind to and inhibit topoisomerase I, high levels of which occur throughout the cell cycle. Diarrhoea and reversible bone marrow depression occur but, in general, these alkaloids have fewer unwanted effects than most other anticancer agents.

❖ **Hormones**

Tumors derived from hormone-sensitive tissues may be hormone-dependent, an effect related to the presence of steroid receptors in the malignant cells. Their growth can be inhibited by hormones with opposing actions, by hormone antagonists or by agents that inhibit the endogenous hormone synthesis. Hormones or their analogues that have inhibitory actions on target tissues can be used in treatment of tumors of those tissues. Such procedures alone rarely affect a cure but do mitigate the symptoms of the cancer and thus play an important part in the clinical management of sex hormone-dependent tumors.
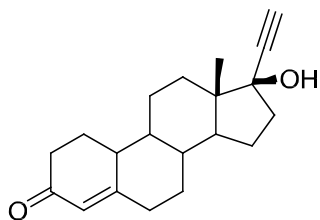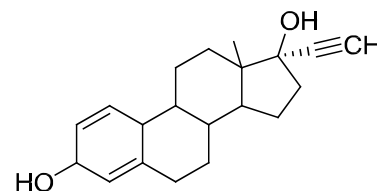
(28)   (29)
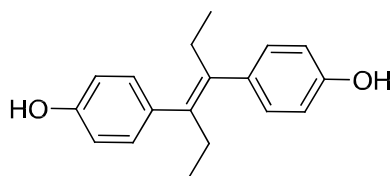
(31)
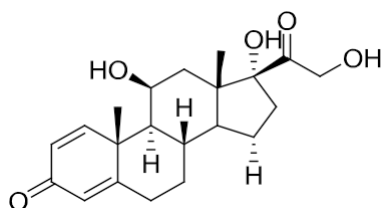
(32)
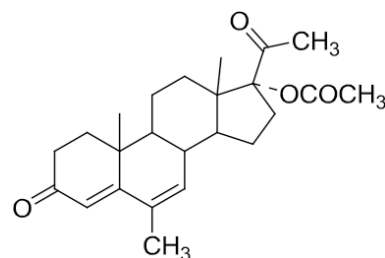
(33)
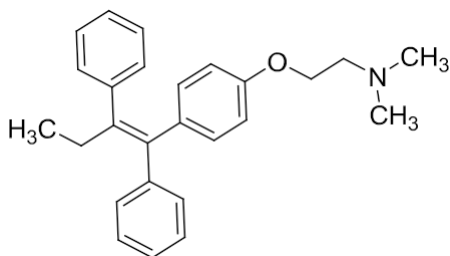
(34)
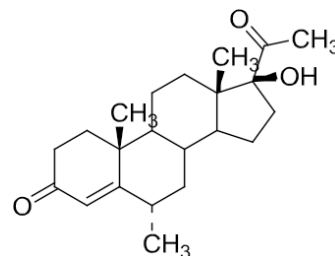
(35)

Glucocorticoid

Glucocorticoids such as **Prednisolone (28)** and **Dexamethasone** (29) have marked inhibitory effects on lymphocyte proliferation and are used in the treatment of leukaemias and lymphomas. Their ability to lower raised intracranial pressure, and to mitigate some of the side effects of anticancer drugs, makes them useful as supportive therapy when treating other cancers, as well as in palliative care.

Oestrogens

Diethylstilbestrol (30) and **Ethinyl estradiol** (31) are two oestrogens used clinically in the palliative treatment of androgen-dependent prostatic tumors. The latter compound has fewer side effects. These tumors are also treated with gonadotrophin-releasing hormone analogues. Oestrogens can be used to recruit resting mammary cancer cells into the proliferating pool of cells, thus facilitating killing by other, cytotoxic drugs.

Progestogens

Progestogens such as **Megestrol** (32), Norehisterone (33) and **Medroxyprogesterone** (34) have been useful in endometrial neoplasms and in renal tumors.

❖ **Hormone Antagonists**

In addition to the hormones themselves, hormone antagonists can also be effective in the treatment of several types of hormone-sensitive tumors.

Antioestrogens

An antioestrogen, **Tamoxifen (35)**, is remarkably effective in some cases of hormone-dependent breast cancer and may have a role in preventing these cancers. In breast tissue, tamoxifen competes with endogenous oestrogens for the oestrogen receptors and therefore inhibits the transcription of oestrogen-responsive genes.
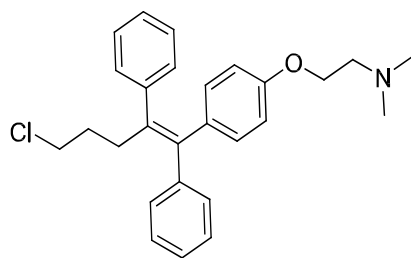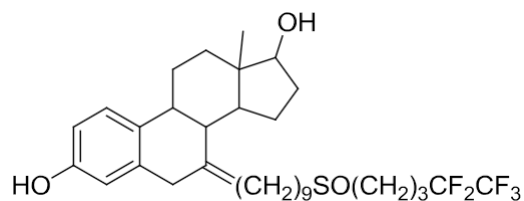
(36)   (37)

Other oestrogen receptor antagonists include **Toremifene (36)** and **fulvestrant (37)**. Aromatase inhibitors such as anastrozole, letrozole and exemestane, which suppress the synthesis of oestrogen from androgens, are also effective in the treatment of breast cancer.

Antiandrogens

The androgen antagonists, flutamide, cyproterone and **Bicalutamide (38),** may be used either alone or in combination with other agents to treat tumors of the prostate. They are also used to control the 'flare' that is seen when treating patients with gonadorelin analogues.
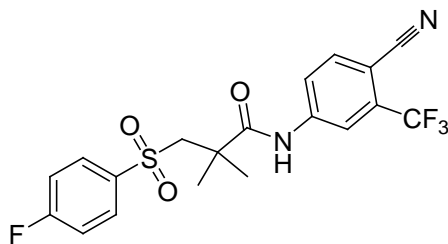
(38)

❖ Radioactive Isotopes

Radioactive isotopes have an important place in the therapy of certain tumors; for example, radioactive iodine (131I) is used in treating thyroid tumors. Anticancer agents: hormones and radioactive isotopes

Hormones or their antagonists are used in hormone-sensitive tumors:

o glucocorticoids for leukaemias and lymphomas

o tamoxifen for breast tumors

o gonadotrophin-releasing hormone analogues for prostate and breast tumors

o antiandrogens for prostate cancer

o inhibitors of sex hormone synthesis for postmenopausal breast cancer.

Radioactive iostopes can be targeted at specific tissues, for example ^{131}I for thyroid tumors.

❖ **Miscellaneous Agents**

Crisantaspase

Crisantaspase (39) is a preparation of the enzyme asparaginase, given intramuscularly or intravenously. It breaks down asparagine to aspartic acid and ammonia, and is active against tumor cells, such as those of acute lymphoblastic leukemia, that have lost the capacity to synthesize asparagine and therefore require an exogenous source. As most normal body cells are able to synthesize asparagine, the drug has a fairly selective action and has very little suppressive effect on the bone marrow, the mucosa of the gastrointestinal tract or hair follicles. It may cause nausea and vomiting, central nervous system depression, anaphylactic reactions and liver damage.
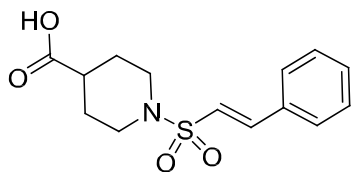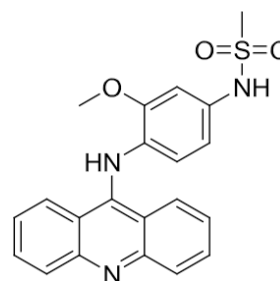
(39)   (40)

Amsacrine

Amsacrine (40) has a mechanism of action similar to that of doxorubicin. Bone marrow depression and cardiac toxicity have been reported.

1.4 Role of Aurora-kinases in Cell Division and Cancer

Aurora kinases are serine/threonine kinases that are essential for cell proliferation. This enzyme helps the dividing cell in dispensing its genetic materials to its daughter cells. More specifically, Aurora kinases play a crucial role in cellular division by controlling chromatid segregation. Defects in this segregation can cause genetic instability, a condition which is highly associated with tumorigenesis. [8]

Three Aurora kinases have been identified in mammalian cells to date. Besides being implicated as mitotic regulators, these three kinases have generated significant interest in the cancer research field due to their elevated expression profiles in many human cancers.

The three isoforms of kinases found in mammals are : Aurora A, Aurora B, and Aurora C. They are expressed during G2/M phaseof the cell cycle and are critical for the proper regulation of mitosis. [9]

Functioning of isoforms in the cell cycle goes as follows:

- Aurora A (aka Aurora 2) functions during prophase of mitosis and is required for correct function of the centrosomes (the microtubule organising centres in eukaryotic cells). controls centrosome maturation and mitotic spindle formation[10]

- Aurora B (aka Aurora 1) ensures chromosome segregation and alignment as part of the chromosomal passenger protein complex . It functions in the attachment of the mitotic spindle to the centromere.[11]

- Aurora C, works in germ-line cells though not well understood, is thought to function similarly to Aurora B.[12]

Over-expression of Aurora kinases is observed in various tumor cells. It is believed that inhibition of Aurora kinases could lead to the G2 arrest of cancer cells and subsequently promote the death of cancer cells. Therefore, Aurora kinases have emerged as attractive oncology targets for small-molecule drug discovery. [13]

FIGURE 1.4 : Expression of Aurora Kinases in Cells[14]
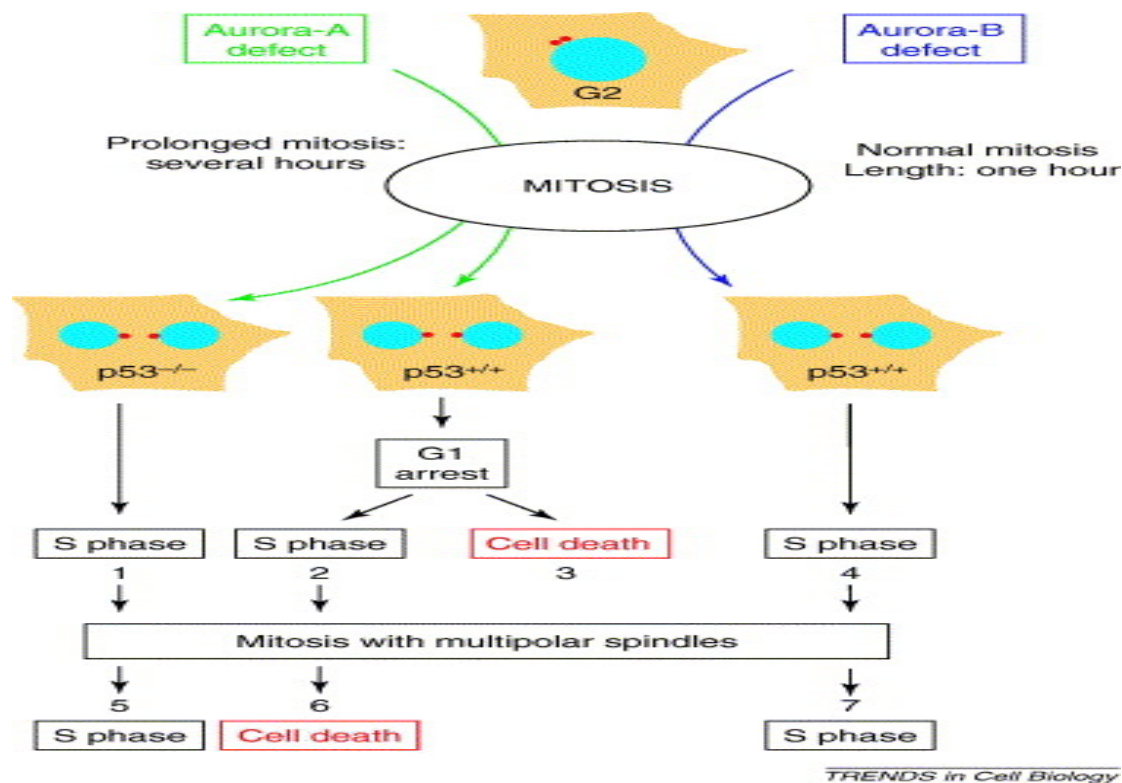
Members of the Aurora-kinase family have recently emerged as key mitiotic regulators required for genome stability . Furthermore, these serine/threonine kinases are frequently overexpressed in human tumours. For example, as shown in Fig 1.4 , Aurora-A is frequently amplified in tumours, indicating that it is important for tumour foration or progression in drug development. Given the amplification of Aurora-A in tumours and the observation that it can act as a bona fide oncogene, transforming cells when ectopically expressed in vitro, its product has been highlighted as a drug target. Several reports have been published describing the first generation of small-molecule inhibitors of Aurora-kinase activity. Importantly and excitingly, one of these has shown antitumour activity in in vivo models A great deal has recently been learned about the basic biology of this family of kinases, in the context of the initiation of cancer and in its therapy. There are, however, inherent difficulties in the

biological approaches that are available at present for validating kinases as small-molecule drug targets. It is believed that inhibition of Aurora kinases could lead to the G2 arrest of cancer cells and subsequently promote the death of cancer cells. Therefore, Aurora kinases have emerged as attractive oncology targets for small-molecule drug discovery.

As a result, many Aurora kinase inhibitors, including Aurora A selective, Aurora B selective, and pan-Aurora kinase inhibitors, have been discovered and advanced to human clinical trials.

FIG: 1.5 : TARGETING AURORA KINASES[15]
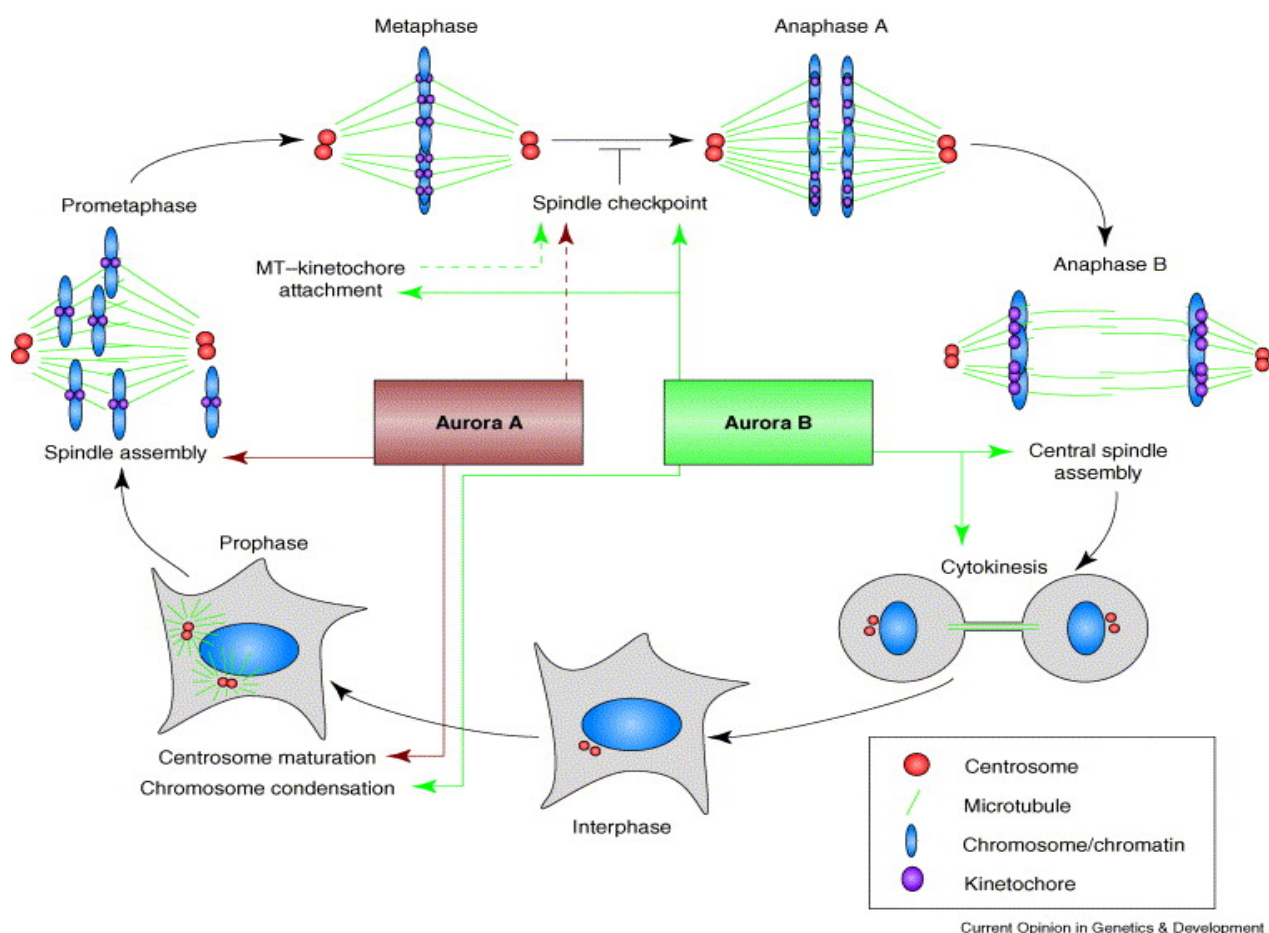
1.4.1 Aurora Kinase-A as cancer target

Aurora A kinase also known as serine/threonine-protein kinase 6 is an enzyme that in humans is encoded by the AURKA gene .

Aurora A is a member of a family of mitotic serine/threonine kinases. It is implicated with important processes during mitosis and meiosis whose proper function is integral for healthy cell proliferation. Aurora A is activated by one or more phosphorylations and its activity peaks during the G2 phase to M phase transition in the cell cycle.

The protein encoded by this gene is a cell cycle-regulated kinase that appears to be involved in microtubule formation and/or stabilization at the spindle pole during chromosome segregation. The encoded protein is found at the centrosome in interphase cells and at the spindle poles in mitosis. This gene may play a role in tumor development and progression

FIGURE 1.6: Structure of Aurora Kinase
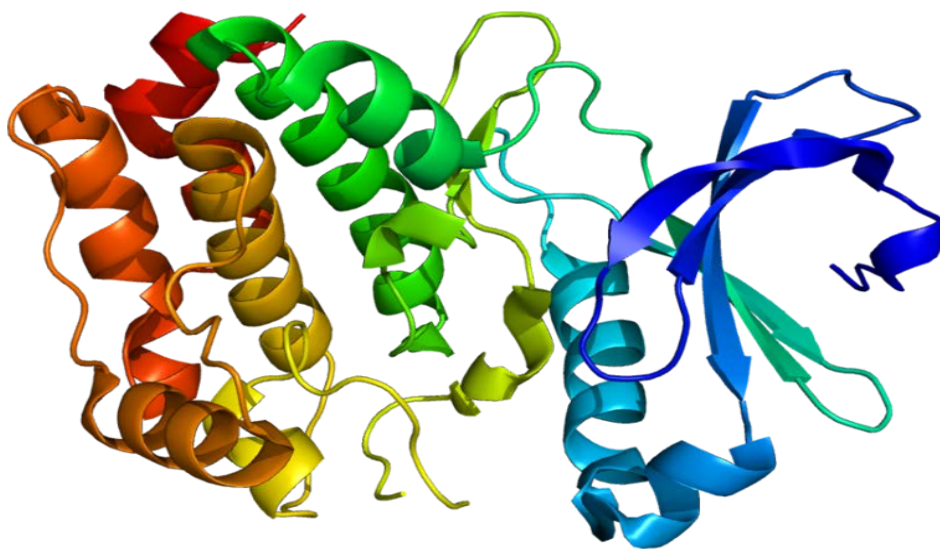
1.4.2 Mechanism of AURKA

AURKA induces p53 degradation by phosphorylation of Ser-315. It was demonstrated that DNA binding and transactivation activity of p53 was abrogated by AURKA. AURKA phosphorylates p53 at Ser-215 in vitro and in vivo. The inhibition of p53 DNA binding and transactivation activity by AURKA depends on phosphorylation of Ser-215 but not Ser-315. Further, AURKA phosphorylation of Ser-215 of p53 is associated with AURKA -regulated cell cycle progression, cell survival, and transformation. The p53 is a physiological substrate of AURKA and that AURKA exerts its function through phosphorylation of Ser-215 of p53. 1.6.3 Role of AURKA in Mitosis

FIGURE 1.7 : Role of AURKA in Mitosis[16]
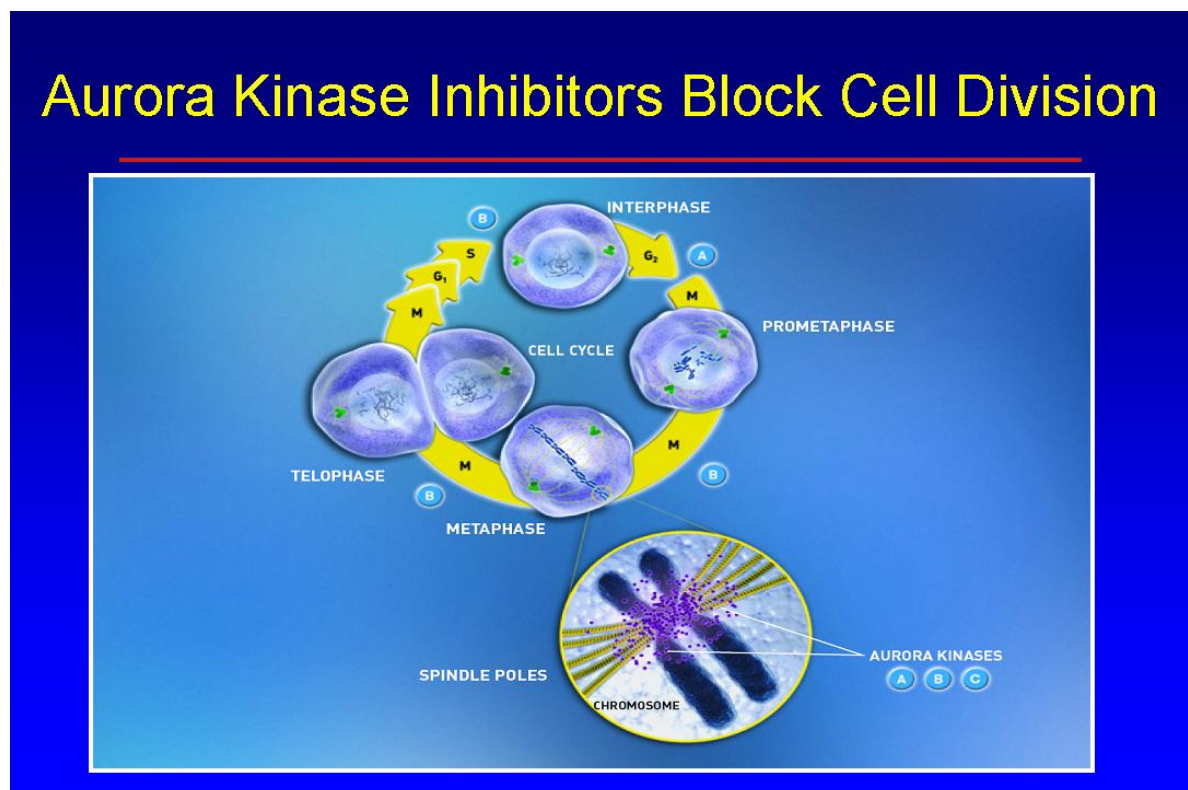
Targeting mitosis is a well known approach in the search for anti-cancer therapies. For example, the taxanes and vinca alkaloids, some of the most effective compounds in the oncology field, are anti-mitotics. Unfortunately the collateral effects related to their activity on microtubules (e.g., neurotoxicity) still remain an unsolved issue. The search for well tolerated anti-mitotic agents continues to represent a challenge in drug discovery. Within the family of Ser/Thr protein kinases, we consider mammalian Aurora kinases, which secure the correct progression of cell cycle during mitosis or meiosis, as biological targets worth pursuing in the quest for new therapeutic agents in the oncology fieldDuring mitosis, a mitotic spindle is assembled by using microtubules to tether together the mother centrosome to its daughter. The resulting mitotic spindle is then used to propel apart the sister chromosomes into what will become the two new daughter cells. Aurora A is critical for proper formation of mitotic spindle. It is required for the recruitment of several different proteins important to the spindle formation. Among these target proteins are TACC, a microtubule-associated protein that stabilizes centrosomal microtubules and Kinesin 5, a motor protein involved in the formation of the bipolar mitotic spindle. γ-tubulins, the base structure from which centrosomal microtubules polymerize, are also recruited by Aurora A. Without Aurora A the centrosome does not accumulate the quantity of γ-tubulin that normal centrosomes recruit prior to entering anaphase. Though the cell cycle continues even in the absence of deficient γ-tubulin, the centrosome never fully matures; it organizes fewer aster microtubules than normal. [17]

Finally, Aurora A helps orchestrate an exit from mitosis by contributing to the completion of cytokinesis- the process by which the cytoplasm of the parent cell is split into two daughter cells. During citokinesis the mother centriole returns to the mid-body of the mitotic cell at the end of mitosis and causes the central microtubules to release from the mid-body. The release allows mitosis to run to completion. Though the exact mechanism by which Aurora A aids cytokinesis is unknown, it is well documented that it relocalizes to the mid-body immediately before the completion of mitosis.

1.4.3 Clinical Significance of AURKA

Aurora A dysregulation has been associated with high occurrence of cancer. For example, one study showed over-expression of Aurora A in 94 percent of the invasive tissue growth in breast cancer, while surrounding, healthy tissues had normal levels of Aurora A expression. Dysregulation of Aurora A may lead to cancer because Aurora A is required for the completion of cytokinesis. If the cell begins mitosis, duplicates its DNA, but is then not able to divide into two separate cells it becomes an aneuploid- containing more chromosomes than normal. Aneuploidy is a trait of many cancerous tumors. Ordinarily, Aurora A expression levels are kept in check by the tumor suppressor protein p53. [18]

1.6 Pharmacophore modeling

A very important part of drug design is predicition of small molecule binding to a target macromolecule. A detailed quantitative predicition of small molecule binding can require sophisticated computational techniques and lots of computer time. Often a reasonable qualitative prediction of binding can be made by just specifying the spatial arrangement of a small number of atoms or functional groups. Such an arrangement is called a pharmacophore. When researchers start on a drug design project, one of the early steps is to assay available compounds in order to obtain some initial active hits. Of course, it is prohibitively costly to simply assay every compound available. Thus, there needs to be a logical process for choosing compounds with some reasonable probability that any one of them might be a useful inhibitor. The tools that fill this need are substructure searches, similarity metrics, and pharmacophore searches. Of the three, pharmacophore searches are best at finding a range of chemical structures with viable features, and are thus the method of choice for the first round of compound selection. The ability of pharmacophore to identify new classes of inhibitors is termed as "scaffold hopping.Thus a pharmacophore can be defined as "an ensemble of steric and electronic features that is necessary to ensure the optimal supramolecular interactions with a specific biological target and to trigger (or block) its biological response".One of the advantages of pharmacophore searching is that it is possible to generate a pharmacophore

model without any direct knowledge of the geometry of the protein's active site. This can be done by analysing a set of known active ligands to find what features they have in common. first step in building a pharmacophore model from a set of ligands is the alignment of the molecules, including position, rotation, and conformation. [19]

1.6.1 Ligand based pharmacophore modeling

One of the advantages of pharmacophore searching is that it is possible to generate a pharmacophore model without any direct knowledge of the geometry of the protein's active site. This can be done by analysing a set of known active ligands to find what features they have in common. In practice, this can be somewhat difficult. One reason for this is that there is no sure way to know what conformer of an active ligand is the active conformer.[76,78] The active site may have an important functional group suggesting a pharmacophore feature that is not present in any of the known ligands. Also, the known ligands may by chance have a feature not required for binding, particularly if they are all derivatives of the same base structure. This is why it is best to perform this analysis with a set of active ligands that are not all derivatives of the same structure. In spite of these difficulties, constructing a pharmacophore model from known ligands may be the best option available at some early stage of the project. The first step in building a pharmacophore model from a set of ligands is the alignment of the molecules, including position, rotation, and conformation. The initial alignment may be done with active compounds only. Later, inactive compounds can be aligned onto this set. Ideally, the alignment starts with the most rigid fused ring compounds; other compounds are then aligned to those. This is a mechanism for finding the correct conformer of each compound to use. If there are no rigid structures, the ―shoot-from-the-hip alternative is aligning the compounds to the lowest energy conformer of the most active compound.

1.6.2 Structure Based Pharmacophore Modeling

The alternative to generating pharmacophore models from active compounds is to generate them from the geometry of the active site. This is usually the preferred option if this geometry is known. Since it is possible to see how the pharmacophore model interacts with the active site, there will not be errors due to having a limited set of training compounds. The process of building a pharmacophore model from the geometry of the active site starts with a three-dimensional molecular structure for the protein, or at least the active site. In some cases, it may be necessary to identify which region of the surface of the protein is the active site. There are crevice detection programs to suggest possible active site locations based on the geometry of the surface.

1. GASP -Genetic Algorithm Superposition Program
2. DISCOtech- It is based on distance geometry approaches
3. GALAHAD -Genetic Algorithm with Linear Assignment for Hypermolecular Alignment of Datasets

1.6.3 GALAHAD

The new pharmacophore alignment method GALAHAD (Genetic Algorithm with Linear Assignment for Hypermolecular Alignment of Datasets) aligns a set of molecules that share a common mode of biological activity and develops corresponding pharmacophore models. Using a sophisticated genetic algorithm and a multi-objective scoring function, GALAHAD takes into account energetics, steric similarity, and pharmacophoric overlap, while accommodating conformational flexibility, ambiguous stereochemistry, alternative ring configurations, multiple partial match constraints, and alternative feature mappings among molecules. GALAHAD aligns a set of molecules that share a common mode of biological activity, and develops a corresponding pharmacophore hypothesis. Pharmacophore models are returned as hypermolecules, which contain information from every molecule in the training set, as well as a 3D search query that can be used to probe databases for new

structures that match the model. New target molecules that were not included in the training set can be fit to the model, yielding scores for energy as well as steric and pharmacophoric similarity that relate directly to ligand affinity. GALAHAD allows researchers to automatically develop pharmacophore hypotheses and structural alignments from a set of molecules that bind at a common site. No prior knowledge of pharmacophore elements, constraints, or molecular alignment is required, making it ideal for exploring new targets and new modes of action. GALAHAD uses a sophisticated new genetic algorithm (GA) that defines each molecule as a core structure plus a set of torsions. To overcome limitations in existing pharmacophore tools, GALAHAD's genetic algorithm was developed on real-world datasets. Pre-processing (or pre-generated conformers) provide torsional biases that speed up calculations, while yielding less strained ligand conformations in output pharmacophore models. Torsions are then applied to the core structure, and 3D similarity among the ligands is rapidly measured using pharmacophoric and steric multiplets. Since each molecule is simultaneously compared to every other molecule, specification of a template molecule is not required and the results are not biased towards any structure. Using pharmacophoric and steric similarity instead of one-to-one feature mapping allows the calculations to be carried out in internal coordinate space, which produces significantly faster convergence of the GA. [20]

ADVANTAGES:

Pareto multi-objective optimization is used to simultaneously balance steric, pharmacophoric, and energy information to build the most valuable hypermolecule models required, so models are unbiased. Run time scales linearly with the number of ligands, unlike other methods.

Partial match and partial coverage models can be created in a timely manner.

There are 12 columns in the MSS result spreadsheet. The first three are model properties generated during post-processing, the next five are model scores components from the genetic algorithm, and the last four are the scores for individual ligands within each model. Results of pharmacophore models generated contain following information:

➤ SPECIFICITY : Specificity is a logarithmic indicator of the expected discrimination of each query, based on the number of features it contains, their allotment across any partial constraints and the degree to which the features are separated in space. This value should be at least 4-5.

➤ N_HITS : The actual number hit. A negative number indicates that no ligands hit the model query.

➤ FEATS: Total number of features in the model query.

➤ PARETO: The values in this column indicate the Pareto rank of the each model. A value of) indicates that no one model is superior to any other by all four of the criteria laid out in the last 4 columns.

➤ ENERGY: The total energy of the model

➤ STERICS: The steric overlap of the model

➤ HBOND : The pharmacophoric concordance

➤ MOL_QRY : The agrrement between the query tuplet and the pharmacophoric tuplets for the ligands as a group

➤ FEATS: The total number of features in the model query.

➤ PARETO: The values in this column indicate the Pareto rank of the each model (see Pareto Ranking). A value of 0 indicates that no one model is superior to any other by all four of the criteria laid out in the last 4 columns.

➤ ENERGY: The total energy of the model.

➤ STERICS: The steric overlap for the model.

➤ HBOND   : The pharmacophoric concordance.

➢ MOL_QRY: The agreement between the query tuplet and the pharmacophoric tuplets for the ligands as a group.

➢ IND_ENERGY: The total energy for each of the individual ligands in the model.

➢ IND_STERICS: The steric overlap for each of the individual ligands in the model.

➢ IND_HBOND: The pharmacophoric concordance for each of the individual ligands in the model.

➢ IND_MOL_QRY: The agreement between the query tuplet and the pharmacophoric tuplets for each of the individual ligands in the model.

➢

1.6 SEARCHING COMPOUND DATABASES

The fit between the molecule and the pharmacophore can be used as an alignment device which is referred as virtual screening. The pharmacophore searching algorithm translates and rotates each molecule in the Cartesian coordinate system to place it in the best possible alignment with the pharmacophore. Virtual screening (VS) is a computational technique used in drug discovery research. By using computers, it deals with the quick search of large libraries of chemical structures in order to identify those structures which are most likely to bind to a drug target, typically a protein receptor or enzyme. [21]

Virtual screening has become an integral part of the drug discovery process. Related to the more general and long pursued concept of database searching, the term "virtual screening" is relatively new. Walters, et al. define virtual screening as "automatically evaluating very large libraries of compounds" using computer programs. As this definition suggests, VS has largely been a numbers game focusing on questions like how can we filter down the enormous chemical space of over 10^{60} conceivable compounds to a manageable number that can be synthesized, purchased, and tested. Although filtering the entire chemical universe might be a fascinating question, more practical VS scenarios focus on designing and

optimizing targeted combinatorial libraries and enriching libraries of available compounds from in-house compound repositories or vendor offerings.

1.7 MOLECULAR DOCKING

Docking is a computer algorithm that predicts the preferred orientation and conformation of the ligand in the binding site of the target and determines how a ligand molecule will bind in the active site of a target. This includes determining the orientation of the compound, its conformational geometry, and the scoring. The scoring may be a binding energy, free energy, or a qualitative numerical measure. Docking is the most accurate method for predicting whether a particular compound will be a good inhibitor of a particular protein.[22]

There are two key components of a docking program:
1) The search algorithm and
2) The scoring function.

The Search algorithm: The search algorithm positions molecules in various locations, orientations, and conformation within the active site. The choice of search
algorithm determines how thoroughly the program checks possible molecule positions,
and how long it takes to run. Some examples of search algorithm are Monte carlo search,
Simulated annealing, genetic algorithm, Multiple Copy Simultaneous search etc.

1.8 3D-QSAR

QSAR is conceptually a way of finding a simple equation that can be used to predict some property from the molecular structure of a compound. This is done by using curve fitting software to find the equation coefficients, which are weights of known molecular properties. The molecular properties in a QSAR equation are called descriptors. A descriptor can be any number that describes the molecule. Descriptors can be as simple as the molecular weight, or

as obtuse as topological indices. QSAR uses descriptors that are a single number describing some aspect of the molecule. 3D-QSAR uses a 3D grid of points around the molecule, each point having properties associated with it, such as electron density or electrostatic potential. In general, conventional QSAR is best used for computing properties that are a function of nonspecific interactions between the molecule and its surroundings. For these properties, small changes in molecular structure generally give small changes in the property. For example, conventional QSAR is the method of choice for computing normal boiling points, passive intestinal adsorption, blood–brain barrier permeability, colligative properties, etc. Conversely, 3D-QSAR is better for computing very specific interactions, such how tightly a compound will bind to the active site in one, specific protein. The rest of this chapter discusses QSAR, but not 3D-QSAR.[23]

1.9 *IN-SILICO* ADMET

The goal of *in-silico* ADME–Toxicity characterization is to provide, with reasonable accuracy, a preliminary prediction of the in vivo behaviour of a compound to assess its potential to become a drug. Many factors combine to determine this, therefore, a variety of experimental assays have been developed to characterize each aspect of the processes. The tools involved include physicochemical methods and biological assays using subcellular fractions, primary cell culture, immortalized cell lines, tissues and whole organs. Two major challenges faced by these assays in the discovery phase are higher throughput and shorter time for data turnaround, both of which are a result of the need to rapidly screen a large number of compounds. To meet these challenges, new formats of in vitro ADME–Tox assays serving early discovery have been developed from traditional assays through protocol simplification and making use of technology advancement. It is important to recognize the similar field known as *in-silico* pharmacology. This field involves the use of computer-assisted (computational) methods for study of chemical and biological drugs in the context of understanding how they may ultimately affect (beneficially or adversely) functions of the body. Even with these broad definitions, it is clear that the *in-silico* toxicology and

pharmacology fields are inter-related and overlapping in their coverage of the study of adverse effects of drugs.[24]

1.10 admetSAR

Various problems associated with ADMET (absorption, distribution, metabolism, excretion and toxicity) have been the central reason for the failure of hundreds of candidates in clinical trials or the withdrawal of few marketed drugs due to unacceptable side effects. So, in-silico ADMET prediction can help in reducing failure rate of drug candidates which are developed by costly and time consuming processes. In silico pharmacokinetic properties and toxicities were predicted using admetSAR which is a free tool for assessment of ADMET properties. It uses 22 highly predictive qualitativeis a free tool for assessment of ADMET properties. Various classification models which were developed using support vector machine classification algorithm and in house substructure pattern recognition method to assess the prediction studies. To predict the ADMET properties of the designed molecules data input was given by SMILES input format obtained by the molecular structure using build-in tool of JSDraw.

CHAPTER-10

IN-SILICO PHARMACOKINETIC AND

TOXICITY PREDICTION

10. *In- silico* Pharmacokinetic and Toxicity Prediction

In-silico pharmacokinetic and toxicity prediction play an important role in drug discovery and development because ADMET (absorption, distribution, metabolism and excretion) and toxicities are major causes for failure of drug candidates during late phases of drug development. *In silico* properties prediction of proposed structure molecules before synthesis can reduce time and cost involved in synthesis of compounds. This approach is more powerful during lead optimization as it can provide guidance regarding modification of structure which will improve physicochemical properties.

10.1 Methods and Materials

Various problems associated with ADMET (absorption, distribution, metabolism, excretion and toxicity) have been the central reason for the failure of hundreds of candidates in clinical trials or the withdrawal of few marketed drugs due to unacceptable side effects. So, in-silico ADMET prediction can help in reducing failure rate of drug candidates which are developed by costly and time consuming processes. In silico pharmacokinetic properties and toxicities were predicted using admetSAR which is a free tool for assessment of ADMET properties. It uses 22 highly predictive qualitativeis a free tool for assessment of ADMET properties. Various classification models which were developed using support vector machine classification algorithm and in house substructure pattern recognition method to assess the prediction studies. To predict the ADMET properties of the designed molecules data input was given by SMILES input format obtained by the molecular structure using build-in tool of JSDraw.

10.2 Results and Discussion

Pharmacokinetic properties and toxicities were determined using free web tool for 10 compounds including Tozasertib. Results of pharmacokinetic properties and toxicities are

shown in **Table 20.** Solubility and partition coefficient were calculated for pharmacokinetic property. Results of *in silico* pharmacokinetic and toxicity study revealed that no compound showed any significant toxicity and all compounds showed good pharmacokinetic properties. The logP value was measured to determine hydrophilicity of both compounds. It has been found that high logP value is associated with poor absorption or permeation and it must be less than 5. This study suggested that all compounds conformed to this limit. Typically, low solubility is associated with bad absorption, so the general aim is to avoid poorly soluble compounds. The aqueous solubility (logS) of a compound significantly affects its absorption and distribution characteristics. This result further encourages us to discover newer inhibitors in treatment of cancer.

Table 20: *In silico* **Pharmacokinetic and Toxicity Study of Synthesized Compounds**

Compound No.	Probability to cross BBB	Human Intestinal Absorption	logS	logP	Carcinogenicity	Rat acute toxicity
59	0.7323	0.9638	-3.6308	0.7882	0.8871	2.4769
60	0.6432	0.9789	-3.5343	0.8067	0.8810	2.4528
61	0.6825	0.9834	-3.8859	0.9266	0.8879	2.4603
62	0.7301	0.9494	-0.3.8202	0.5759	0.8488	2.4886
63	0.5526	0.9858	-0.3882	0.8272	0.7525	2.5460
64	0.7517	0.9689	-3.8920	0.8653	0.8567	2.4923
65	0.7407	0.9561	-3.7963	0.8299	0.8730	2.5155
66	0.7517	0.9689	-3.8920	0.8653	0.8567	2.4923
67	0.7292	0.8877	-3.5798	0.7583	0.9128	2.4754
68	0.7571	0.9273	-3.8462	0.8738	0.8992	2.4647

CHAPTER- 11
CONCLUSION

10. Conclusion

In course of our research to find novel anti-cancer agents, ligand based pharmacophore modeling was performed using GALAHAD. 11 molecules were used to perform pharmacophore mapping. Model 5 was considered as the best model on the basis of specificity from the 20 models which were generated. A best pharmacophore hypothesis contains 2 donor sites, 1 acceptor atom and 2 hydrophobic regions which was chosen for substructure searching in NCI and Maybridge Hit Finder databases. A total number of 16829 molecules were obtained from 58,591 molecules after virtual screening. Virtual screening was applied in order to filter drug like compounds after applying Lipinski's rule of five. Pharmacophore models were chosen for virtual screening method to retrieve the potential leads against Aurora Kinase-A inhibitors. In order to predict the biological activity of synthesized compounds, 3D QSAR (CoMFA and CoMSIA) study was performed on 48 (38 training and 10 test set molecules) Pyrolo-triazene derivatives. Both CoMFA and CoMSIA models were good in prediction of activity of external set molecules Different molecules were designed based on 3D QSAR studies, pharmacophore modeling and knowledge based SAR. These molecules contained mercaptopurine ring as core structure. They were docked on Aurora Kinase-A protein. Docking results suggest comparitive docking score compared to Tozasertib. 10 molecules bearing mercaptopurine ring moiety were synthesized and structures of synthesized compounds were confirmed by IR spectroscopy, Mass spectroscopy and ^{1}H NMR spectroscopy.. *In silico* pharmacokinetic and toxicities were also predicted for 10 molecules in order to explore these molecules as drug candidate. Pharmacokinetic and toxicities study reveals that there is as such no significant toxicity found in any of the molecule. Hence, it is concluded that our pharmacophore model, model 5 is able to identify new hits from different chemical databases and does not give only potent molecules but also having good pharmacokinetic properties which may act as good leads against cancer.

CHAPTER-12

REFERENCES

1. Mohammad Neaz Morshed: Computational approach to the identification of novel Aurora-A inhibitors, Bioorganic & Medicinal Chemistry, 19, 2011, 907–916

2. Barré, F., Chermann, J. S.; Rey, P.; Nugeyre, M. T.; Chamaret, S.; Gruest, J.; Dauguet, C.; Blin, C.; Vezinet, F.; Rouzioux, C.; Rozenbaum, W.; Montagnier, L. Isolation of a T-lymphotropic retrovirus from a patient at risk for acquired immune deficiency syndrome (AIDS). Science 1989, 220, 868-871.

3. Gottlieb, M. S.; Schroff, R.; Schranker, H. M. Pneumocystis carinii pneumonia and mucosal candidiasis in previously healthy homosexual men: evidence of a new acquired cellular immunodeficiency. N. Engl. J. Med. 1981, 305, 1425-31.

4. Bhatt, H.G., Patel, P.K., Pharmacophore Modeling, Virtual Screening and 3D-QSAR Studies of 5-tetrahydroquinolinylidine Aminoguanidine Derivatives as Sodium Hydrogen Exchanger Inhibitors. Bioorg. Med. Chem. Lett. **2012**, 22, 3758-3765.

5. Zhao, Ligand-based pharmacophore model of N-Aryl and N-Heteroaryl piperazine, 1A-adrenoceptors antagonists using GALAHADJournal of Molecular Graphics and Modelling for Aurora kinase inhibitors, **2010**, 29 , 126–136

6. Sugunadevi Sakkiah, Identification of critical chemical features for Aurora kinase-B inhibitors using Hip-Hop, virtual screening and molecular docking, 985 , **2011**, 14–26

7. Barreca, M. L.; Ferro, M.; Rao, A.; Luca, L. D.; Maria, M. J.; Debyser, M. Z.; Chimirri, A. Pharmacophore-Based Design of HIV-1 Integrase Strand-Transfer Inhibitors. J. Med. Chem. **2005**, 48, 7084-7089

8. Khanfar, M. A.; Asal, B. A.; Mudit, M.; Kaddoumi, A.; Sayed, K. A. The marine natural-derived inhibitors of glycogen synthase kinase-3b phenylmethylene hydantoins: In vitro and in vivo activities and pharmacophore modeling. Bioorg. Med. Chem. Lett. **2009**, 17, 6032-6039.

9. Vadivelan, S.; Sinha, B. N.; Rambabu, G.; Boppana, K.; Jagarlapudi, S. A. Pharmacophore modeling and virtual screening studies to design some potential histone deacetylase inhibitors as new leads. J. Mol. Graphics Model. **2008**, 26, 935–946.

10. Bandgar, B. P.; Gawande, S. S.; Bodade, R. G.; Gawande, N. M.; Khobragade, C. N. Synthesis and biological evaluation of a novel series of pyrazole chalcones as anti-inflammatory, antioxidant and antimicrobial agents. Bioorg. Med. Chem.**2009**, 17, 8168-8173.

11. Pignatello, R.; Intravaia, V. D.; Puglisi, G. A calorimetric evaluation of the interaction of amphiphilic prodrugs of idebenone with a biomembrane model. Journal of Colloid and Interface Science. **2006**, 299, 626–635

12. Cabrera CM, Identity tests: Determination of cross contamination. Cytotechnology; **2006**; 51: 45–50

13. Bernas T, Dobrucki. Mitochondrial and nonmitochondrial reduction of MTT: interaction of MTT with TMRE, JC-1, and NAO mitochondrial fluorescent probes. J. Cytometry; 1; **2002**, 47(4): 236-42.

14. Banks-Schlegel SP, Intermediate filament and cross-linked envelope expression in human lung tumor cell lines. Cancer Res. 45: **1985**, 1187-1197

15. Bruce A. Chabner, In Defense of Cell-Line Screening, Journal of the National Cancer Institute; **1990**, 82(13).

16. Bussey KJ, Integrating data on DNA copy number with gene expression levels and drug sensitivities in the NCI-60 cell line panel. Mol Cancer Ther; **2006**,5: 853-67.

17. Cabrera CM et al., Identity tests: Determination of cross contamination. Cytotechnology; **2006**, 51: 45–50.

18. Canavan TP, Doshi NR (2000). "Cervical cancer.".Am Fam Physician 61 (5): 1369–76.PMID 10735343.

19. Chatterjee R. (2007). Cell biology. Cases of mistaken identity. Science; 315: 928–931.

20. Cory AH, Owen TC, Barltrop JA, Cory JG (1991). "Use of an aqueous soluble tetrazolium/formazan assay for cell growth assays in culture". Cancer communications; 3(7): 207–12.

21. Sybyl-X 1.3, http://www.tripos.com, St. Louis, MO, **2010.**

22. GALAHAD,. Tripos, St. Louis, MO; http://www.tripos.com/.

23. Meng, X.Y.; Zhang, H. K.; Mezei, M.; Cui, M. Molecular Docking: A Powerful Approach for Structure Based Drug Discovery. Curr Comput Aided Drug Des. **2011**, 7, 146-157

24. Jorgensen, W.L. The many roles of computation in drug discovery. *Science*, **2009**, *303*, 1813-1818

25. Kitchen, D.B.; Decornez, H.; Furr, J.R.; Bajorath, J. Docking and scoring in virtual screening for drug discovery: methods and applications. *Nat. Rev. Drug Discov.,* **2010**, *3*, 935-949.

26. Zhang, J.; Pan, X., Wang, C., Wang, F., Li, P., Xu, W., He, L. Pharmacophore modeling, 3D-QSAR studies, and in-silico ADME prediction of pyrrolidine derivatives as neuraminidase inhibitors. *Chem Biol Drug Des.* **2012**, 79, 353-359.

27. Lee, K.; Jeong, W.; Kim, Y. Pharmacophore modeling and virtual screening studies for new VEGFR-2 kinase inhibitors. *Eur. J. Med. Chem.* **2010**, *45*, 5420-5427

28. Pirhadi, S.; Ghasemi, J. B. 3D-QSAR analysis of human immunodeficiency virus entry-1 inhibitors by CoMFA and CoMSIA. *Eur. J. Med. Chem.* **2010**, *45*, 4897-4503

29. Davood azarifar, Acetic acid-promoted condensation of *o*-phenylenediamine with aldehydes into 2-aryl-1-(arylmethyl)-1*H*-benzimidazoles under microwave irradiation*J. Serb. Chem. Soc. 75* (9) 1181–1189 (**2010**).

30. Synthesis and characterization of 9-methyl-2-morpholin-4-yl-8-substituted phenyl-1H-purine derivatives using polyphosphoric acid (PPA) as an efficient catalyst Tetrahedron Letters 52 (**2011**) 5521–5524.

31. Simona Bindi , Thieno[3,2-c]pyrazoles: A novel class of Aurora inhibitors with favorableantitumor activityBioorganic & Medicinal Chemistry 18 (**2010**) 7113–7120

32. Duman R. K.; Heath R. T.; Bose R. N. FEBS Letters, **1999**, 455, 49-54.

33. Nicholas Keen & Stephen Taylor, Nature Reviews Cancer, **2004**

34. Rıhova, B. 2-(R)-benzylaminoquinoxalines as non classical antifolate agents. Journal of Controlled Release, **2000,** 13, 241–261.

35. Schott, H. Quinoxaline analogues of TMQ and 10-propargyl-5,8-dideaza folic acid and its precursors. Bioorganic & Medicinal Chemistry, **2009**, 17, 6824–6831

36. Szumilak, M. Pirrolo[1,2-a]quinoxalines analogues of antifolic trimetrexate andMethotrexate. European Journal of Medicinal Chemistry, **2010**, 45, 5744-5751.

37. Bhupender S. European Journal of Medicinal Chemistry, 2011, 11, 1-6.

38. Rıhova, B., Journal of Controlled Release, 2000, 13, 241–261

39. Wei, J.; Li, H.; Qu, W.; Gao, Q. Molecular docking study of A3 adenosine receptor antagonists and pharmacophore-based drug design. *Neurochemistry International* **2009***, 5, 637–642.

40. Jinyi, X. Recent advances in the synthesis of antibacterial quinolones. Bioorganic & Medicinal Chemistry Letters, **2008**, 18, 4741–4744.

41. . Krauth, F. Status of the NCI preclinical antitumor drug discovery screen. Bioorganic & Medicinal Chemistry, **2010**, 18, 1816–1821.

42. Rang, H. P.; Dale, M. M.; Ritter, J. M.; Flower, R. J. Text Book of Pharmacology, **2007**, 6th edition, 722-731

43. Bolanos-garcia V M. Aurora kinases. The International Journal of Biochemistry & Cell Biology 37 (**2005**) 1572–1577

44. Gautschi O, Heighway J, Mack PC, Purnell PR, Lara PN Jr, Gandara DR Clin Cancer Res. **2008** Mar 15; Aurora kinases as anticancer drug targets, 14(6):1639-48,

45. Giet R, Prigent C. Aurora/Ipl1p-related kinases, a new oncogenic family of mitotic serine-threonine kinases. Journal of Cell Science 112 (**1999**) 3591–3601.

46. Ma C, Cummings C, Liu XJ (March 2003). "Biphasic activation of Aurora-A kinase during the meiosis I- meiosis II transition in Xenopus oocytes". Mol. Cell. Biol. 23 (5): 1703–16. doi:10.1128/MCB.23.5.1703-1716.2003

47. Marumoto T, Honda S, Hara T, Nitta M, Hirota T, Kohmura E, Saya H (December **2003**). "Aurora-A kinase maintains the fidelity of early and late mitotic events in HeLa cells". J. Biol. Chem. 278 (51): 51786–95.

48. Ouchi M, Fujiuchi N, Sasai K, Katayama H, Minamishima YA, Ongusaha PP, Deng C, Sen S, Lee SW, Ouchi T (May **2004**). "BRCA1 phosphorylation by Aurora-A in the regulation of G2 to M transition". J. Biol. Chem. 279 (19): 19643–8.

49. Roles of Aurora Kinases in Mitosis and Tumorigenesis Jingyan Fu, Minglei Bian, Qing Jiang and Chuanmao Zhang Mol Cancer Res January **2007** 5; 1-10

50. Wolber, G.; Langer, T. LigandScout: 3D Pharmacophores derived from protein-bound ligands and their use as virtual screening filters. J. Chem. Inf. Comput. Sci**. 2004**, 18, 147-165

51. Curhan, S. G.; Eavey, R.; Shargorodsky, J.; Curhan, G. C. "Analgesic Use and the Risk of Hearing Loss in Men". *The American Journal of Medicine,* **2011**, *123 (3),*231–237.

52. Venkatesh, P.; Pandeya, S.N. "Synthesis, characterization and anti-inflammatory activity of some 2-amino benzothiazole derivatives". *International Journal of ChemTech research,* **2009**, *1(4)*, 1354-1358

53. Sachan, S.; Tiwari, S.; Pandey, V. "Structure-Based Optimization of Benzothiazole Derivatives as Potent Anticancer Agents: A QSAR/QSPR Approach", *Int. J. of Pharm. & Life Sci. (IJPLS),* **2011**, *Vol. 2, 5*, 746-750.

54. Patel, Y.; Gillet, V. J.; Bravi, G.; Leach, A. R. Pharmacophore Perception, Development and Use in Drug Design, *J. Comput.-Aided Mol. Des.,* **2002**, *16*, 653–681.

55. Jorgensen, W.L. The many roles of computation in drug discovery. *Science*, **2004**, *303*, 1813-1818.

56. Jorgensen, W.L. The many roles of computation in drug discovery. *Science*, **2004**, *303*, 1813-1818.

57. Zhang, J.; Pan, X., Wang, C., Wang, F., Li, P., Xu, W., He, L. Pharmacophore modeling, 3D-QSAR studies, and in-silico ADME prediction of pyrrolidine derivatives as neuraminidase inhibitors. *Chem Biol Drug Des.* **2012**, 79, 353-359.

58. Ajala, A. O.; Okoro, C. O. CoMFA and CoMSIA studies on fluorinated hexahydropyrimidine derivatives. *Bioorg. Med. Chem. Lett.* **2012**, *21,* 7392-7398.

59. Bandgar, B. P.; Gawande, S. S.; Bodade, R. G.; Gawande, N. M.; Khobragade, C. N. Synthesis and biological evaluation of a novel series of pyrazole chalcones as anti-inflammatory, antioxidant and antimicrobial agents. *Bioorg. Med. Chem.***2009***, 17,* 8168-8173

60. Pignatello, R.; Intravaia, V. D.; Puglisi, G. A calorimetric evaluation of the interaction of amphiphilic prodrugs of idebenone with a biomembrane model. *Journal of Colloid and Interface Science.* **2006**, *299*, 626–635.

61. www.admetexp.org as accessed on 5th May, 2013.

CHAPTER-2

LITERATURE

REVIEW

2. LITERATURE REVIEW

Literature review was done both , in the fields of computational chemistry and synthetic approaches which were used in development and discovery of Aurora Kinase- A inhibitors. Literature survey was carried out for Pharmacophore modeling, Virtual screening, 3D Qsar approaches, Molecular approaches as well as various synthetic methods.

2.1 Morshed. *et.al* reported the development of a new five dimensional pharmacophore model for Aurora kinase A inhibitors as shown in **Fig 2.1** which led to the discovery of some novel derivatives using Hypogen. The best pharmacophore hypothesis consists of two hydrophobic regions, 2 hydrogen bond acceptors, one aromatic ring and two hydrogen bond donors. [26]

2.2 Barreca *et al.* described pharmacophore mapping of diketoacid derivatives of integrase inhibitors using HYPOGEN which conatin 4 features including one hydrophobic aromatic region, two hydrogen-bond acceptors, and one hydrogen-bond donor. The resulting pharmacophore model guided the rational design of new potent IN inhibitors.[27]
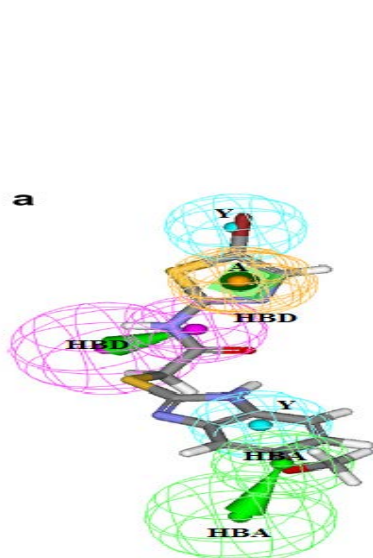

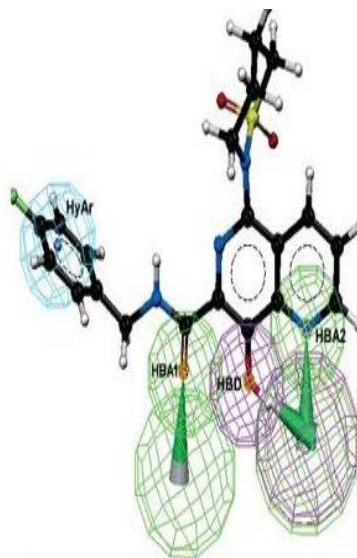**FIGURE 2.1**: **Pharmacophore modelling**   **FIGURE 2.2 : Pharmacophore Mapping**

2.3 Bhatt *et al.* generated three dimensional pharmacophore modeling of 5-Tetrahydroquinolinylidine aminoguanidine derivatives as sodium hydrogen exchanger inhibitors (SHE) using Genetic Algorithm Similarity Program (GASP) method. The best pharmacophore model contained 2 donor sites. 2 acceptor atoms and 2 hydrophobic regions **(Fig 2.3).** The best pharmacophore model was used for substructure searching and virtual screening. 3D-QSAR, CoMFA and CoMSIA study were performed on same compounds.[28]
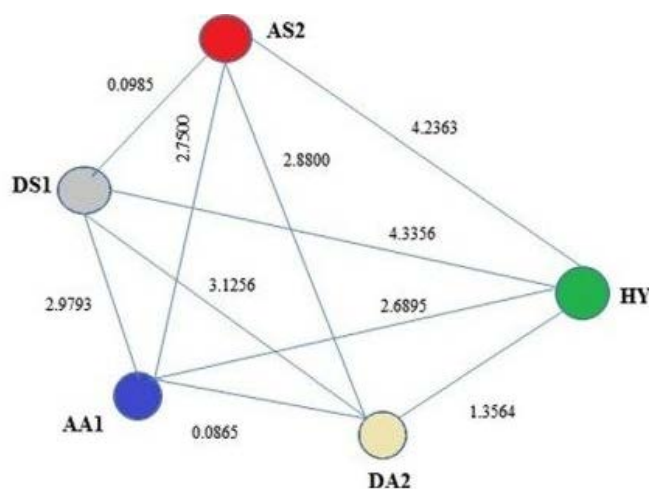
FIGURE 2.3 : **Pharmacophore Model using GASP**

2.4 Zhao *et.al.* developed Ligand-based pharmacophore models of N-Aryl and N-Heteroaryl piperazine - 1A-antagonists using two separate training sets. Pharmacophore models were generated using the flexible align method within the GALAHAD module, implemented in SYBYL8.1 software **(Fig. 2.4).** The most significant pharmacophore hypothesis, characterized by the conflicting demands of maximizing pharmacophore consensus, maximizing steric consensus, and minimizing energy, consisted of one positive nitrogen center, one donor atom center, two acceptor atom centers, and two hydrophobic groups.[29]
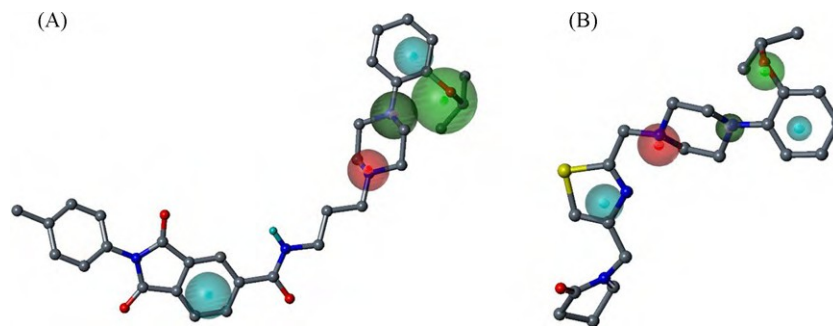
FIGURE 2.4 : **Pharmacophore mapping using GALAHAD**

2.5 Khanfar *et al.* derived three dimension pharmacophore model to discover GSK-3β inhibitor using DISCOtech modeule of SYBYL. **(Fig 2.5)** The generated pharmacophore model was validated using in-house database of active and inactive GSK-3β inhibitors. Molecular docking study was also within the binding pocket of glycogen synthase kinase-3β (GSK-3β). [30]

FIGURE 2.5 : **Pharmacophore Mapping using DISCOtech**

2.6 Sakkiah *et. al.* performed studies to find the selective chemical features for Aurora kinase-B inhibitors using the potent methods like Hip-Hop**,(Fig 2.6a)** virtual screening, homology modeling, molecular dynamics and docking. The best hypothesis, Hypo1 was

validated toward a wide range of test set containing the selective inhibitors of Aurora kinase-B. Homology modeling and molecular dynamics studies were carried out to perform the molecular docking studies. The best hypothesis Hypo1 was used as a 3D query to screen the chemical databases. The screened molecules from the databases were sorted based on ADME and drug like properties. The selective hit compounds were docked and the hydrogen bond interactions with the critical amino acids present in Aurora kinase-B were compared with the chemical features present in the Hypo1 [31]
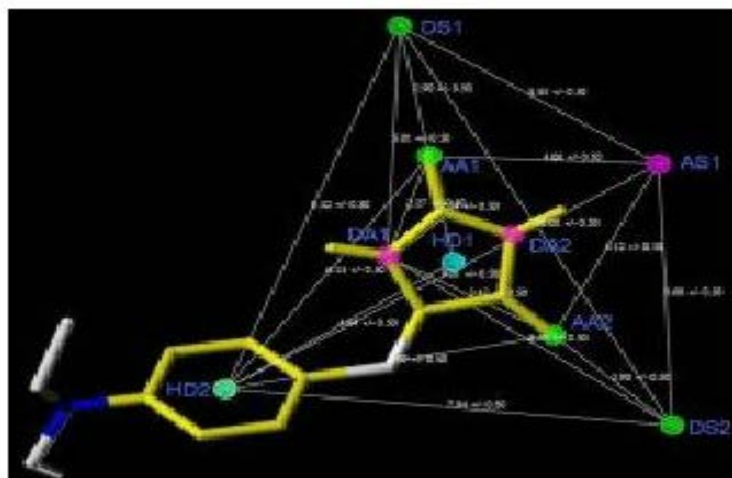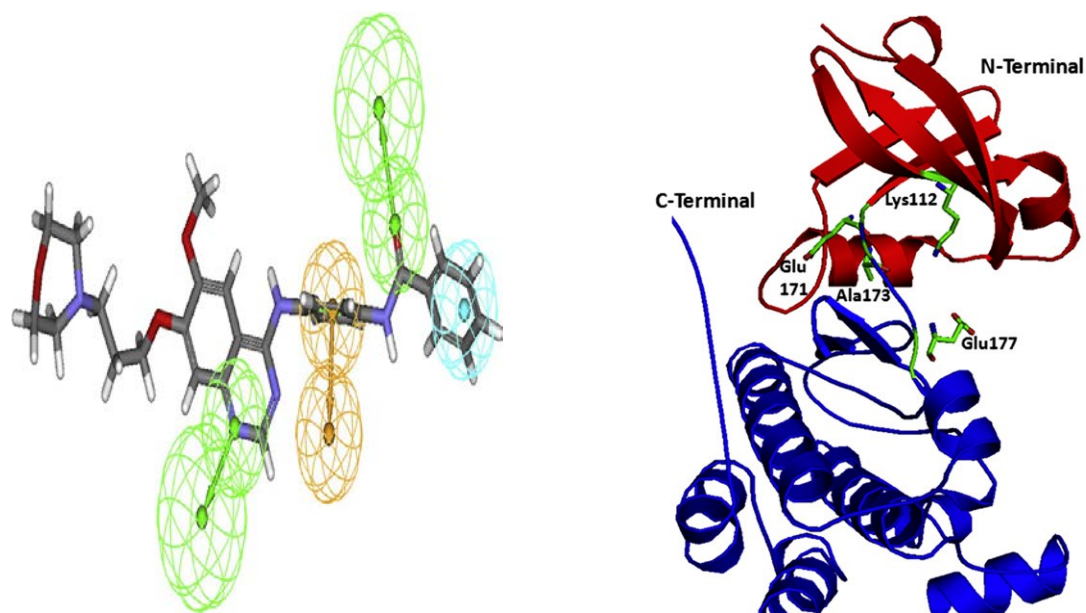

FIGURE 2.6 (a) : Pharmacophore mapping using HIP-HOP
             (b) Docking studies on Aurora Kinase

2.7. Yuan *et al*. described pharmacophore model of piperidine-based analogues of cocaine at dopamine transporter using Genetic Algorithm Similarity Program (GASP) method. (Fig 2.7) The flexible superposition of all studied compounds was performed for each pharmacophore model using the FlexS algorithm. All sets of the overlaid structures with the top-ranked conformers were used for CoMFA modeling. A successful strategy of pharmacophore-based alignment of the fittest conformers was designed and applied to determine the details of the

DAT binding site in proximity to the 3R-substituent of the piperidine-based analogues of cocaine.[32]
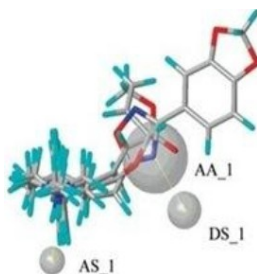
FIGURE 2.7: Pharmacophore modelling using GASP

2.8 Li *et. al*. designed, synthesized and evaluated a series of N,1,3-triphenyl-1H-pyrazole-4-carboxamide derivatives for their potential antiproliferation activity and Aurora-A kinase inhibitory activity. Docking simulation was performed to position various compounds into the active site of Aurora-A kinase, in order to get the probable binding model for further study**.(Fig 2.8)** The results of Westernblot assay demonstrated that compound 10e possessed good Aurora-A kinase inhibitory activity against HCT116 to develop potential anti cancer newer agents.[33]
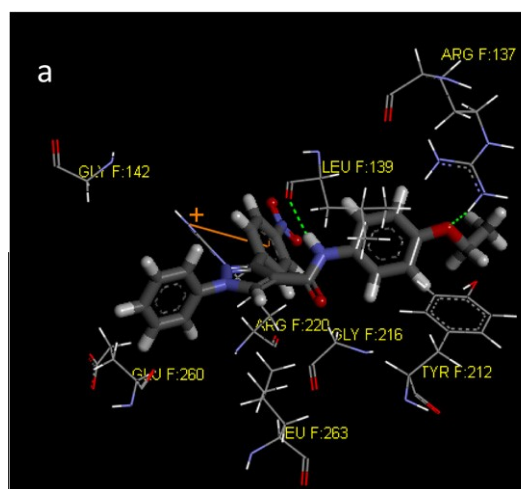
FIGURE 2.8: **Docking Studies on Aurora Kinase-A**

2.9 Vadivelan.s.*et.al* used pharmacophore modelling and virtual screening to design novel histone deacetylase inhibitors. They used 20 molecules of 3 different chemical groups, a generated pharmacophore **(Fig 2.9)** was used as a query in substructure searching of NCI database. A total of 4638 molecules from a pool of 2,38,819 molecules were identified as hits while 297 molecules were indicated as highly active. This type of Similarity analysis would prove to be efficient not only for lead generation but also for lead optimization. [34]
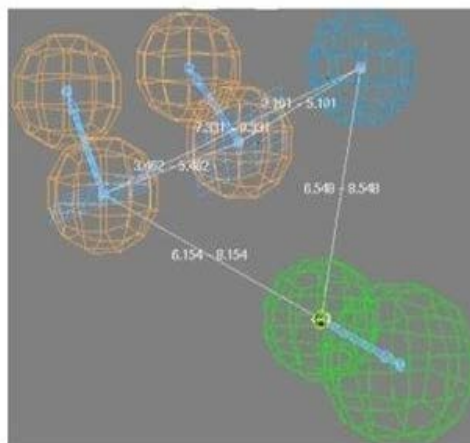
FIGURE 2.9: **Pharmacophore model used for virtual sreening**

**2.10 Coumar** *et.al.* identified tricyclic 6,7-dihydro-4H-pyrazolo[1,5-a pyrrolo[3,4-d] pyrimidine-5,8-dione as a novel scaffold for Aurora kinase A inhibition through virtual screening by SAR exploration coupled with molecular modeling of 8a reveals the minimum pharmacophore requirements for Aurora kinase A inhibition.[35]

2.11 Fu *et.al* desgined four series of dihydropyrazolo [3,4-b]pyridines and benzo[4,5]imidazo[1,2-a] pyrimidines **(Fig 2.10)** and synthesized as dual KSP and Aurora-A kinase inhibitors for anti-cancer agents . This was done by introducing some fragments of Aurora-A kinase inhibitors into our KSP inhibitor CPUYL064. A total of 19 target compounds were evaluated by two related enzyme inhibition assays and a cytotoxicity assay in vitro. The results showed that some target compounds could inhibit both enzymes, and several of them showed significant inhibition activity against HCT116 cell line. [36]
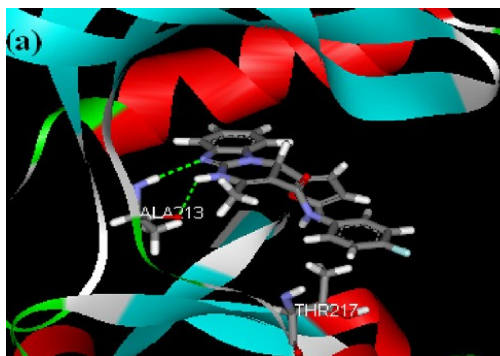
FIGURE 2.10: **Docking studies of substituted pyrimidines for carrying out anticancer activity**

2.12 Lee *et.al*. performed virtual screening to determine potent vascular endothelial growth factor receptor (VEGFR)-2 kinase inhibitors. A database of approximately 820,000 commercial compounds was used for screening, and 100 compounds were chosen as candidate VEGFR-2 inhibitors through pharmacophore modeling and docking studies. These 100 compounds were tested for their biological activities: 10 compounds were found to inhibit the enzyme, with IC50 values ranging from 10 to 1 mM. (Fig. 2.11) [37]
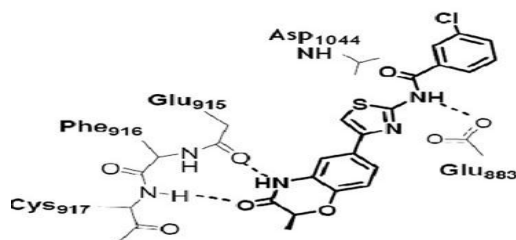
FIGURE 2.11 : **Docking studies on VEGFR-2 for anti-cancer activity**

2.13 Brazidec *et.al* performed Docking studies on the series of pyrazolopyrimidine core. The studies for this series is exemplified in (**Fig 2.12**) showing the key interactions between the compound and the ATP binding site of AKA. Two hydrogen bonds are predicted between the pyrazolopyrimidine core and the hinge region. [38]
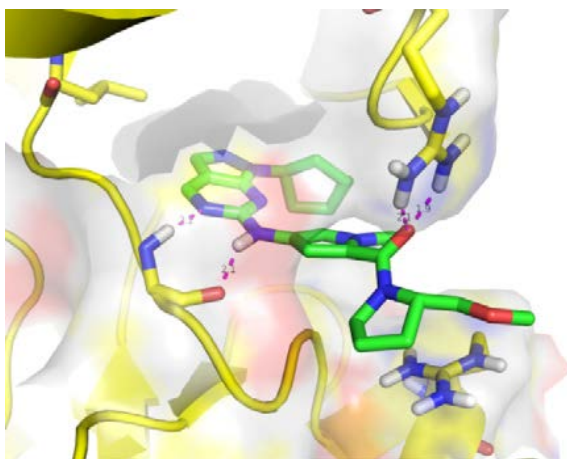
FIGURE 2.12 : **Binding pose of structure with AKA**

2.14   Talele *et.al* studied the binding modes of a known 1,4,5,6-tetrahydropyrrolo[3,4-c]pyrazole, quinazoline, pyrimidine and indolinone series of Aurora A kinase inhibitors using molecular docking and molecular dynamics (MD) simulations. Crystallographic bound compound was precisely predicted by our docking procedure as evident from 0.43 A ° root mean square (rms) deviations. The structure-based drug design strategy described in this study will be highly useful for the development of new inhibitors with high potency and selectivity. [39]
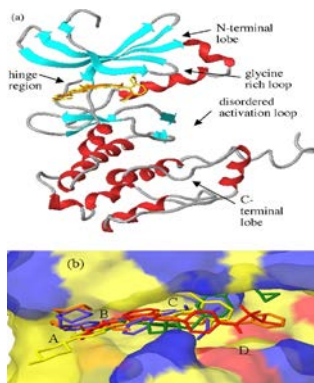
FIGURE 2.13 : Docking Interactions

2.15 Lan *et.al* carried out 3D-QSAR studies namely CoMFA, and CoMSIA on a series (48 compounds) of Aurora kinase-A inhibitors. An alignment rule for the compounds was defined using Distill. Models were validated using a data set obtained by dividing the data set into a training set and test set using hierarchical clustering. The resulting 3D CoMFA/CoMSIA contour maps provide useful guidance for designing highly active inhibitors. **(Fig 2.14)**[40]
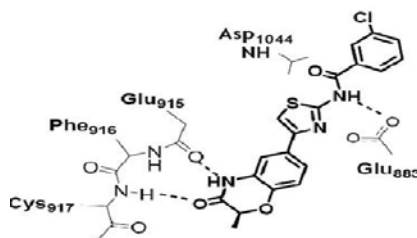
FIGURE 2.14: **Docking studies**

2.16 Yan *et.al* developed several QSAR models for predicting the inhibitory activity of 117 Aurora-A kinase inhibitors were developed. The whole dataset was split into a training set and a test set based on two different methods, (1) by a random selection; and (2) on the basis of a Kohonen's self-organizing map (SOM). Then the inhibitory activity of 117 Aurora-A kinase inhibitors was predicted using multilinear regression (MLR) analysis and support vector machine (SVM) methods, respectively. For the two MLR models and the two SVM models, for the test sets, the correlation coefficients of over 0.92 were achieved. [41]

2.17 Lan *et.al* performed 3D-QSAR and docking studies on sixty imidazo[4,5-b] pyridine derivatives as Aurora A kinase inhibitors. The CoMFA and CoMSIA models using forthy-eight molecules in the training set, gave r2 cv values of 0.774 and 0.800, r2 values of 0.975 and 0.977, respectively**.(Fig. 2.15)** [42]
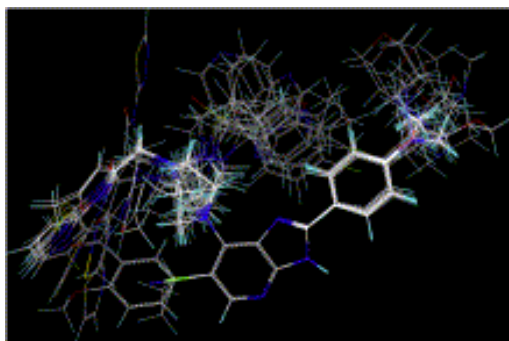
FIGURE 2.15 : **Molecular Alignment for 3D QSAR Studies**

2.18 Ajala *et.al.* developed 3D-QSAR models of a series of fluorinated hexahydropyrimidine derivatives with cytotoxic activities using CoMFA and CoMSIA The models will inspire the design and synthesis of novel hexahydropyrimidines with enhanced potency and selectivity. **(Fig. 2.16)[43]**

.
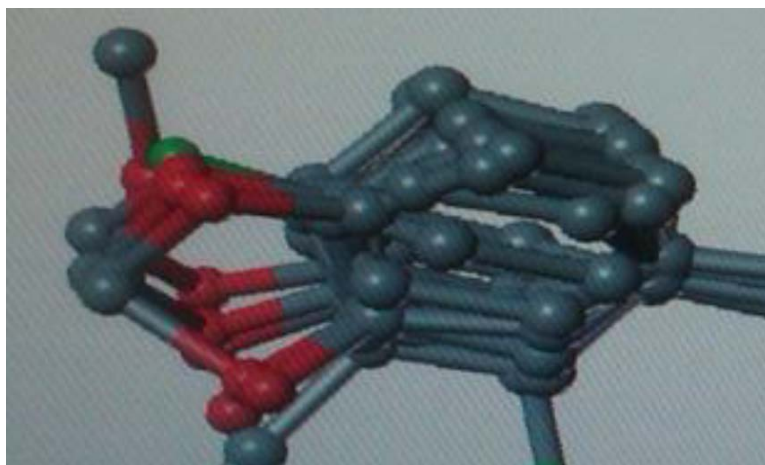
FIGURE 2.16 : **Molecular Alignment of hexahydropyrimidine derivatives**

2.19 Leng *et.al* carried out QSAR studies on imidazopyrazine derivatives as Aurora A kinase inhibitors. A combined study of molecular docking, pharmacophore modelling and 3D-QSAR was performed on a series of imidazo [1, 2-a] pyrazines as novel Aurora kinase inhibitors to gain insights into the structural determinants and their structure-activity relationship. An ensemble of conformations based on molecular docking was used for PHASE pharmacophore studies. The developed best-fitted pharmacophore model was validated by diverse chemotypes of Aurora A kinase inhibitors and was consistent with the structural requirements for the docked binding mechanism. Subsequently, the pharmacophore-based alignment was used to develop PHASE and comparative molecular similarity indices analysis (CoMSIA) 3D-QSAR models. The best CoMSIA model showed good statistics (q (2)= 0.567, r (2)= 0.992), and the predictive ability of the model was validated using an external test set of 13 compounds giving a satisfactory prediction. Based on the PHASE and CoMSIA 3D-QSAR results, a set of novel Aurora A inhibitors were designed that showed excellent potencies.[44]

2.20 Moriarty *et.al* synthesized   new class of Aurora-A inhibitors, which have been identified based on the 2-amino-pyrrolo[2,3-d]pyrimidine scaffold and also contain n-methyl piperazine moiety**.(Fig 2.17**) [45]

FIGURE 2.17 : Identification of new scaffold for synthetic work

2.21 García *et.al* carried out the Mitsunobu reaction between (RS)-2,3-dihydro-1,4-benzoxathiin-3-methanol and the heterocyclic bases 6- chloro-, 2,6-dichloro, and 6-bromo-purines under microwave-assisted conditions, a formal 1,4-sulfur migration takes place through two consecutive oxyranium and episulfonium rings, giving rise to the corresponding (RS)-9-(2,3-dihydro-1,4-benzodioxin-3-ylmethyl)-9H-purine derivatives (41). The induction of the G2/M cell cycle arrest and apoptosis by the three most active compounds was observed in human breast cancer cells.[46]
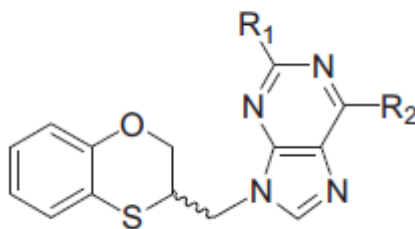
(41)

2.22 Hughes *et.al* synthesized a novel series of 7-[1H-indol-2-yl]-2,3-dihydro-isoindol-1-ones (42) designed to be inhibitors of VEGF-R2 kinase was synthesized and found to potently inhibit VEGF-R2 and Aurora-A kinases. The structure-based design, synthesis, and initial SAR of the series are discussed by Terry V. Hughes et. al.[47]
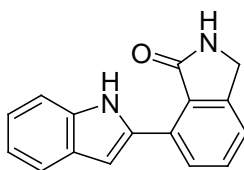
(42)

2.23 Sadanandam *et.al*. demonstrated the synthesis of various purine derivatives through the coupling of N4-methyl-2-morpholin-4-yl-pyrimidine-4,5-diamine (43) with various aldehydes by using polyphosphoric acid (PPA) as an efficient catalyst in DMF at reflux temperature. The PPA catalyst gave better yields (70–85%) in short reaction times (45–60 min). [48]

(43)
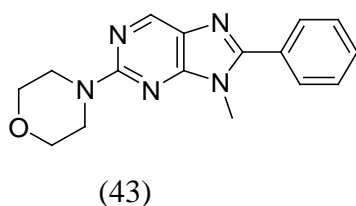
2.24 Azarifar *et.al*. developed an efficient and simple procedure was developed for the green synthesis of various 2-aryl-1-(arylmethyl)-1H-benzimidazoles in high yields by acetic acid-promoted condensation of o-phenylenediamine with aldehydes in air under microwave irradiation and transition metal catalyst-free conditions**.(Fig 2.18)** [49]
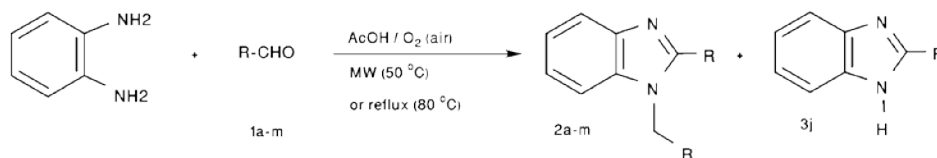
FIGURE 2.18: **Procedure for Synthetic scheme**

2.25 Sattar.*et.al*. synthesized a series of novel purine and pyrimidine derivatives (44) and biologically evaluated for their in vitro anti-CDK2/cyclin A3 and antitumor activities in Ehrlich ascites carcinoma (EAC) cell based assay. [50]
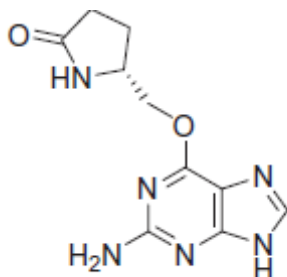
(44)

2.26 Bindi *et.al* synthesized several Aurora kinase inhibitors **(Fig 2.19)** and tested in vitro against three cancer cell lines, HCT-116 cell line. All tested compounds can serve as novel templates for the anticancer chemotherapy and can serve as new leads in cancer chemotherapy. [51]
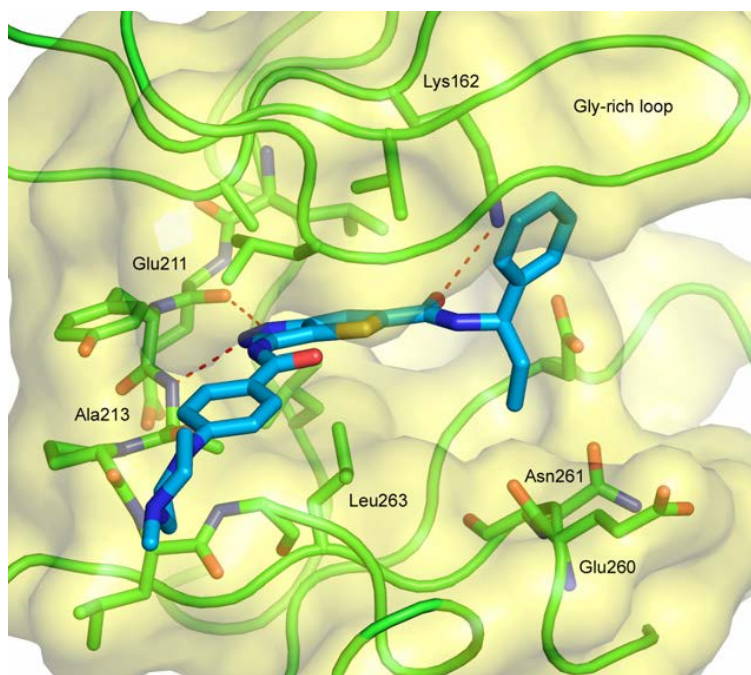
FIGURE 2.19 : Docking Interactions

2.27 Zatloukal *et.al* evaluated several inhibitors of cyclin-dependent kinases (CDKs), including the 2,6,9-trisubstituted purine derivative roscovitine, in clinical trials as potential anticancer drugs. The most potent compounds were investigated further to assess their ability to influence cell cycle progression, p53-regulated transcription and apoptosis. All the observed biological effects were consistent with inhibition of CDKs involved in the regulation of cell cycle and transcription. (Fig 2.20) [52]
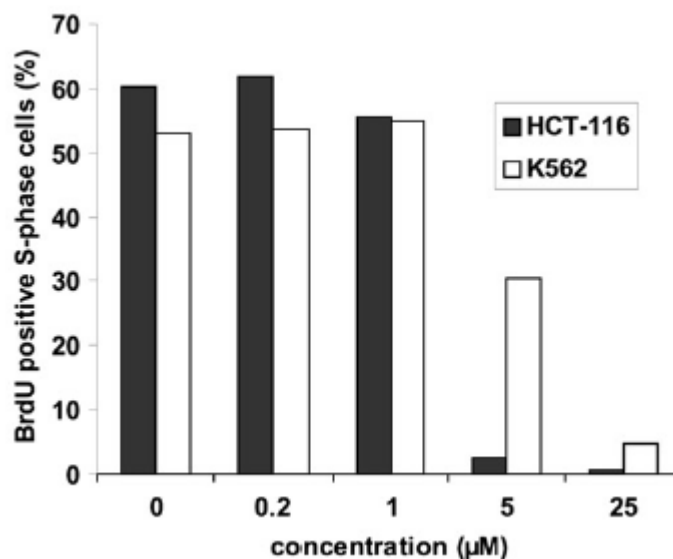
FIGURE 2.20 : **Evaluation of Biological Activity**

2.28 Chauhan *et al.* synthesized several pteridine and tested in vitro against three cancer cell lines, MCF7 (breast), NCI-H460 (lung) and SF-268 (CNS). All tested pteridines can serve as novel templates for the anticancer chemotherapy and can serve as new leads in cancer chemotherapy. [53]

(45)
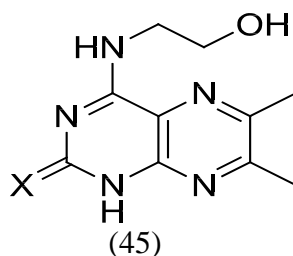
2.29 Bandgar *et al.* confirmed the structures through in silico drug relevant properties (HBD, HBA, PSA, c Log P, EHOMO and ELUMO) and further sassured that the compounds are potential lead compounds for future drug discovery study. Toxicity of the compounds was evaluated theoretically using OSIRIS property explorer and revealed to be nontoxic. [54]

2.30 Macias *et al.* calculated pharmacokinetic parameters and studied toxicity profile of benzoxazepines derivatives. Lipophilicity and solubility were calculated which are crucial in early drug discovery process. [55]

2.31 Pignatello *et al.* calculated clogP antioxidant drug idebenone to determine Lipophilicity and modified it to improve bioavailability. [56]

CHAPTER-3

AIM AND OBJECTIVES

3 AIM AND OBJECTIVES

- Development of inhibitors against Aurora kinases as anticancer molecules gained attention because of the facts that aberrant expression of these kinases leads to chromosomal instability and derangement of multiple tumor suppressor. A new approach for inhibiting cancer growth that shows great promise for structure-based drug development is targeting enzymes central to cellular mitosis.

- Hence, Aurora kinase A has proved to be an emerging target for cancer therapy. The aim of this project is to design and synthesise novel compounds that could act as Aurora kinase A inhibitors..

- The research include the following objectives:

➢ To carry out **literature survey** of various computational and synthetic approaches to design and synthesis novel anti-cancer agents.

➢ To derive a ligand based pharmacophore model from diverse class of Aurora-A inhibitors by using **GALAHAD**. Virtual screening of these compounds by applying Lipinski's rule of five to filter drug like compounds.

➢ To perform **3D QSAR (COMFA and COMSIA)** on a selected series of compounds by using Sybyl X1.3

➢ To **design molecules** by applying both Pharmacophore and knowledge based structure based relationship approaches which might act as potential anti-cancer agents.

- ➢ To perform docking study of designed molecules by using **Surflex- dock** module of Sybyl X1.3. To establish the method of synthesis for best compounds based on docking result.

- ➢ To confirm the structure of the synthesised compounds by **FT-IR, ^{1}H NMR, Mass spectroscopy**.

- ➢ To **evaluate** the compound for their anti-cancer activity.

- ➢ To predict In silico pharmacokinetic and toxicities study using **admetSAR.**

CHAPTER-4

PHARMACOPHORE

MODELING

4. Pharmacophore Modeling
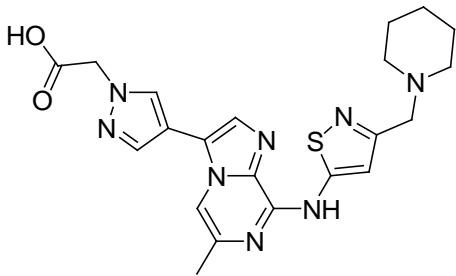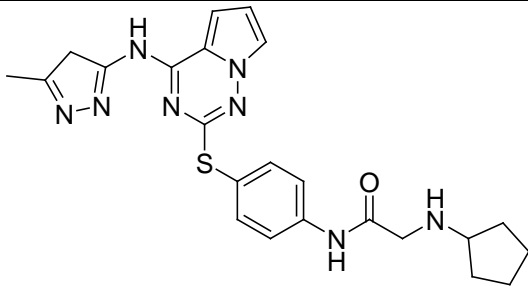
A pharmacophore is an abstract description of molecular features which are necessary for molecular recognition of a ligand by a biological macromolecule. A pharmacophore model explains how structurally diverse ligands can bind to a common receptor site. Furthermore pharmacophore models can be used to identify through denovo design or virtual screening novel ligands that will bind to the same receptor. Sometimes, it is very time consuming and costly to assay every compound in order to find some initial HITS. Thus, there needs to be a logical process for identifying compounds with some probability that any one of them might be a useful inhibitor. Pharmacophore modeling is the method of choice for the first round of compound selection. This ability of a pharmacophore model is used to find new classes of inhibitors when one class is known. Pharmacophore modeling can thus be useful in such cases. Thus a pharmacophore can be defined as "an ensemble of steric and electronic features that is necessary to ensure the optimal supramolecular interactions with a specific biological target and to trigger (or block) its biological response".
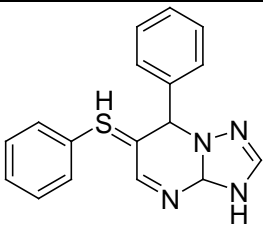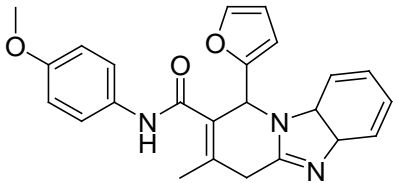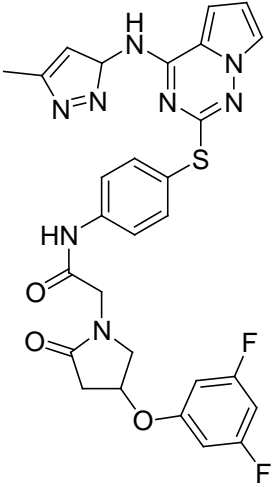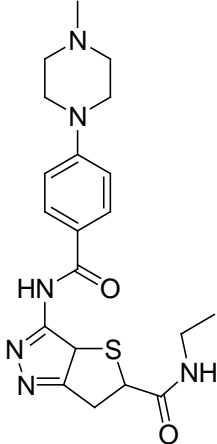
4.1 Methods and materials:
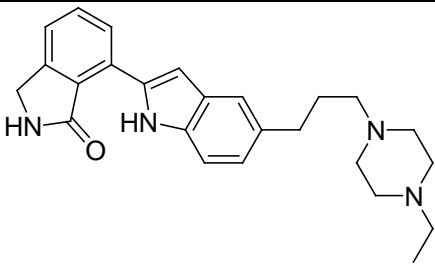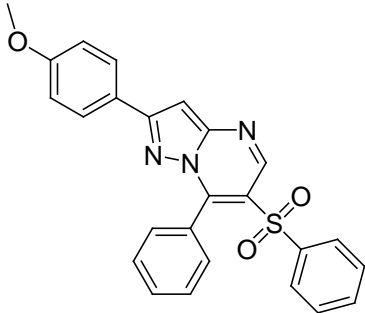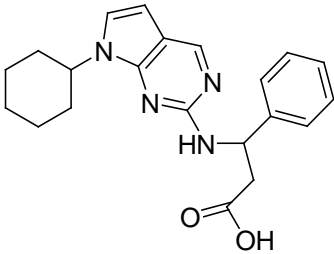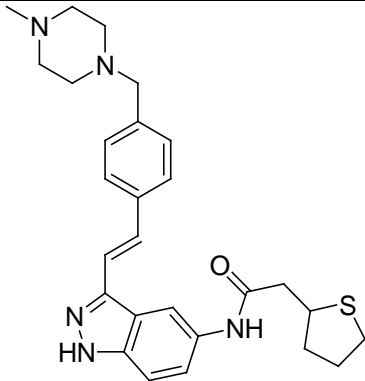
The pharmacophore mapping and database searching were performed using the SYBYLX 1.3 software from Tripos Inc., St. Louis, MO, USA. All the compounds were sketched using SKETCH function of SYBYL X 1.3. Partial atomic charges were calculated by the Gasteiger Huckel method and energy minimizations were performed using the Tripos force field with a distance-dependent dielectric and the Powell conjugate gradient algorithm convergence criterion of 0.01 kcal/mol Å. Eleven molecules (46-56) were selected to generate twenty pharmacophore models using GALAHAD module. Chemical structures, chemical class and activity are shown in **Table-1**. GALAHAD (Genetic Algorithm with Linear Assignment for Hypermolecular Alignment of Datasets) aligns a set of molecules that share a common mode of biological activity and develops corresponding pharmacophore models. Using a sophisticated genetic algorithm and a multi-objective scoring function, GALAHAD takes into account energetics, steric similarity, and pharmacophoric overlap, while accommodating

conformational flexibility, ambiguous stereochemistry, alternative ring configurations, multiple partial match constraints, and alternative feature mappings among molecules. Pharmacophore models are returned as hypermolecules, which contain information from every molecule in the training set, as well as a 3D search query that can be used to probe databases for new structures that match the model. All parameters were kept as default except population size (125), mutation weight (96), fitness increment (0.02) and number of alignment (10).

Table 1: Training set molecules used to develop Pharmacophore Hypothesis for Aurora Kinase-A inhibitors: [58-67]

.Compound No.	Structure	Class	Activity
46		Pyrazine	1828 nM
47		Triazene	553 nM

48		Triazolo pyrimidine	121 nM
49		Triazene	0.037μM
50		Triazene	426 nM
51		Carboxamide	0.048μM

52		Isoindoline	54 µM
53		Pyrimidine	0.025 µM
54		Pyrimidine	84 µM
55		Indazole	222 nM

56		Pyrrole	166 nM

4.2 Results and Discussion

Results of pharmacophore hypothesis generated by GALAHAD are shown in table-2. Model 6 was considered the best model and used for further analysis. There are 12 columns in the MSS result spreadsheet. The first three are model properties generated during post-processing, the next five are model scores components from the genetic algorithm, and the last four are the scores for individual ligands within each model. Results of pharmacophore models generated is mainly evaluated on the basis of following information:

➢ SPECIFICITY : Specificity is a logarithmic indicator of the expected discrimination of each query, based on the number of features it contains, their allotment across any partial constraints and the degree to which the features are separated in space. This value should be at least 4-5.

➢ N_HITS : The actual number hit. A negative number indicates that no ligands hit the model query.

➢ FEATS: Total number of features in the model query.

➢ PARETO: The values in this column indicate the Pareto rank of the each model. A value of) indicates that no one model is superior to any other by all four of the criteria laid out in the last 4 columns.

➢ ENERGY: The total energy of the model.

Model 5 is considered as the best model as it has higher specificity compared to remaining 19 models. A two dimensional and three dimensional pharmacophore hypothesis are shown in figure--- and -- respectively. The best model contained 2 donor sites, 1 acceptor atom and 2 hydrophobic regions. These features for inhibitory activity were also highlighted through 3D space modelling approach which explored importance of critical inter-feature distances among the features for the Aurora-A kinase activity.

Table 2: Result of Pharmacophore Hypothesis Generated by GALAHAD

Model No.	Specificity	No. of Hits	Features	Pareto	Energy
1	2.4360	9	4	0	17.6300
2	2.6240	10	4	0	43.6200
3	4.7920	9	7	0	39.4000
4	3.7490	9	3	0	67.0000
5	**4.8900**	**10**	**5**	**0**	**526.7600**
6	3.9700	10	5	0	56.5400
7	4.1390	11	5	0	7039.7900
8	3.2450	8	4	0	35.4900
9	3.4100	7	6	0	32.2000
10	3.5840	10	6	0	41.5900
11	2.3250	9	7	0	5229.2900

12	2.3740	6	2	0	1824.7200
13	3.9030	8	5	0	33.0300
14	3.7880	9	7	0	53311.1602
15	1.9590	7	2	0	3459.8301
16	2.8770	8	4	0	20.1200
17	3.1400	10	4	0	186.4400
18	3.2580	11	7	0	156.9300
19	2.4770	9	4	0	37.9500
20	3.1030	10	5	0	4481.4902

FIGURE 4.1 : Three Dimension Pharmacophore Hypothesis Generated by GALAHAD
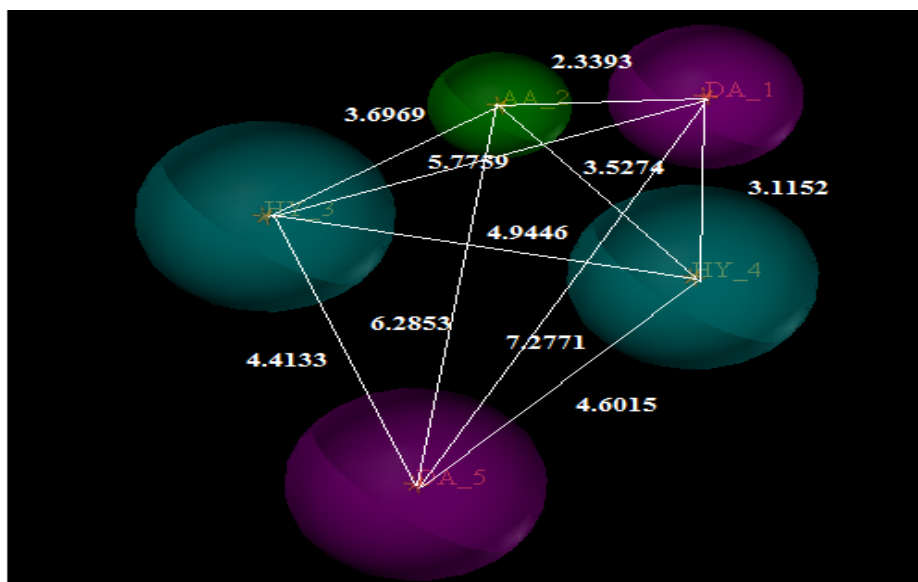
FIGURE 4.2 : Two Dimension Pharmacophore Hypothesis Generated by GALAHAD
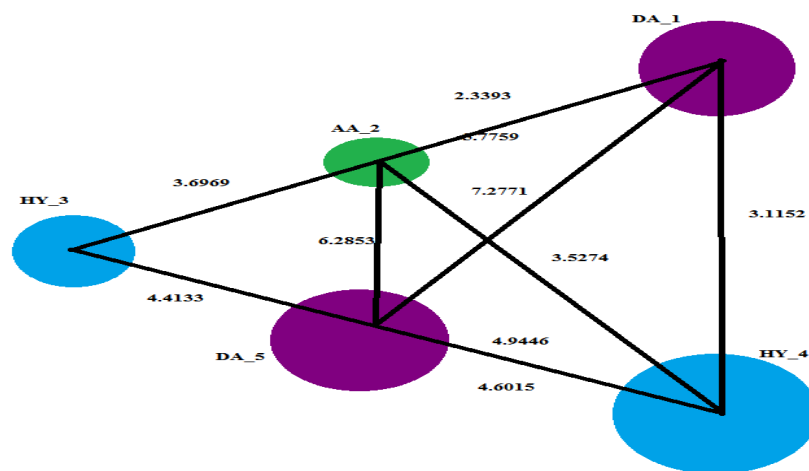
Here,

HY – Hydrophobic region

DA- Donor Atom

AA- Acceptor atom

4.3 Pharmacophore Validation

The generated pharmacophore model should be statistically significant, and should identify active compound from a database. Therefore, the derived pharmacophore was validated using following methods.

4.3.1 Screening Best Pharmacophore Model on Marketed Aurora Kinase-A inhibitors.

The model was validated by screening a database containing 6 known inhibitors. The model picked up all 4 known inhibitors including VX-680, MLN8237 and R547 giving a comparable Q_{fit} of 81.35%. These functions were performed by using UNITY module in the SYBYL X 1.3 software from Tripos Inc., St. Louis, MO, USA.

4.3.2 Screening Best Pharmacophore Model on Test Set Compounds

The model was further validated by screening a database containing 81 test inhibitors. The model picked up 39 inhibitors giving a Qfit value up to 90.1 %. These functions were performed by using UNITY module in the SYBYL X 1.3 software from Tripos Inc., St. Louis, MO, USA.During this process, Query type was set as 'FLEX' and all other options were kept as default.

4.3.3 Validation of the Best pharmacophore Model using Reciever Operating Characteristic (ROC) Curve

- ROC Curve is the plot of sensitivity vs specificity of the pharmacophore model generated.

- Furthermore, the validation of the model was carried out using a database of 30 test compounds. 20 conformers were generated for each test compound using Genetic Algorithm (GA) Conformer Search. So, a total of 600 compounds were obtained. Decoy set consists of a total number of 2074 compounds. Hence, a total of 2674

compounds (Test + decoy) were used for further validation. 2328 compounds were retrieved after completion of the process.

- Validation and analysis of the results were done using SPSS Evaluation Version 15.0. , a software for statistical analysis. These functions were performed by using UNITY module in the SYBYL X 1.3 software from Tripos Inc., St. Louis, MO, USA. During this process, Query type was set as 'FLEX' and all other options were kept as default.
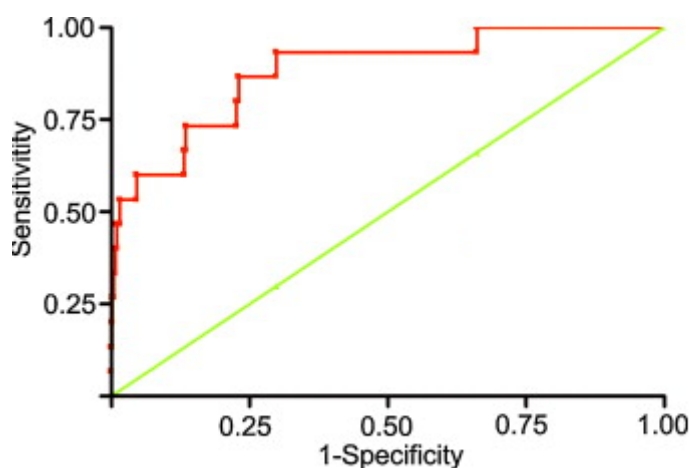
Area Under Curve (AUC) = 0.782

Fig 4.3 : Pharmacophore Validation : ROC Curve

4.3.3 Sensitivity and Specificity of Model.

Sensitivity and specificity are statistical measures of the performance of a binary classification test, also known in statistics as classification function. Sensitivity measures the proportion of actual positives which are correctly identified as such. Specificity measures the proportion of negatives which are correctly identified. Sensitivity relates to the test's ability to identify positive results.

Sensitivity =   Number of true positives
_____

                 Number of true positives + Number of False negatives

Specificity =   Number of true negatives
_____

                 Number of true negatives+ Number of false positives

➢ Sensitivity and specificity of best model was evaluated by using separate Decoy set of
   2074 compounds. Pharmacophore based screening of Decoy database resulted into:

      1) No. of True Positives: 974
      2) No. of True Negatives: 632
      3) No. of False Positives: 180
      4) No. of False Negatives: 289

Sensitivity and specificity were obtained from above equations which are as follows :

   1) **Sensitivity = 0.77**
   2) **Specificity = 0.78**

Pharmacophore validation results show good sensitivity and specificity. This validation results suggest that generated pharmacophore model can be successfully used in virtual screening to search the substructures from databases to retrieve initial hits. Further these pharmacophoric features were co-related with the 3D QSAR studies and compounds were desgined on the basis of these results.

CHAPTER-5

VIRTUAL SCREENING

5. VIRTUAL SCREENING

Virtual screening emerged as an important tool in our quest to access novel drug like compounds. .The fit between the molecule and the pharmacophore can be used as an alignment device which is referred as virtual screening. The pharmacophore searching algorithm translates and rotates each molecule in the Cartesian coordinate system to place it in the best possible alignment with the pharmacophore. Virtual screening (VS) is a computational technique used in drug discovery research. By using computers, it deals with the quick search of large libraries of chemical structures in order to identify those structures which are most likely to bind to a drug target, typically a protein receptor or enzyme. Thus, success of a virtual screen is defined in terms of finding interesting new scaffolds rather than many of these hits. Interpretations of virtual screening accuracy should therefore be considered with caution. Low hit rates of interesting scaffolds are clearly preferable over high hit rates of already known scaffolds.

5.1 Materials and Methods:

After 3D-pharmacophore model generation, NCI (National Cancer Institute) and Maybridge Hit Finder database were used for substructure searching. As the drug discovery and development arm of the National Cancer Institute (NCI), the Developmental Therapeutics Program (DTP) plans, conducts, and facilitates development of therapeutic agents for cancer . The data in this database focuses on research in the cancer . The hits from both databases were filtered by applying Lipinski's rule-of-five and other filters like remove bad fragments etc.83 Lipinski's Rule of Five is a rule of thumb to evaluate druglikeness or determine if a chemical compound with a certain pharmacological or biological activity has properties that would make it a likely orally active drug. The rule was formulated by Christopher A. Lipinski in 1997. Lipinski's rule states that, in general, an orally active drug has no more than one violation of the following criteria: Not more than 5 hydrogen bond donors (nitrogen or oxygen atoms with one or more hydrogen atoms) Not more than 10 hydrogen bond acceptors

(nitrogen or oxygen atoms) A molecular mass less than 500 Daltons. An octanol-water partition coefficient log P must not greater than 5.

5.2 Results and Discussion

The best pharmacophore model was selected to search substructure in NCI and Maybridge Hit Finder database. All parameters were unchanged except priority was kept high. A total number of 58591 molecules were obtained after substructure searching from both databases. These molecules were again screened for drug like compounds by applying Lipinski's rule of five and finally 16829 compounds were obtained which might be useful in rational design of new Aurora Kinase A inhibitors. Among these 16829 molecules, 17 molecules exhibit Qfit value more than 80%. The stepwise description of screening procedure is shown in **Fig. 5.1.**

FIGURE 5.1: **Flow Chart of virtual Screening Procedure of NCI and Maybridge Hit Finder Databases**
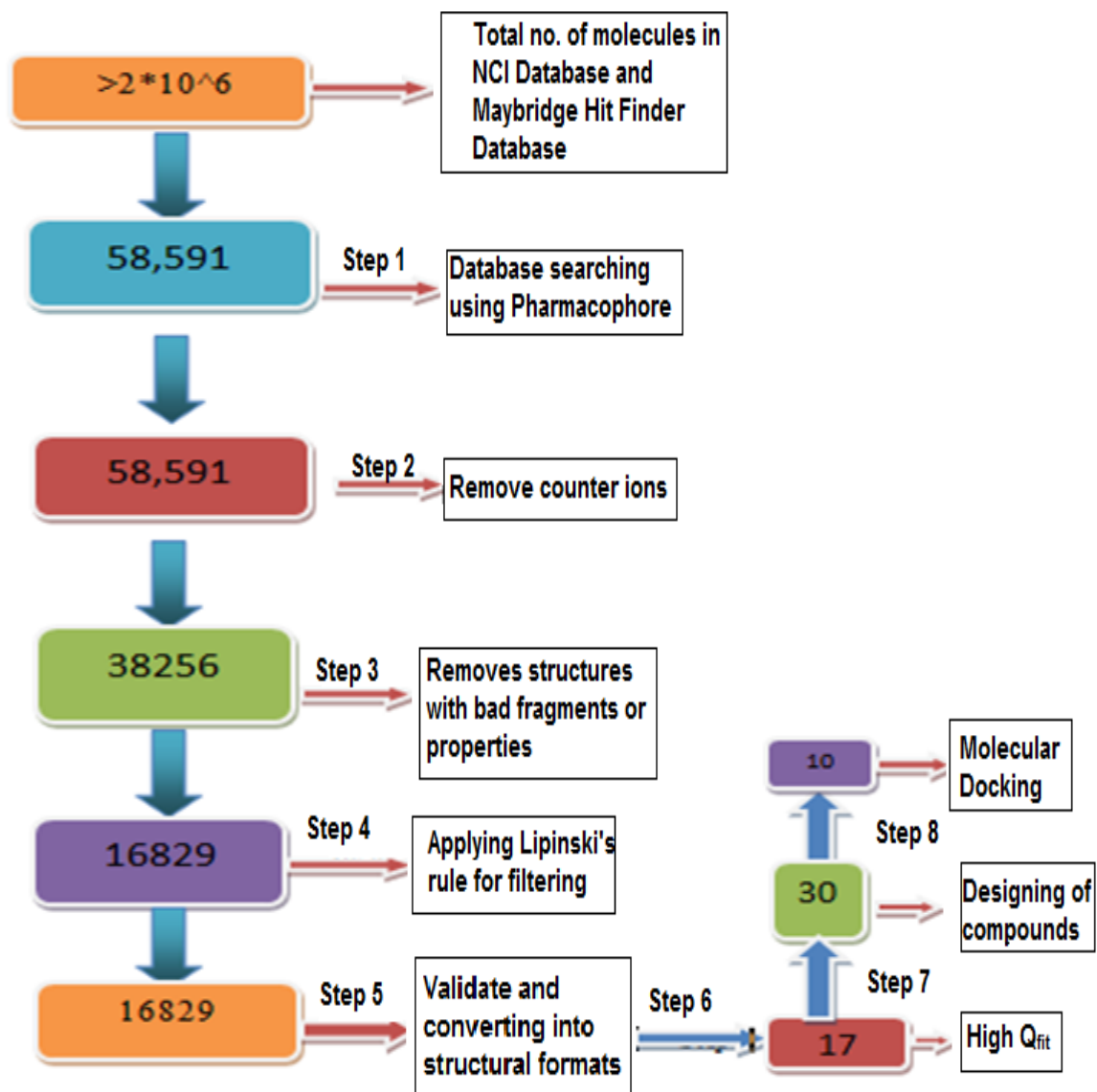
CHAPTER-6

3D QSAR STUDY

6. 3D-QSAR (CoMFA and CoMSIA)

QSAR is conceptually a way of finding a simple equation that can be used to predict some property from the molecular structure of a compound. This is done by using curve fitting software to find the equation coefficients, which are weights of known molecular properties. In this study, 3D-QSAR model was built using Comparative Molecular Field Analysis (CoMFA) and Comparative Similarity Indices Analysis (CoMSIA) methods. CoMFA and CoMSIA are computer programs which are used to correlate the 3D structure of molecules with biological activity based on statistical techniques. CoMFA is most commonly used 3D-QSAR technique in drug discovery which was developed by Cramer et al. CoMFA describes steric (Lenard Jones) and electrostatic (Coulomb) fields. In CoMSIA, similarity indices are calculated at regularly placed grid points for the aligned molecules. Besides electrostatic and steric fields, CoMSIA also calculates other descriptors like hydrophobic, hydrogen bond donor and hydrogen bond acceptor.

6.1 Material and method

Many Aurora Kinase-A inhibitors were synthesized and their inhibitory activity was measured by different method. It is unreliable to build 3D-QSAR models with mixed biological data and to avoid this situation; we selected 48 pyrolo-triazene derivatives reported by Abraham et al. The chemical structures of compounds are listed in **Table 3**. Molecular alignment is one of the most crucial components in 3D-QSAR studies as it affects the statistical analysis of CoMFA and CoMSIA. Several methods have been described like pharmacophore- based alignment, rigid alignment of molecules by Distill, etc. A Distill based alignment method was used in development of CoMFA and CoMSIA models. **Figure 6.1** shows alignment of training set molecules used in 3D-QSAR models. All aligned molecules were placed in grid box with grid spacing of 2.0 Å on three axes of the Cartesian coordinate system. CoMFA steric and electrostatic fields were calculated using QSAR module of Sybyl X1.3. CoMFA uses Lenard jones potential and coulomb potential to calculate steric and electrostatic fields, respectively. Both steric and electrostatic fields were calculated for each molecule using sp^3

hybridized carbon atom with 1.52 Å Van der Waals radiuses and a charge of +1.0. The energy cut-off values for both

r2 pred= SD-PRESS/SD

Where SD is the sum of the squared deviations between the biological activity of molecules in the test set and the mean biological activity of the training set molecules and PRESS is the sum of the squared deviations between predicted and actual activity values for every molecule in the test set.

The training set was initially checked for outliers. If the residual of an inhibitor between observed pIC50 and predicted pIC50 values is greater than one logarithm unit, the inhibitor is considered as outlier. The experimental activities, predicted activities and their residues of the 38 training set inhibitors and 10 test set inhibitors are listed in **Table 4**. It is clear from Table 3 that there is no outlier in CoMFA and CoMSIA models. The statistical results obtained from standard CoMFA model is given in **Table 5**. The q^2, r^2 pred, r^2ncv, F and SEE (standard error of estimation) values were computed. PLS analysis showed a high cross validated r^2 (q^2) value of 0.492 with six components. The regression lines for the experimental and predicted activity of training and test sets are shown **in Figure 6.2 and 6.3** . By comparison of the experimentally observed and theoretically predicted pIC_{50} values of inhibitory activity of a series of triazene derivatives, it can be seen that both CoMFA and CoMSIA models performed well. in the prediction of the activities of the test inhibitors (**Table 4**). In almost all the cases, the predicted values were close to the observed pIC_{50}. The non-cross-validated PLS analysis results in a conventional r^2 of 0.963, F of 134.886 and a standard error of estimation (SEE) of 0.112. Field contribution for both steric and electrostatic fields account for 0.688 and 0.312, respectively.

The steric contour map for the CoMFA model with the most active inhibitor compound 25 is shown in **figure 6.4(a)**. In this figure, the green contours represent regions of high steric tolerance (80% contribution), while the yellow contours represent regions of low steric bulk tolerance (20% contribution). The steric green contour map of CoMFA model indicates that steric bulky group near amide linkage region favours anti-cancer activity. A small yellow

region is observed away from molecular structure indicates that there is no significance of HBD property in this region. It is evidence by comparing compound 7 and 8. Compound 8 (pIC_{50}=7.9393) is more potent than compound 7 (pIC_{50}= 7.93) as more bulky substitution is present on the pyrolidine ring on Compound 8 as compared to compound 7.

CoMFA electrostatic contour map is shown in **figure 6.4(b).** In electrostatic contour map, positive charge favourable region is indicated in blue colour and negative charge favourable region is indicated in red colour. A large red region is seen near benzene ring of pyrolo-triazene derivatives indicates that electronegative groups at this position favour activity. A large polyhedron is displayed in figure. A blue polyhedral is observed near pyrazole substitution which links benzene ring through amide linkage .Compound 25 having the highest activity (pIC_{50} =8.6) has highly electronegative substitutions (-F) and hence has higher activity.
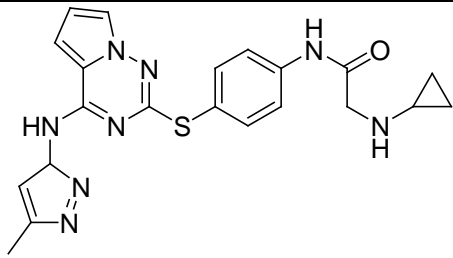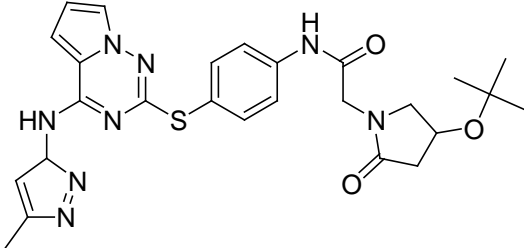
The CoMSIA model with the combination of all fields yielded a cross-validated r^2 value of 0.524 with 6 components, non-cross-validated r^2 of 0.962, F value of 126.47 and predictive r^2 of 0.500. Contribution of steric, electrostatic, hydrogen bond donor (HBD), hydrogen bond acceptor (HBA) and hydrophobic fields were 0.154, 0.155, 0.210, 0.212 and 0.269 respectively. The advantage of CoMSIA contour maps over CoMFA is that they are easier to interpret. Apart from calculating steric and electrostatic fields as in CoMFA, CoMSIA additionally uses hydrophobic, hydrogen bond donor and hydrogen bond acceptor fields. A correlation between actual and predicted activity of training are shown in **figure 6.3**.
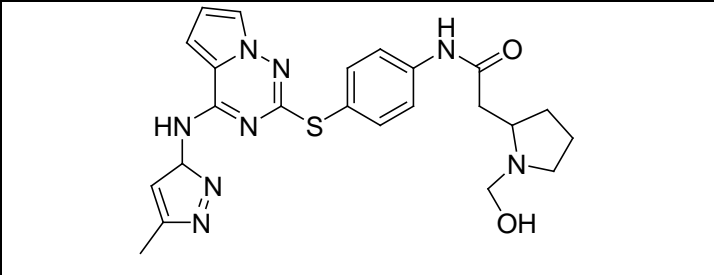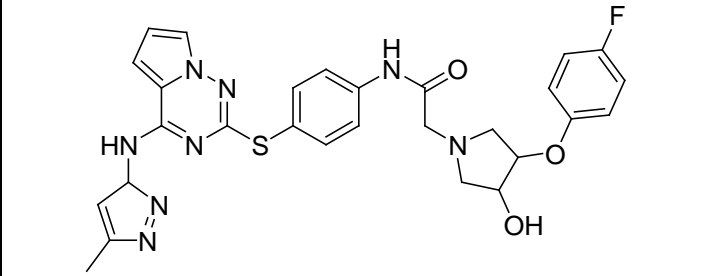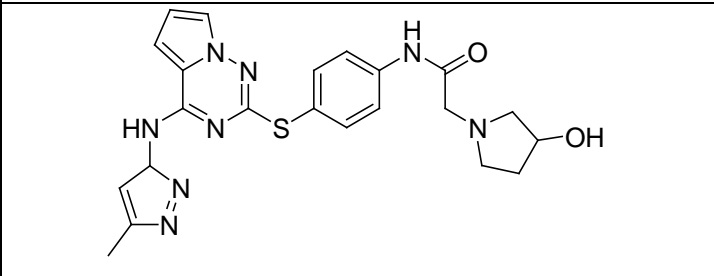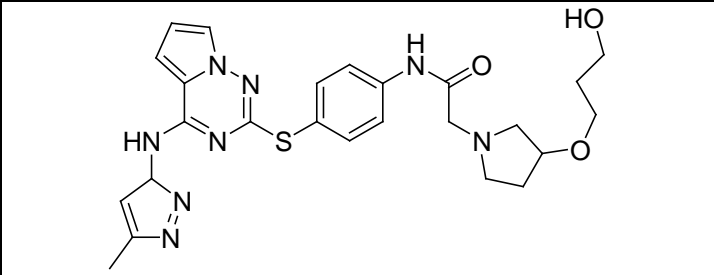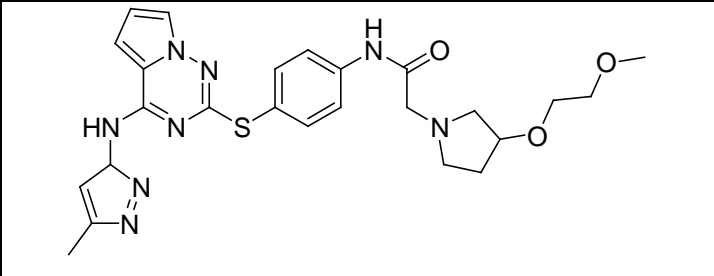
CoMSIA hydrophobic contour map is displayed in **figure 6.5(a).** Yellow polyhedral regions and white polyhedral regions indicate areas where hydrophobic and hydrophilic properties are preferred. One large yellow region is observed near nitrogen of triazene ring indicates that hydrophobic groups in this region are beneficial for anti-cancer activity. It is evidence by comparing compound 37 and 38. Compound 37 (pIC50=7.27) is less potent than compound 38 (pIC50= 8.5) as hydrophobic ring is present in 37.
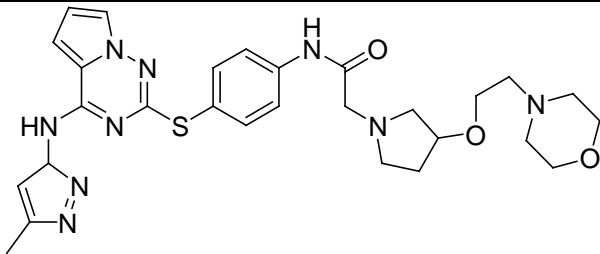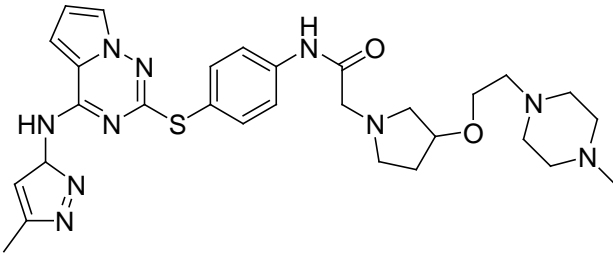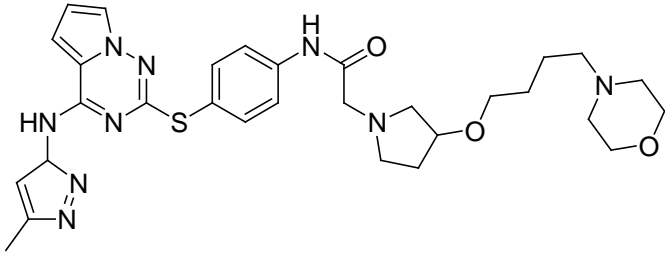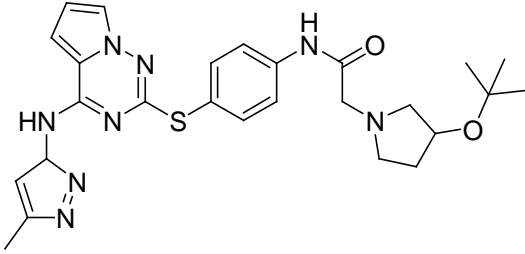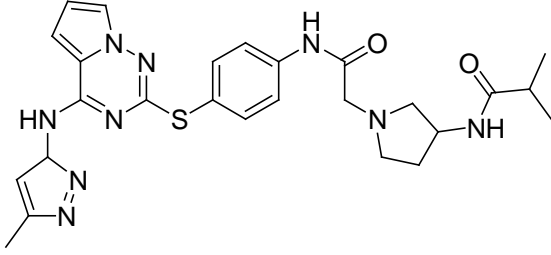
CoMSIA hydrogen bond donor (HBD) contour map is represented in **figure 6.5(b).** Cyan contour (80% contribution) indicates regions where HBD substituents are favoured while purple contour (20% contribution) indicates areas where HBD are disfavoured. One large cyan contour is observed near pyrazole ring and amide linkage suggests that HBD groups in this region favours integrase inhibitory activity. A small purple region is observed away from molecular structure indicates that there is no significance of HBD property in this region. Compound 20 is more potent than compound 26 as it has –OH substitution.
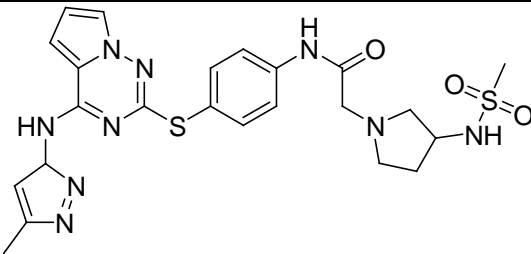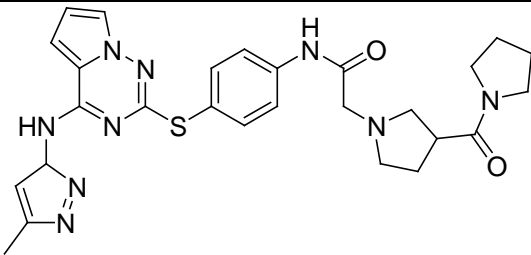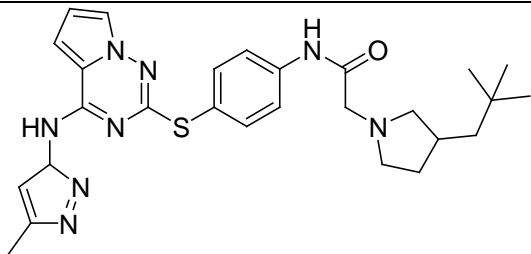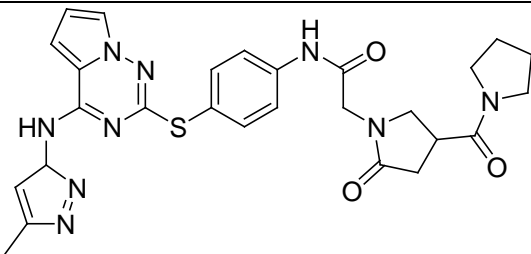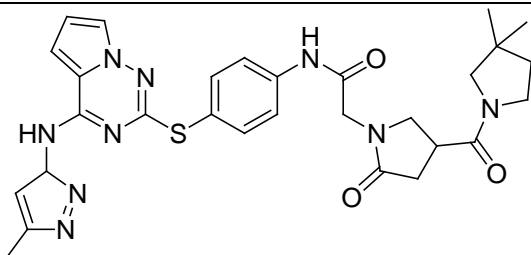
The hydrogen bond acceptor (HBA) contour map of CoMSIA model is displayed in **figure 6.5 (c)**. In CoMSIA HBA field, the magenta (favourable) and red (unfavourable) contour represents 80% and 20% contributions respectively. A medium size magenta contour is seen near amide linkage suggests that HBA groups in this area are preferred for anti-cancer activity. A red polyhedral is seen away from molecular structure indicates that there is no significance of HBA property in this region. Compound 25 shows highest activity as it consists of carbonyl substitution.
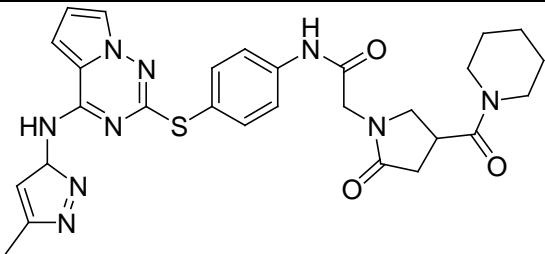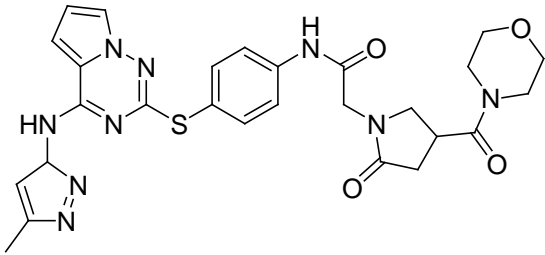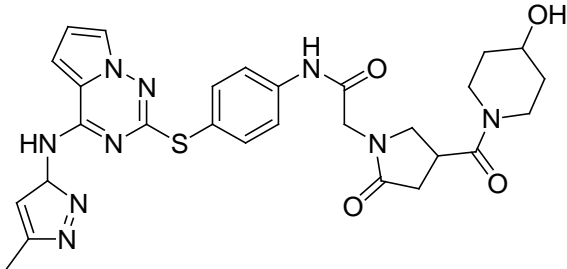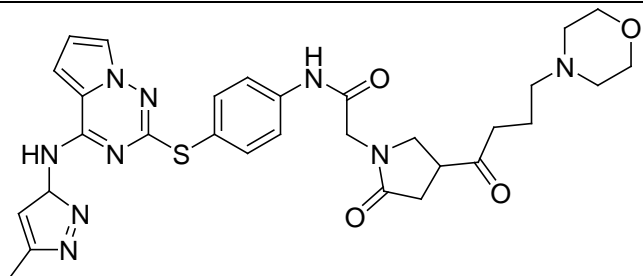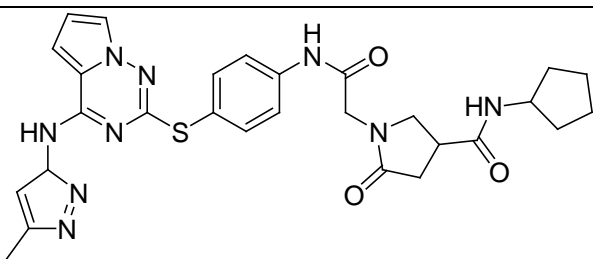
Table 3: Chemical Structures of Pyrolo Triazene derivatives:
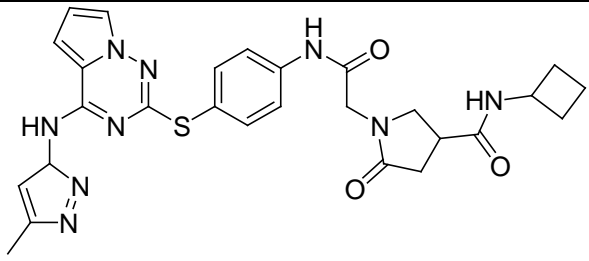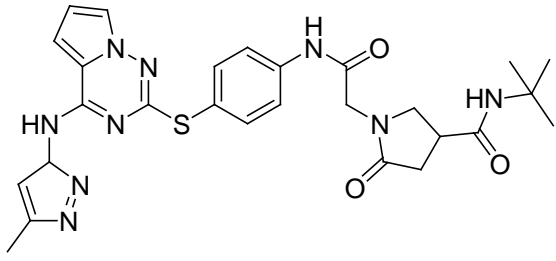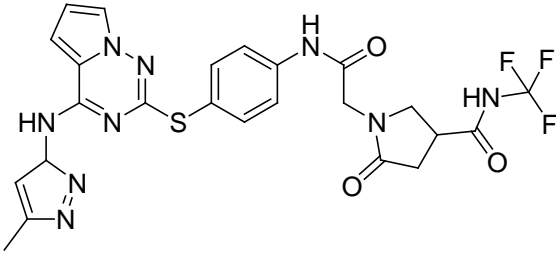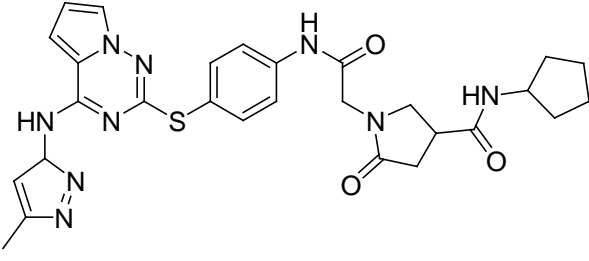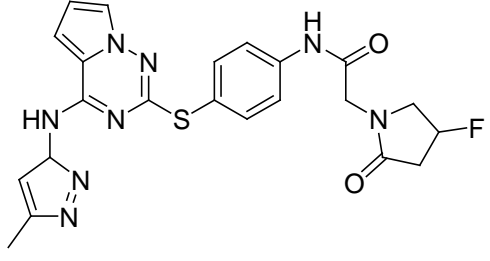
Compound No.	Structure	pIC$_{50}$
1		7.4949
2*		7.9208
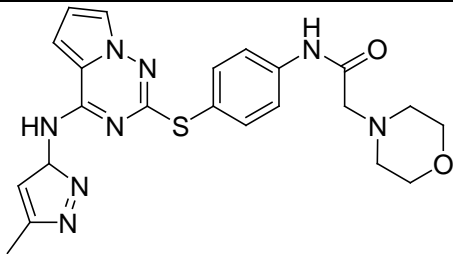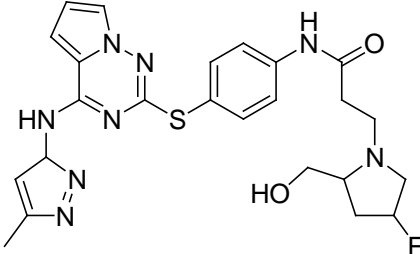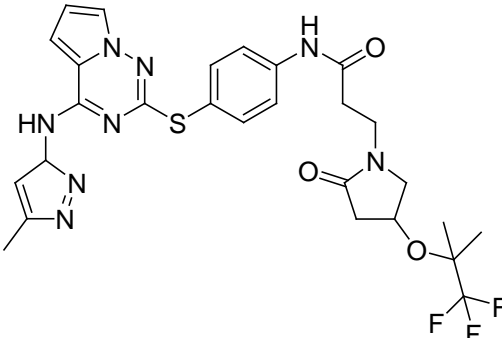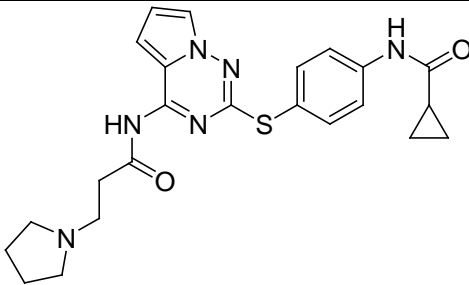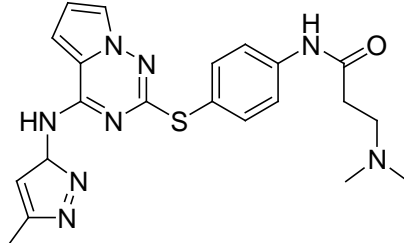
3		7.4202
4		7.8239
5		7.4089
6		8.3468
7*		7.9393
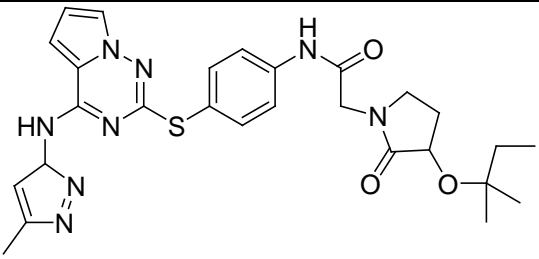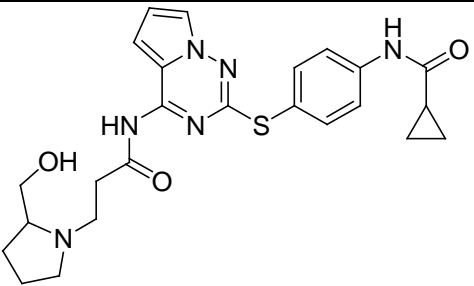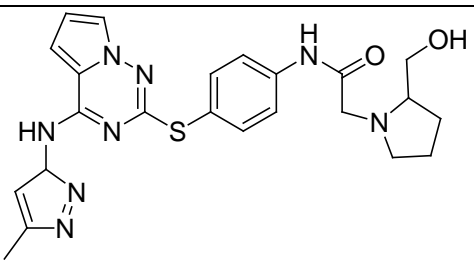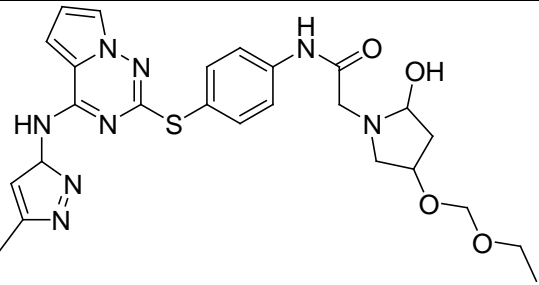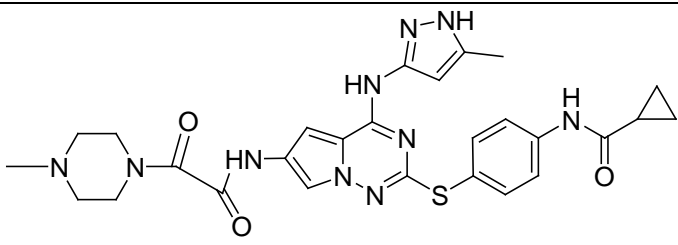
8		7.9586
9		7.9031
10*		8.2924
11		7.6021
12		7.8827
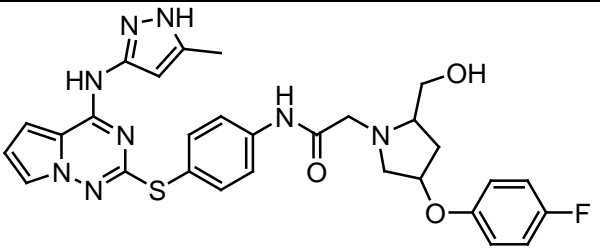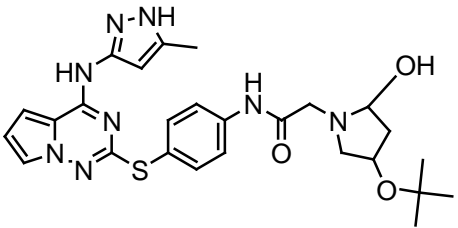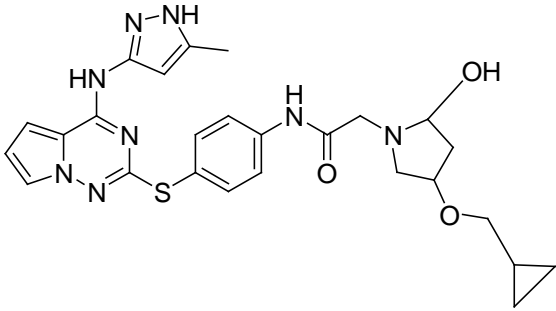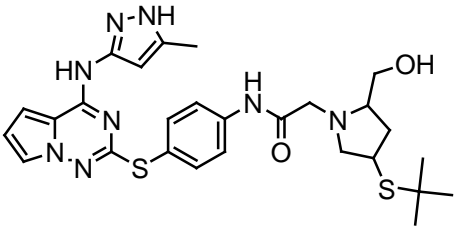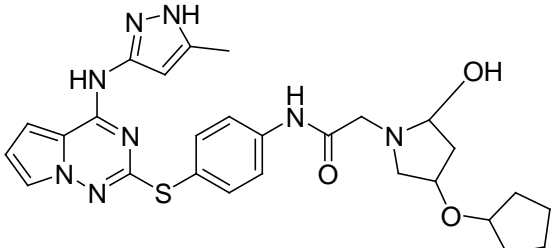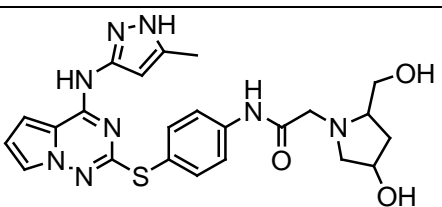
13		7.9101
14		8.0555
15		7.5986
16*		7.9957
17		8.2366
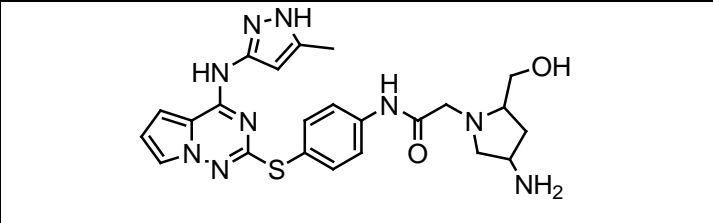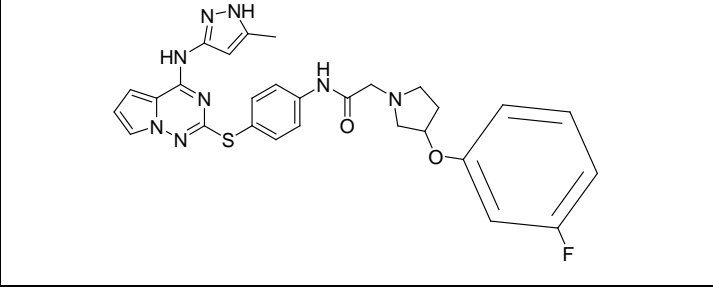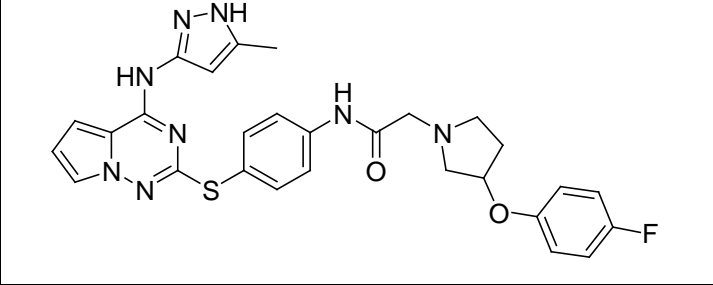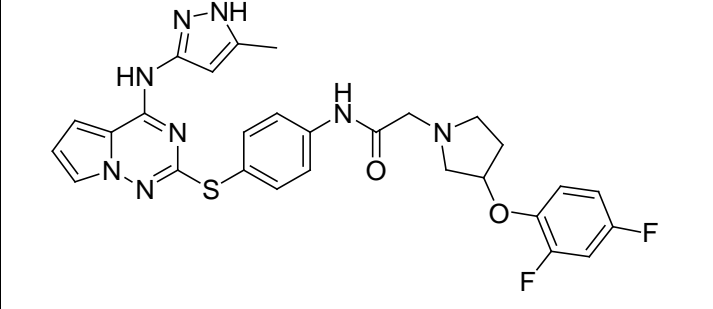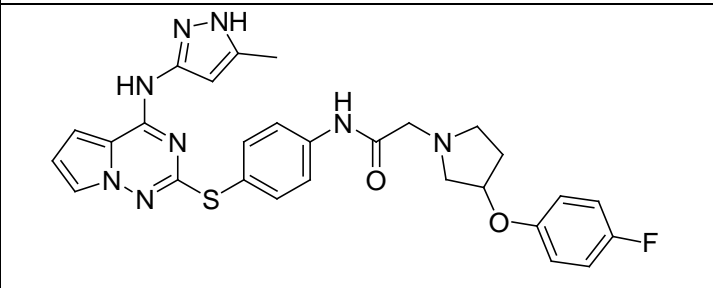
18		8.1938
19		8.3979
20		8.3979
21		8.2007
22		8.0315

23		8.3768
24		8.2518
25		8.6021
26		6.8447
27*		8.3010

28		7.0706
29		7.8239
30		8.2218
31*		7.6383
32		7.5086

33		8.0969
34		8.0000
35		7.7696
36		8.3010
37*		8.1549

38		7.2757
39		6.5214
40		8.1549
41		6.9547
42*		7.9586
43		7.2366

44		6.4191
45*		7.7696
46*		7.8239
47		7.8861
48		8.1549

* Test set molecules

Table 4 : Experimental and Predicted pIC50 of the Training and Test Sets Using CoMFA and CoMSIA Models

Compound No.	Actual pIC_{50}	CoMFA Predicted pIC_{50}	CoMSIA Predicted pIC_{50}
1	7.4949	7.421	7.356
2*	7.9208	8.065	8.066
3	7.4202	7.518	7.560
4	7.8239	7.882	7.891
5	7.4089	7.362	7.479
6	8.3468	8.375	8.342
7*	7.7393	7.653	7.382
8	7.9586	7.911	7.914
9	7.9031	7.922	7.867
10*	8.2494	8.00	8.042
11	7.6021	7.504	7.624
12	7.8827	7.880	7.906
13	7.9101	7.821	7.972
14	8.0555	7.849	7.872
15	7.5986	7.722	7.529
16*	7.9957	8.17	8.033
17	8.2366	8.280	8.294
18	8.1938	8.265	8.215
19	8.3979	8.315	8.473
20	8.3979	8.486	8.291
21	8.2007	8.201	8.235
22	8.0315	7.963	7.976
23	8.3768	8.482	8.513
24	8.2518	8.213	8.217
25	8.6021	8.654	8.505
26	6.8447	6.969	6.873
27*	8.3010	7.904	8.215
28	7.0706	7.087	7.144
29	7.8239	7.612	7.498
30	8.2218	8.197	8.286
31*	7.6383	7.328	7.388
32	7.5086	7.472	7.432
33	8.0969	8.110	7.965
34	8.0000	8.092	8.165
35	7.7696	7.919	7.805
36	8.3010	8.338	8.249
37*	7.85	7.308	7.518

38	7.2757	7.096	7.234
39	6.5214	6.649	6.721
40	8.1549	7.977	8.122
41	6.9547	6.833	7.067
42*	8.09	8.371	8.237
43	7.2366	7.240	7.261
44	6.4191	6.658	6.345
45*	8.00	8.155	8.23
46*	7.7696	7.983	8.041
47	7.8861	7.886	8.051
48	8.1549	8.176	8.084

*Test set molecules

Table 5 : Summary of CoMFA and CoMSIA Results.

Components	Ligand Based Models	
	CoMFA	**CoMSIA**
q^2	**0.491**	**0.500**
r^2_{ncv}	**0.963**	**0.961**
n	**6**	**6**
F-values	**134.886**	**126.472**
SEE	**0.112**	**0.116**
$r^2_{Predicted}$	**0.607**	**0.519**
Probability of r^2_{ncv}	**0.000**	**0.000**
Field contribution	**-**	**-**
Steric	**0.688**	**0.154**
Electrostatic	**0.312**	**0.155**
Hydrophobic	**-**	**0.212**
Hydrogen bond Donor	**-**	**0.210**
Hydrogen bond Acceptor	**-**	**0.269**
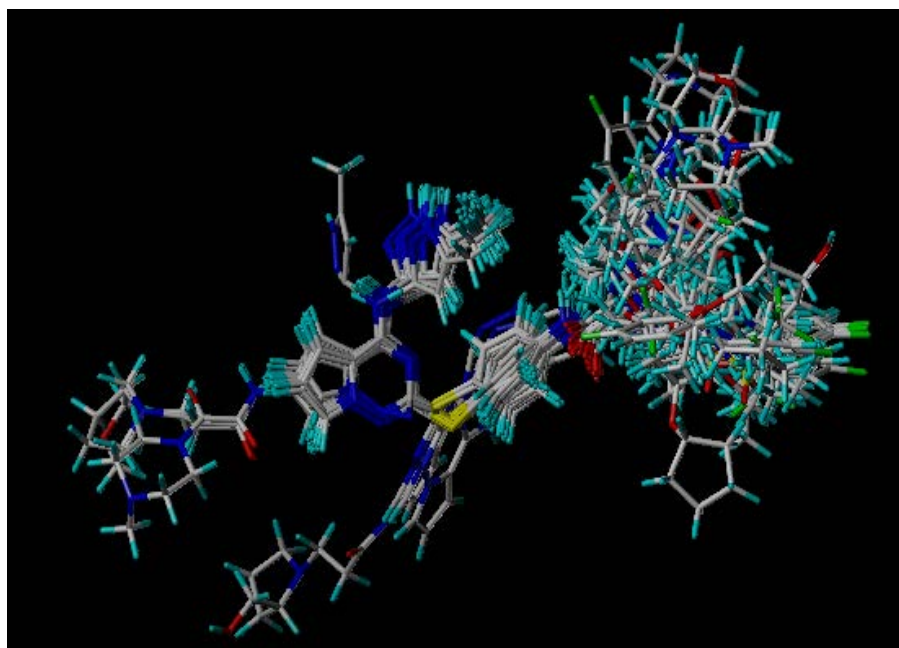
FIGURE 6.1 : Alignment of inhibitory compounds in training set

Figure 6.2. A graph of actual versus predicted activities of the training and test set molecules from CoMFA analysis.
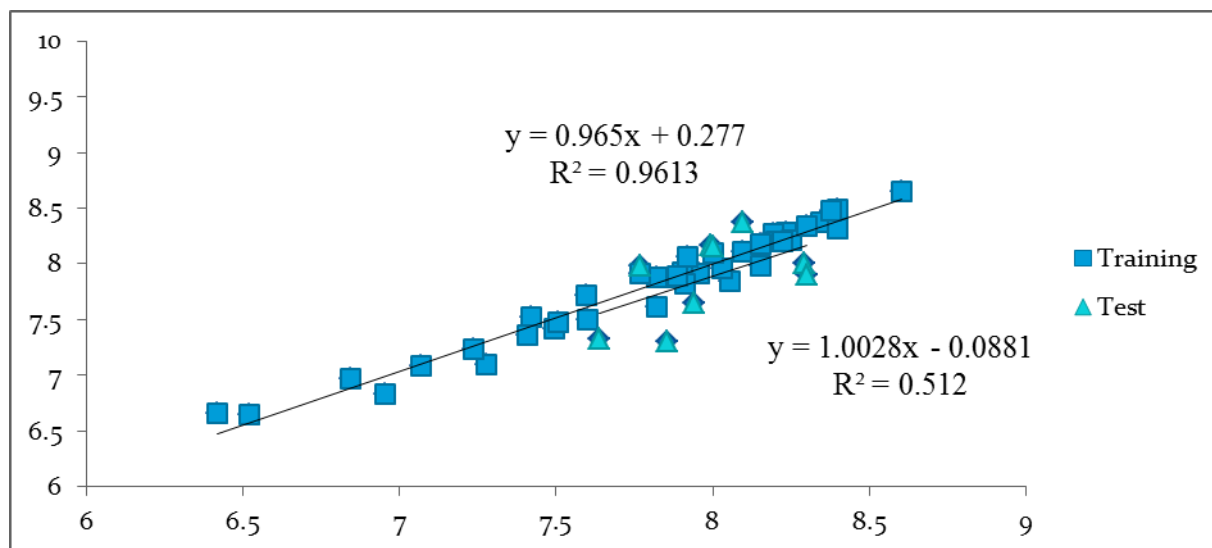
Figure 6.3. A graph of actual versus predicted activities of the training set molecules from CoMSIA analysis.
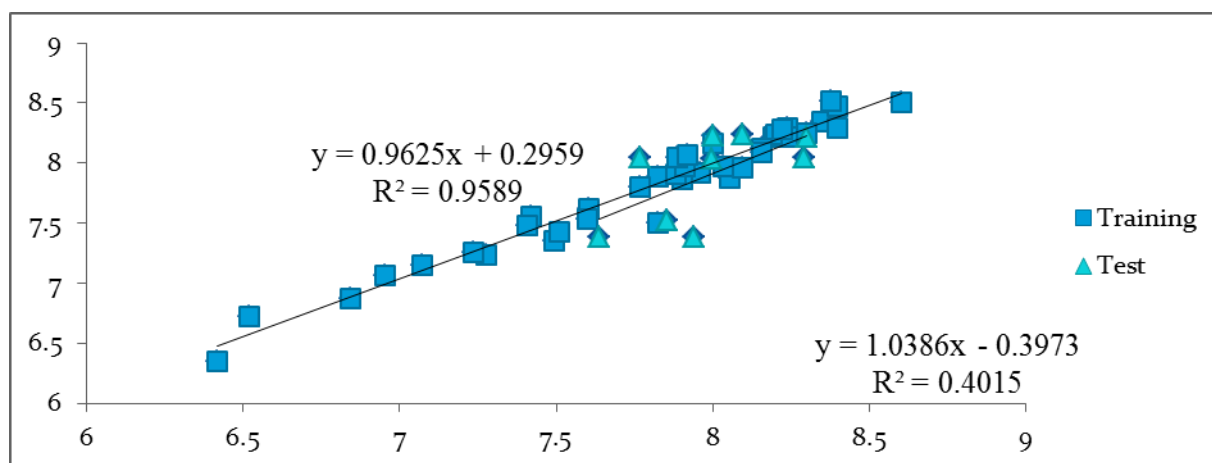
Figure 6.4 CoMFA contour maps in combination with compound 25. (A) Steric contour map (B) Electrostatic contour map.
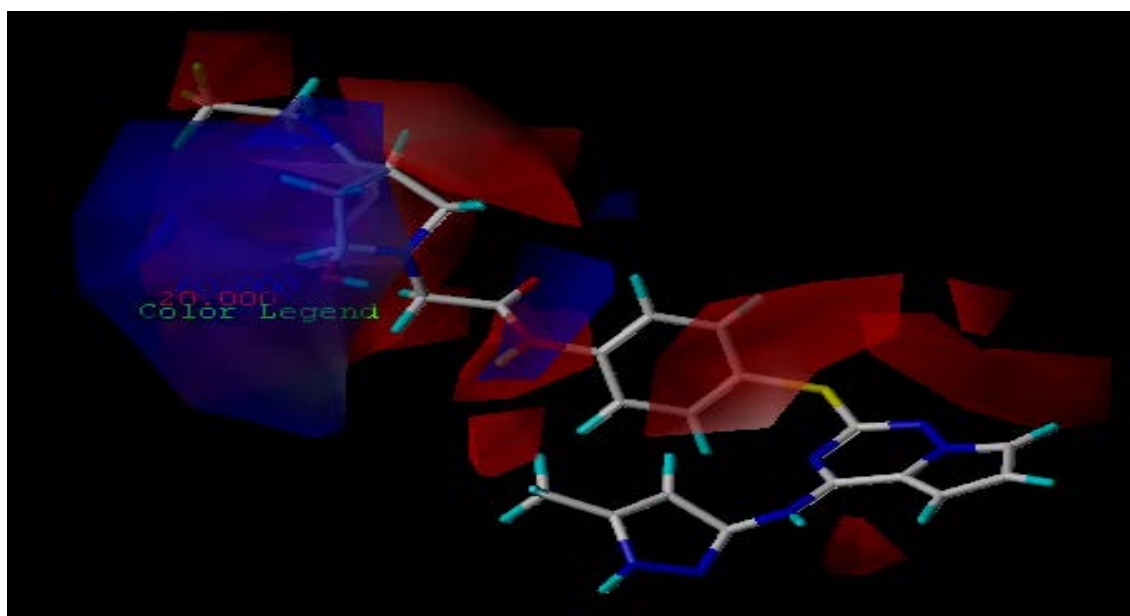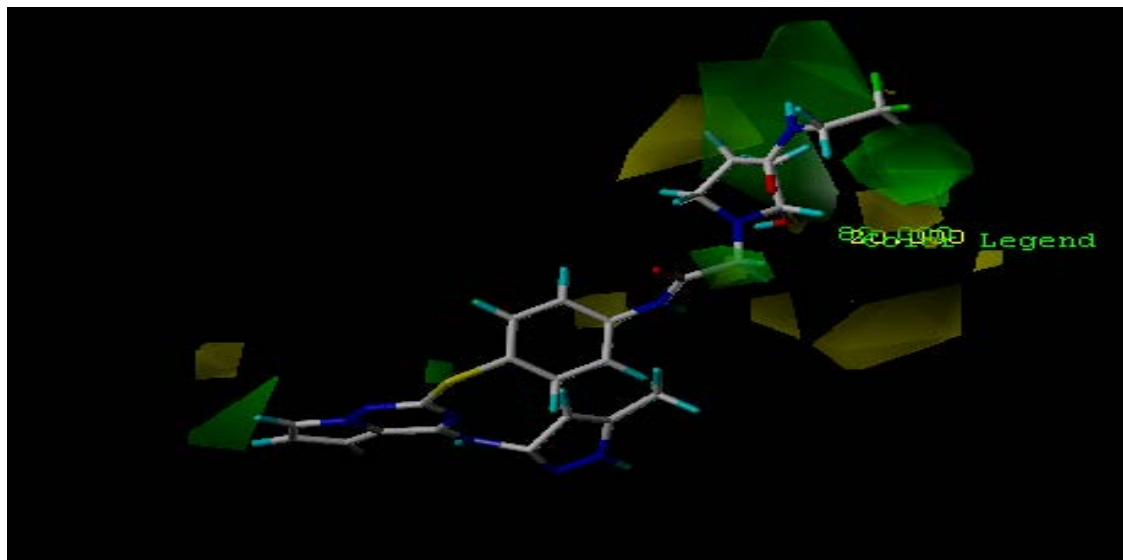
Fig 6.5 CoMSIA contour maps in combination with compound 25. (A) Hydrophobic contour map (B) hydrogen bond donor (C) hydrogen bond acceptor
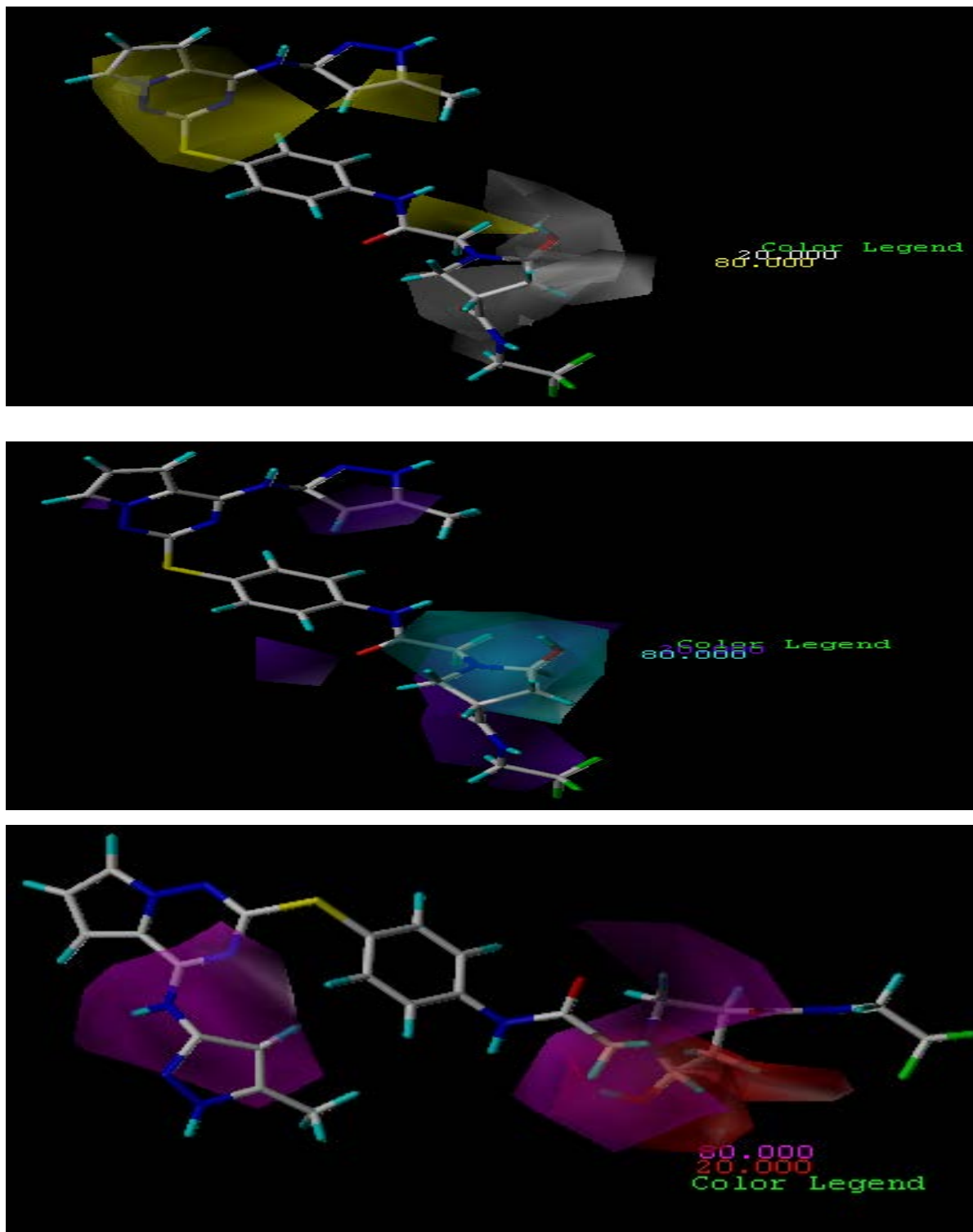
CHAPTER-7

DESIGNING AND

MOLECULAR

DOCKING

7. Designing of Molecules and Molecular Docking

7.1 Designing of Molecules

➢ A total number of 17 molecules have Qfit value more than 80 %. The major ring systems obtained were dihydroanthracene, thioxanthenes, anthracin dione, purine derivates, etc. Purine ring system has higher Qfit value than other scaffold.

➢ So compounds were designed on various position of Purine which might be act as Aurora Kinase-A inhibitors.

➢ Pharmacophore modeling, 3D-QSAR studies and knowledge based structure activity relationship (SAR) was used to design molecules which contain purine ring (57) as a core structure.
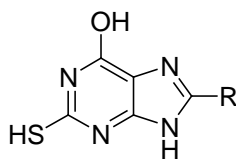
(57)

7.2 Molecular Docking

Docking is an automated computer algorithm that determines how a compound will bind in the active site of a protein. This includes determining the orientation of the compound, its conformational geometry, and the scoring. The scoring may be a binding energy, free energy, or a qualitative numerical measure. In some way, every docking algorithm automatically tries to put the compound in many different orientations and conformations in the active site, and then computes a score for each. Some programs store the data for all of the tested orientations, but most only keep a number of those with the best scores. Hence docking plays an important role in the rational design of drugs.

7.2.1 Materials and methods

Surflex was used for molecular docking. AURKA complex with external ligand [PDB:3K5U] was taken from protein data bank (PDB) and modified for docking calculations. Co-crystalized ligand was removed from the structure, water molecules were removed, H atoms were added and side chains were fixed during protein preparation. Protein structure minimization was performed by applying Tripos force field and partial atomic charges were calculated by Gasteiger Huckel method. Twenty conformers were generated for each molecule.

7.2.2 Results and Discussion:

In this study, designed molecules were selected for docking purpose which was designed by studying structure activity relationship from literature. Co-crystal structure of AURKA was retrieved from the protein data bank. After running Surflex– Dock, the scores of 20 docked conformers were ranked in a molecular spread sheet. We selected the best total score conformer and speculated regarding the detailed binding patterns in the cavity. Results of docking study are shown in table. Docking results **(TABLE-6)** revealed that 2 molecules showed comparative good score compared to standard drugs, Doxorubicin, AZD1152 and VX-680. Surflex dock results contain three information – total score, crash value and polar value. Total score is the total Surflex-Dock score expressed as -log (Kd) to represent binding affinities which include hydrophobic, polar, repulsive, entropic and solvation terms. Crash value is the degree of inappropriate penetration by the ligand into the protein and of interpenetration between ligand atoms (self-clash) that are separated by rotatable bonds. Crash scores close to 0 are favorable. Polar value is contribution of the hydrogen bonding and salt bridge interactions to the total score. The polar score may be useful for excluding docking results that make no hydrogen bonds.

Table 6 : Docking Results of 10 Compounds using Surflex

Structure	Total Score	Crash Value	Polar Score
60	5.4134	-0.6346	2.1160
Doxorubicin	5.0484	-2.1632	4.1917
61	4.9646	-0.6278	4.9774
AZD1152	4.9500	-0.1222	3.7890
VX-680	4.9495	-0.4522	2.7834
62	4.9100	-0.6987	2.8234
67	4.5998	-1.8422	2.6910
66	3.9501	-0.3132	1.1258
63	3.6581	-0.2182	2.8144
64	3.5005	-0.3200	1.7349
68	3.2321	-0.3575	1.5467
59	2.0092	-0.3878	0.0487
65	1.4401	-0.6642	1.0881

Table 7 : AMINO-ACIDS INVOLVED IN DOCKING-INTERACTIONS

Compound	Interacting amino-acids
AZD1152	PRO214, ALA213, TYR212, GLU211
Tozasertib	PRO214, GLY216
Doxorubicin	PRO214, TYR212, ALA213
60	PRO214, TYR212
61	PRO214, GLY142
62	ASP256, GLY276, ASP274
67	TYR212, ALA213
66	TYR148, LEU139
63	GLY216,ASP274
64	TYR212, ALA213
68	TYR212, GLY142, ALA213
59	ASP274, ALA273, ASN261
65	GLY142, GLY140

7.2.3 Binding poses of compounds 60 and 62 in AURKA

Binding pose of both compounds 60 and 62 are shown in figures. Compound 60 shows one hydrogen bond interaction with 6-hydroxyl group of 2-mercapto-8-p-toluyl-9H-purine-6-ol and N1 of purine ring shows interaction with TYR212. **(Fig 7.1a)**.Compound 62 complexed

with AURKA showed occurrence of two hydrogen bonds. PRO214 with 6-hydroxyl group of 8-(4-aminophenyl)-2-mercapto-9H-purin-6-ol and second hydrogen bond is formed between-OH group of substituted acid and GLY142.. **(Fig. 7.1b)**

Fig 7.1 (a) Binding pose of Compound 60 in Aurora Kinase-A
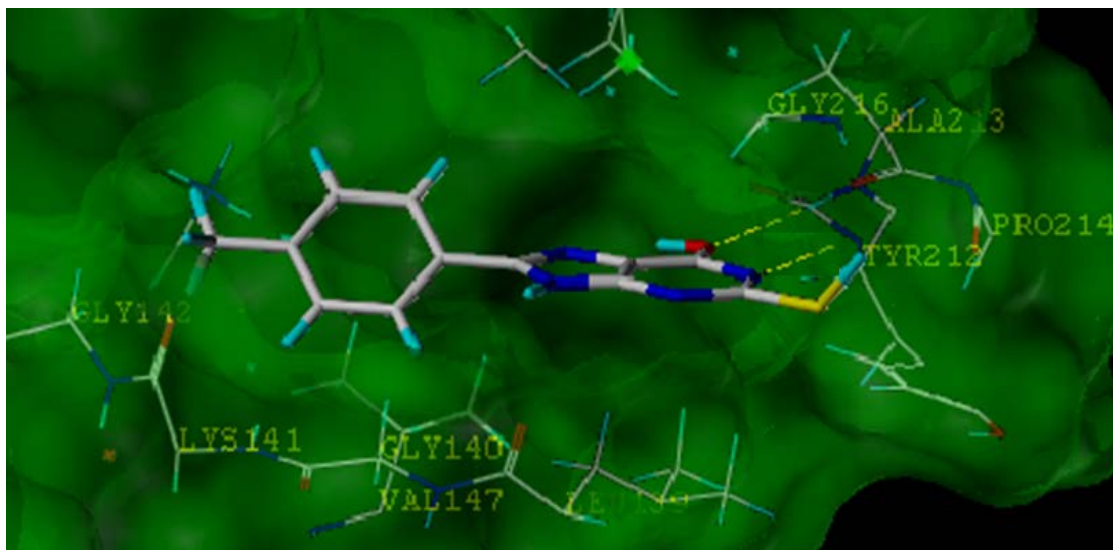
Fig 7.1 (b) Binding pose of Compound 62 in Aurora Kinase-A
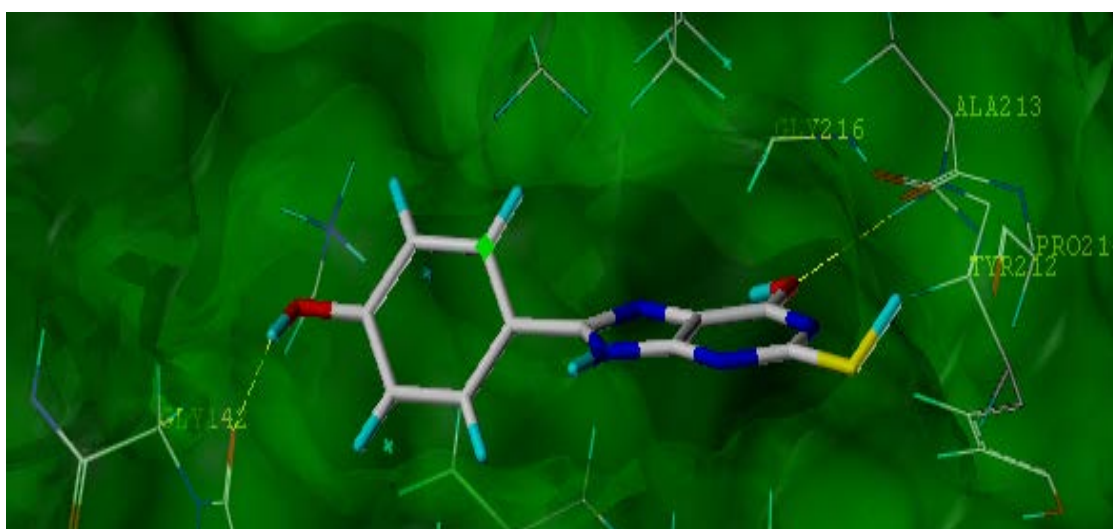
CHAPTER-8

EXPERIMENTAL WORK

8. Experimental Work

8.1 Requirements

Table 8: Chemicals required for synthesis

Sr. No.	Chemical Name	Company
1.	4,5-diamino-6 hydroxy-2-mercaptopurine	Sigma Aldrich
2.	Benzoic acid	CDH
3.	*p*-toluic acid	CDH
4.	*p*-hydroxy benzoic acid	CDH
5.	*p*-amino benzoic acid	CDH
6.	*p*-nitro benzoic acid	CDH
7.	*p*-chloro benzoic acid	CDH
8.	*p*-bromo benzoic acid	CDH
9.	*o*-chloro benzoic acid	CDH
10.	Cinnamic acid	CDH
11.	Phenyl acetic acid	CDH
12.	Glacial acetic acid	CDH
13.	Potassium carbonate	CDH
14.	Benzene	CDH
15.	Methanol	Merck

8.2 Instruments and Apparatus:

- All the reactions were performed in dried Borosilicate glasswares.
- Precoated Silica Gel Plates (MERCK) were used for TLC to monitor progress of the reaction.
- UV Chamber was used for detection of spots in TLC.
- The difference in Rf value between starting material and product were indicative of the conversion of one into the other.
- Melting Point was recorded on VEEGO Corporation Melting point apparatus and the reported melting points are uncorrected.
- REMI Rota-mantle were used for refluxing the reactions and stirring the reactions.
- I.R lamp was used for drying of products.
- Rotary vacuum evaporator (BUCHI type) was used for the recovery of the solvents.
- IR spectra were recorded on SHIMADZU FTIR 8400 at, by KBr dispersion method.
- Mass spectra were recorded using ESI as ion source at Oxygen Healthcare Research P. Ltd, Ahmedabad.
- The proton NMR spectra were recorded at Bruker Avance II 400 spectrometer Saurashtra University, Rajkot.

8.3 Outline for Synthetic Protocol

8.3.1 General Scheme for Synthesis of Compounds

4,5-diamino-6-hydroxy
-2-mercaptopurine

(58)

Substituted acids

2-mercapto-8-substituted-6,9-dihydro-1*H*-purin-6-ol
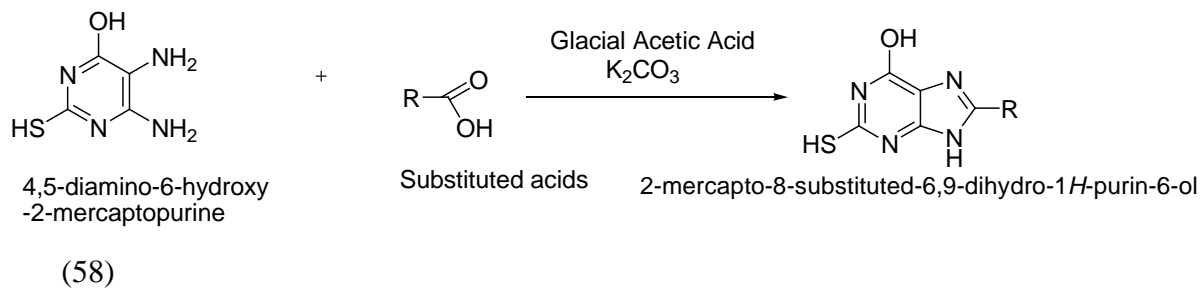
Table 9 : List of Products synthesized

Compound No.	R	Molecular Formula
59	-C$_6$H$_5$	C$_{11}$H$_{10}$N$_4$OS
60	*p*-CH$_3$-C$_6$H$_5$	C$_{12}$H$_{10}$N$_4$OS
61	*p*-OH -C$_6$H$_5$	C$_{11}$H$_8$N$_4$O$_2$S
62	*p*-NH$_2$- C$_6$H$_5$-	C$_{11}$H$_9$N$_5$OS
63	*p*-NO$_2$-C$_6$H$_5$	C$_{11}$H$_7$N$_5$O$_3$S
64	*p*-Cl- C$_6$H$_5$	C$_{11}$H$_7$ClN$_4$OS
65	*p*-Br- C$_6$H$_5$	C$_{11}$H$_7$BrN$_4$OS
66	*o*- Cl -C$_6$H$_5$	C$_{11}$H$_7$ClN$_4$OS
67	-CH=CH-C$_6$H$_5$	C$_{13}$H$_{10}$N$_4$OS
68	-O- C$_6$H$_5$	C$_{10}$H$_{10}$N$_4$O$_2$S

8.4 Procedure for synthesis of substituted purine Derivatives:

Synthesis was carried out using both conventional as well as microwave irradiation method. Conventional method took around 35-45 hours as compared to few minute synthesis using microwave.

8.4.1   Synthesis of 2-mercapto-8-phenyl-6,9-dihydro-1H-purin-6-ol (59)

A mixture of 4,5-diamino-6-hydroxy-2-mercaptopurine (0.5g, 0.0006 mol) was mixed with benzoic acid (0.45g, 0.0009 mol). 1 g of potassium carbonate and 30 ml of glacial acetic acid were added to the above mixture. Synthesis was carried out using both conventional reflux as well as microwave irradiation method . The solid obtained was washed with water and collected by vacuum filtration. Percentage yield, melting point and R_f value were reported.

OH

N   NH$_2$

HS   N   NH$_2$

4,5-diamino-6-hydroxy
-2-mercaptopurine

(58)

+

HO

O

benzoic acid

59 (a)

Glacial Acetic Acid
K$_2$CO$_3$

OH

HN   N

HS   N   N
              H

2-mercapto-8-phenyl-6,9-dihydro-1H-purin-6-ol

(59)
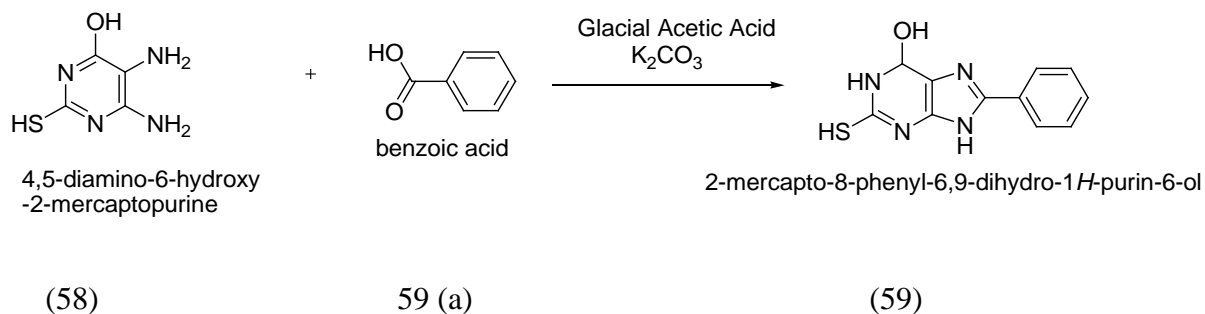
8.4.2   Synthesis of 2-mercapto-8-p-tolyl-9H-purin-6-ol (60)

A mixture of 4,5-diamino-6-hydroxy-2-mercaptopurine (0.5g, 0.0006 mol) was mixed with *p*-toluic acid (0.45g, 1.5 mol). 1 g of potassium carbonate and 30 ml of glacial acetic acid were added to the above mixture. Synthesis was carried out using both conventional reflux as

well as microwave irradiation method. The solid obtained was washed with water and
collected by vacuum filtration. Percentage yield, melting point and R_f value were reported.

OH

NH₂

HS   N   NH₂

4,5-diamino-6-hydroxy
-2-mercaptopurine

(58)

+

HO

O

p-toluic acid

60 (a)

Glacial Acetic Acid
K₂CO₃

OH

N   N

HS   N   N
          H

CH₃

2-mercapto-8-*p*-tolyl-9*H*-purin-6-ol

(60)
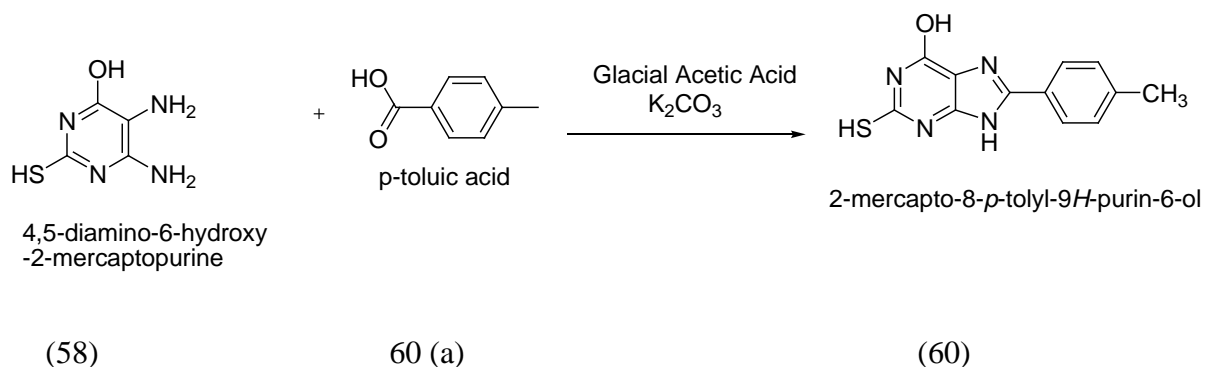
8.4.3   Synthesis of 8-(4-hydroxyphenyl)-2-mercapto-9H-purin-6-ol (61)

A mixture of 4,5-diamino-6-hydroxy-2-mercaptopurine (0.5g, 0.0006 mol) was mixed with
p- hydroxyl benzoic acid (0.45g, 0.00062 mol). 1 g of potassium carbonate and 30 ml of
glacial acetic acid were added to the above mixture. Synthesis was carried out using both
conventional reflux as well as microwave irradiation method. The solid obtained was
washed with water and collected by vacuum filtration. Percentage yield, melting point and R_f
value were reported.

OH

NH₂

HS   N   NH₂

4,5-diamino-6-hydroxy
-2-mercaptopurine

(58)

+

O

HO   OH

p-hydroxy benzoic acid

61 (a)

Glacial Acetic Acid
K₂CO₃

OH

N   N

HS   N   N
          H

OH

8-(4-hydroxyphenyl)-2-mercapto-9*H*-purin-6-ol

(61)
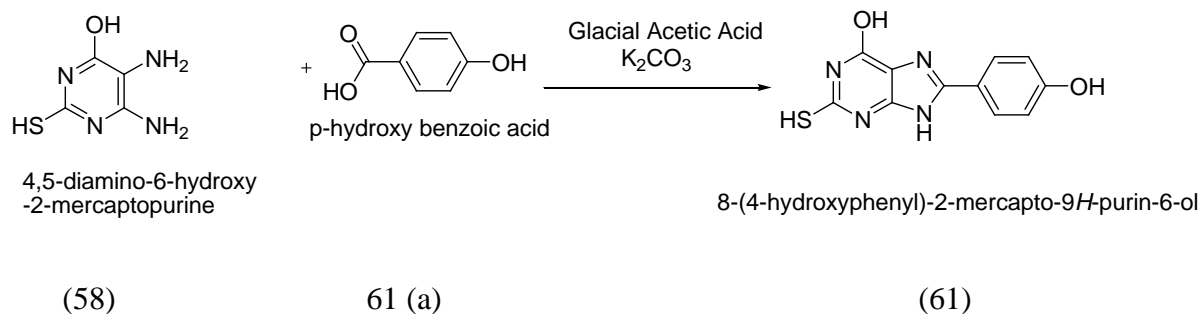
8.4.4   Synthesis of 8-(4-aminophenyl)-2-mercapto-9H-purin-6-ol (62)

A mixture of 4,5-diamino-6-hydroxy-2-mercaptopurine (0.5g, 0.0006 mol) was mixed with
p- amino benzoic acid (0.45g, 0.00064 mol). 1 g of potassium carbonate and 30 ml of glacial
acetic acid were added to the above mixture. Synthesis was carried out using both
conventional reflux as well as microwave irradiation method. The solid obtained was
washed with water and collected by vacuum filtration. Percentage yield, melting point and R_f
value were reported.

4,5-diamino-6-hydroxy
-2-mercaptopurine

p-amino benzoic acid

8-(4-aminophenyl)-2-mercapto-9*H*-purin-6-ol

(58)   62 (a)   (62)
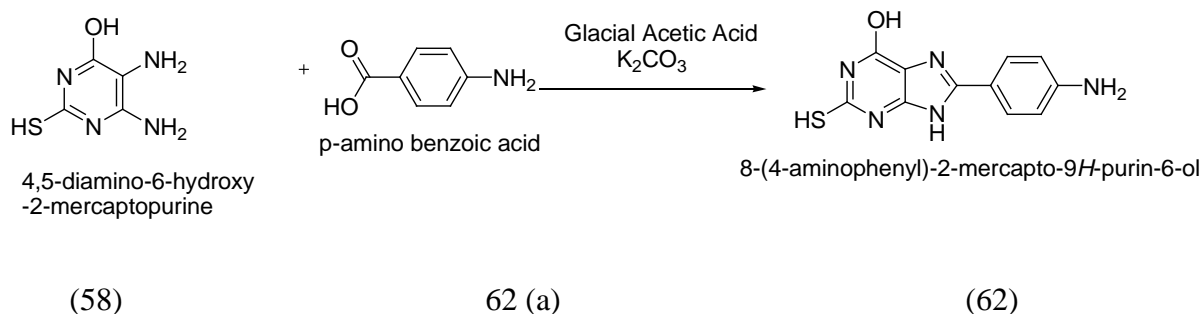
8.4.5   Synthesis of 2-mercapto-8-(4-nitrophenyl)-9H-purin-6-ol (63)

A mixture of 4,5-diamino-6-hydroxy-2-mercaptopurine (0.5g, 0.00062 mol) was mixed with
p- nitro benzoic acid (0.45g, 0.00062 mol). 1 g of potassium carbonate and 30 ml of glacial
acetic acid were added to the above mixture. Synthesis was carried out using both
conventional reflux as well as microwave irradiation method. The solid obtained was
washed with water and collected by vacuum filtration. Percentage yield, melting point and R_f
value were reported

4,5-diamino-6-hydroxy
-2-mercaptopurine

p-nitro benzoic acid

2-mercapto-8-(4-nitrophenyl)-9*H*-purin-6-ol

(58)   63 (a)   (63)
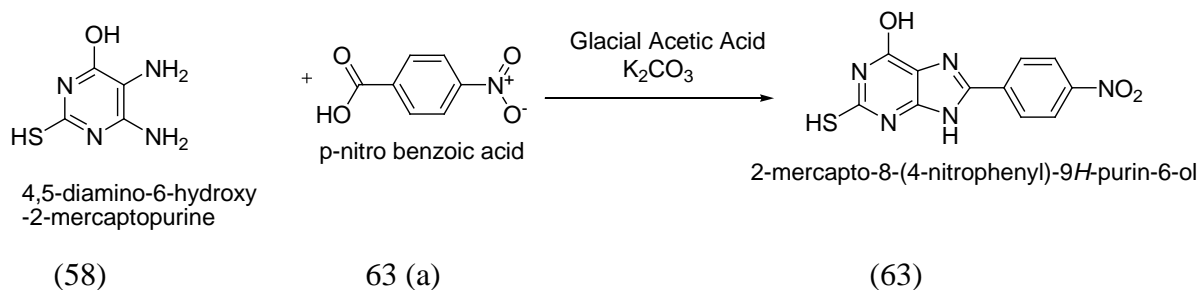
8.4.6 Synthesis of 8-(4-chlorophenyl)-2-mercapto-9H-purin-6-ol (64)

A mixture of 4,5-diamino-6-hydroxy-2-mercaptopurine (0.5g, 0.00062 mol) was mixed with *p*-chloro benzoic acid (0.45g, 0.000616 mol). 1 g of potassium carbonate and 30 ml of glacial acetic acid were added to the above mixture Synthesis was carried out using both conventional reflux as well as microwave irradiation method. The solid obtained was washed with water and collected by vacuum filtration. Percentage yield, melting point and R_f value were reported.

4,5-diamino-6-hydroxy
-2-mercaptopurine

p-chloro benzoic acid

8-(4-chlorophenyl)-2-mercapto-9*H*-purin-6-ol

(58)   64(a)   (64)
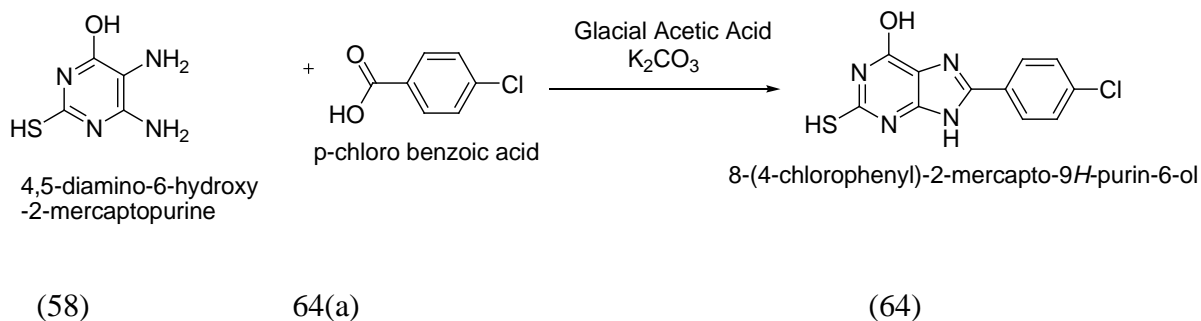
8.4.7 Synthesis of 8-(4-bromophenyl)-2-mercapto-9H-purin-6-ol (65)

A mixture of 4,5-diamino-6-hydroxy-2-mercaptopurine (0.5g,0.00062 mol) was mixed with *p*-bromo benzoic acid (0.45g, 0.0009 mol). 1 g of potassium carbonate and 30 ml of glacial acetic acid were added to the above mixture. Synthesis was carried out using both conventional reflux as well as microwave irradiation method. The solid obtained was washed with water and collected by vacuum filtration. Percentage yield, melting point and R_f value were reported.

OH
NH₂
HS   N
         N

4,5-diamino-6-hydroxy
-2-mercaptopurine

(58)

+

p-bromo benzoic acid

65(a)

Glacial Acetic Acid
K₂CO₃

8-(4-bromophenyl)-2-mercapto-9*H*-purin-6-ol

(65)
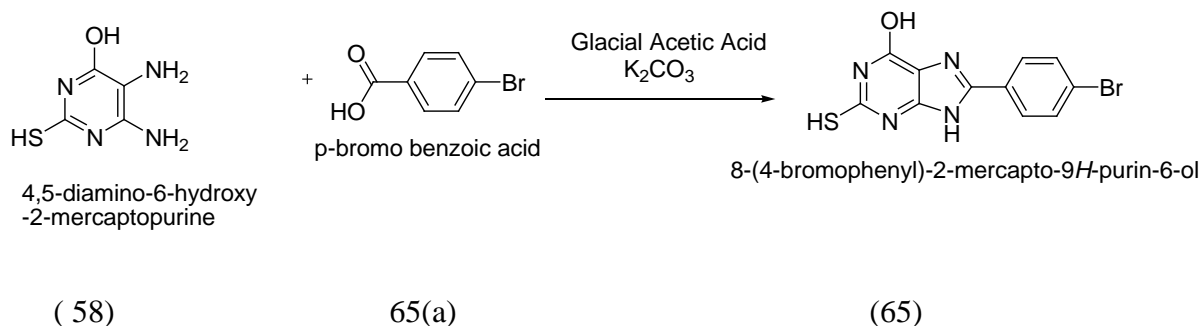
8.4.8   Synthesis of 8-(3-chlorophenyl)-2-mercapto-9H-purin-6-ol (66)

A mixture of 4,5-diamino-6-hydroxy-2-mercaptopurine (0.5g, 0.00062 mol) was mixed with *o*-chloro benzoic acid (0.45g, 0.0007 mol). 1 g of potassium carbonate and 30 ml of glacial acetic acid were added to the above mixture. Synthesis was carried out using both conventional reflux as well as microwave irradiation method. The solid obtained was washed with water and collected by vacuum filtration. Percentage yield, melting point and R_f value were reported

OH
NH₂
HS   N
         N

4,5-diamino-6-hydroxy
-2-mercaptopurine

(58)

+

o-chloro benzoic acid

66(a)

Glacial Acetic Acid
K₂CO₃

8-(3-chlorophenyl)-2-mercapto-9*H*-purin-6-ol

(66)
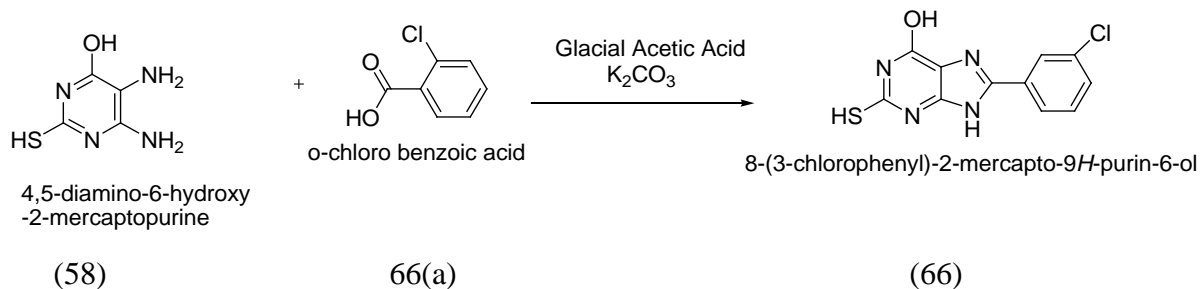
8.4.9   Synthesis of 2-mercapto-8-styryl-9H-purin-6-ol (67)

A mixture of 4,5-diamino-6-hydroxy-2-mercaptopurine (0.5g,0.00062 mol) was mixed with cinnamic acid (0.45g, 0.0008 mol). 1 g of potassium carbonate and 30 ml of glacial acetic acid were added to the above mixture. Synthesis was carried out using both conventional reflux as well as microwave irradiation method. The solid obtained was washed with water

and collected by vacuum filtration. Percentage yield, melting point and R_f value were reported

| (58) | 67 (a) | (67) |
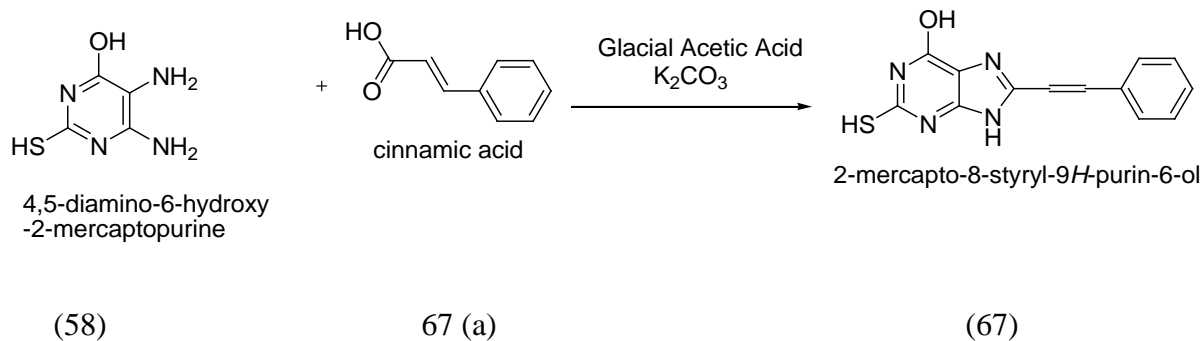
8.4.10 Synthesis of 2-mercapto-8-phenoxy-9H-purin-6-ol (68)

A mixture of 4,5-diamino-6-hydroxy-2-mercaptopurine (0.5g, 0.00062 mol) was mixed with phenyl acetic acid (0.45g, 0.00062 mol). 1 g of potassium carbonate and 30 ml of glacial acetic acid were added to the above mixture. Synthesis was carried out using both conventional reflux as well as microwave irradiation method. The solid obtained was washed with water and collected by vacuum filtration. Percentage yield, melting point and R_f value were reported**.**

| (58) | 68(a) | (68) |
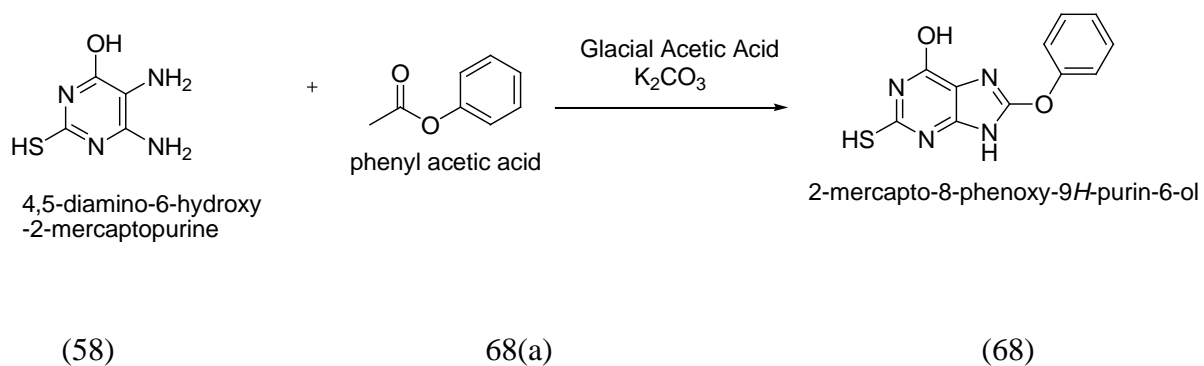
8.5 Results and Discussion

In order to obtain effective anti-Aurora Kinase-A agents , purine derivatives were successfully synthesized. A total of 10 compounds having 2-mercaptopurin-6-ol moiety which are shown as following were prepared. Synthesized compounds along with their IUPAC name are shown in Table 10.

Table 10: List of Synthesized compounds with IUPAC Name

Compound No.	IUPAC Name
59	2-mercapto-8-phenyl-6,9-dihydro-1H-purin-6-ol
60	2-mercapto-8-p-tolyl-9H-purin-6-ol
61	8-(4-hydroxyphenyl)-2-mercapto-9H-purin-6-ol
62	8-(4-aminophenyl)-2-mercapto-9H-purin-6-ol
63	2-mercapto-8-(4-nitrophenyl)-9H-purin-6-ol
64	8-(4-chlorophenyl)-2-mercapto-9H-purin-6-ol
65	8-(4-bromophenyl)-2-mercapto-9H-purin-6-ol
66	8-(3-chlorophenyl)-2-mercapto-9H-purin-6-ol
67	2-mercapto-8-styryl-9H-purin-6-ol
68	2-mercapto-8-phenoxy-9H-purin-6-ol

Table 11 (a) : Synthesis Data

No.	Conventional Method Temperature (120-130 °C)		Microwave Irradiation	
	Time (Hours)	% Yield	Time (min)	% Yield
59	42	30.36%	6	39.48%
60	46	45.6%	8	64.01%
61	48	25.65%	6	83.83%
62	50	20.3%	9	32.19%
63	40	50.4%	5	67.12%
64	36	35.5%	9	42.60%
65	45	25.5%	11	34.30%
66	44	20.5%	5	21.38%
67	50	19.8%	8	34.6%
68	40	30.3%	9	38.46%

Table 11 (b) : Summary of the Physical Data of Synthesized compounds:

Compound No.	R	Molecular Formula	Melting Point °C	R_f Value
59	$-C_6H_5$	$C_{11}H_{10}N_4OS$	284-286	0.60*
60	p-CH_3-C_6H_5	$C_{12}H_{10}N_4OS$	268-270	0.44*
61	p-OH -C_6H_5	$C_{11}H_8N_4O_2S$	270-272	0.54*
62	p-NH_2- C_6H_{5-}	$C_{11}H_9N_5OS$	292-294	0.52*
63	p-NO_2-C_6H_5	$C_{11}H_7N_5O_3S$	>300	0.31*
64	p-Cl- C_6H_5	$C_{11}H_7ClN_4OS$	286-288	0.56*
65	p-Br- C_6H_5	$C_{11}H_7BrN_4OS$	>300	0.40*
66	o- Cl -C_6H_5	$C_{11}H_7ClN_4OS$	278-280	0.32*
67	-CH=CH-C_6H_5	$C_{13}H_{10}N_4OS$	264-266	0.36*
68	-O- C_6H_5	$C_{10}H_{10}N_4O_2S$	>300	0.41*

*Solvent system : Benzene : Methanol – 4:1

8.6 Spectral Analysis of Synthesized Compounds

Chemical Structures of synthesized compounds were FT-IR spectroscopy , mass spectroscopy and ^{1}H NMR spectroscopy.

8.6.1.1 I.R. Spectra of Compound 63
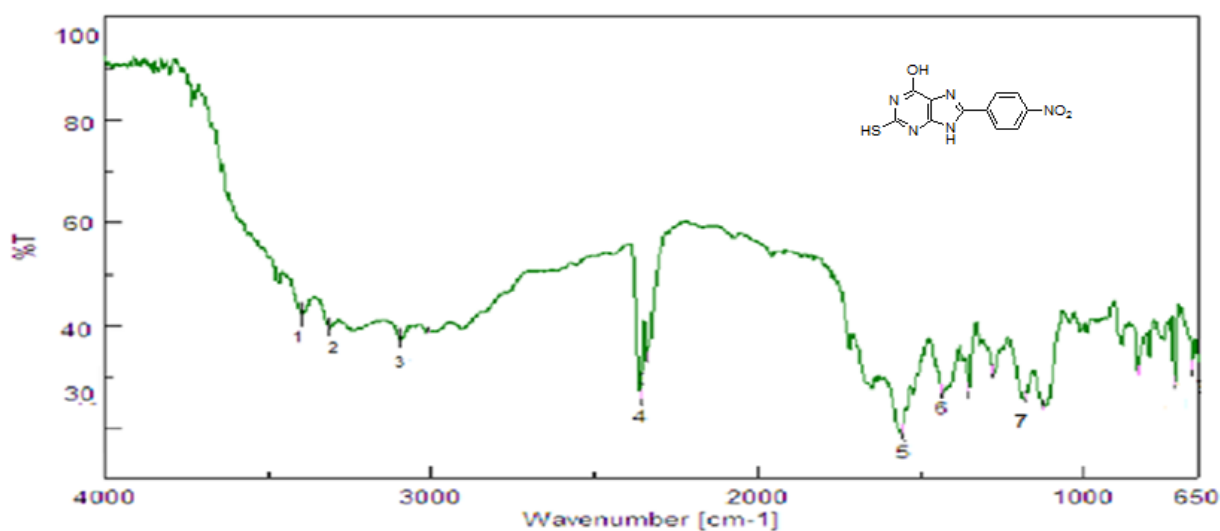
Peak No.	Wave Number (cm-1)	Functional Group
1	3398	N-H stretching
2	3300-3100	O-H aromatic stretching
3	3315	C-H stretching
4	2361	S-H stretching
5	1563	C-O stretching
6	1431	C=N stretching

8.6.1.2 Mass Spectra of Compound 63
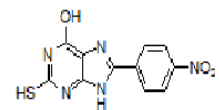
M.wt : 289
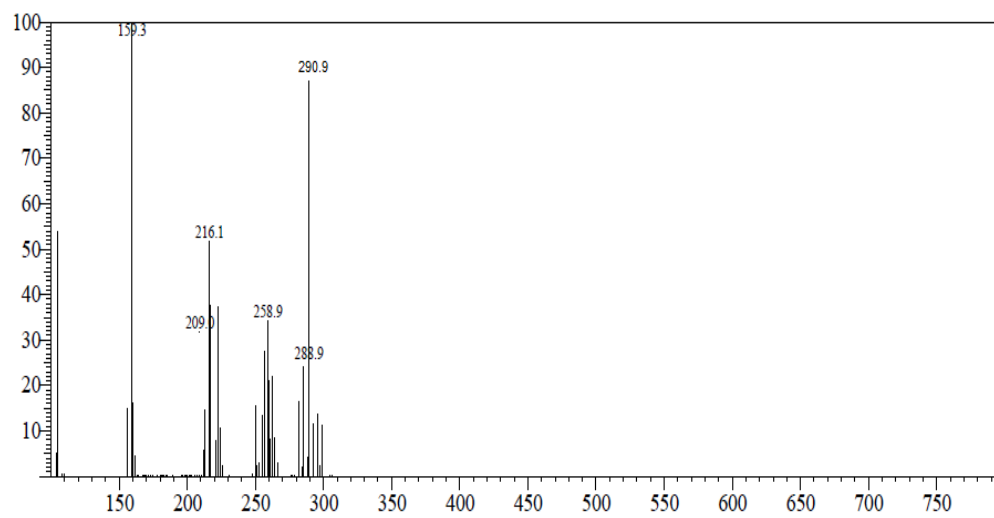
8.6.2.1 I.R. Spectra of Compound 66
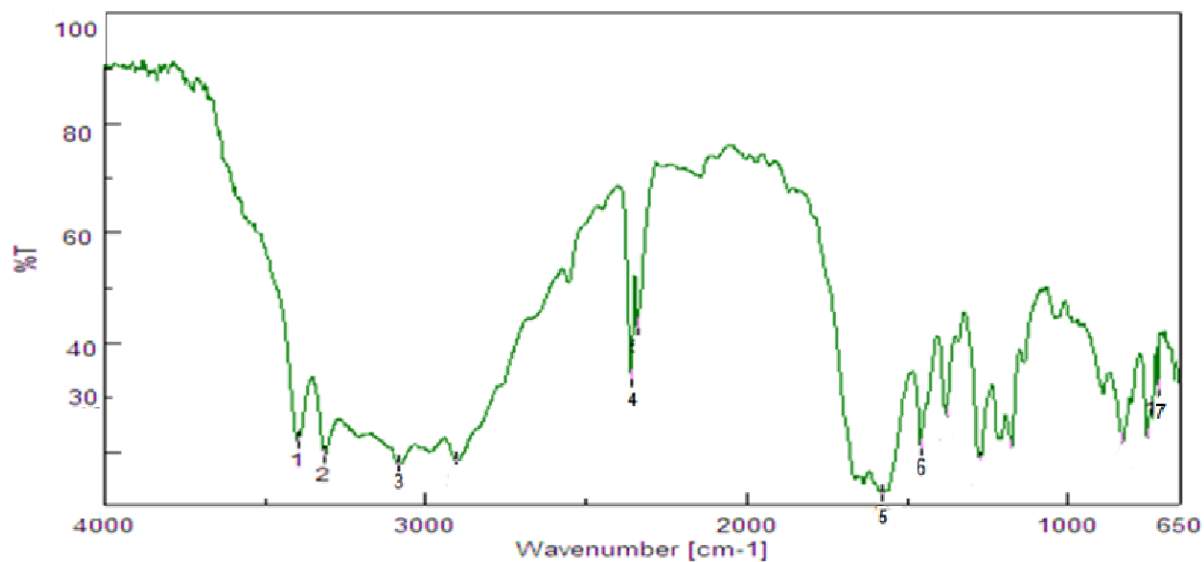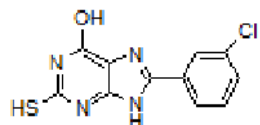
Peak No.	Wave Number (cm-1)	Functional Group
1	3398	N-H stretching
2	3314	C-H aromatic stretching
3	3300-3100	O-H stretching
4	2361	S-H stretching
5	1665	C-O stretching
6	1457	C=N stretching
7	754	C-Cl stretching

8.6.2.2 Mass Spectra of Compound 66
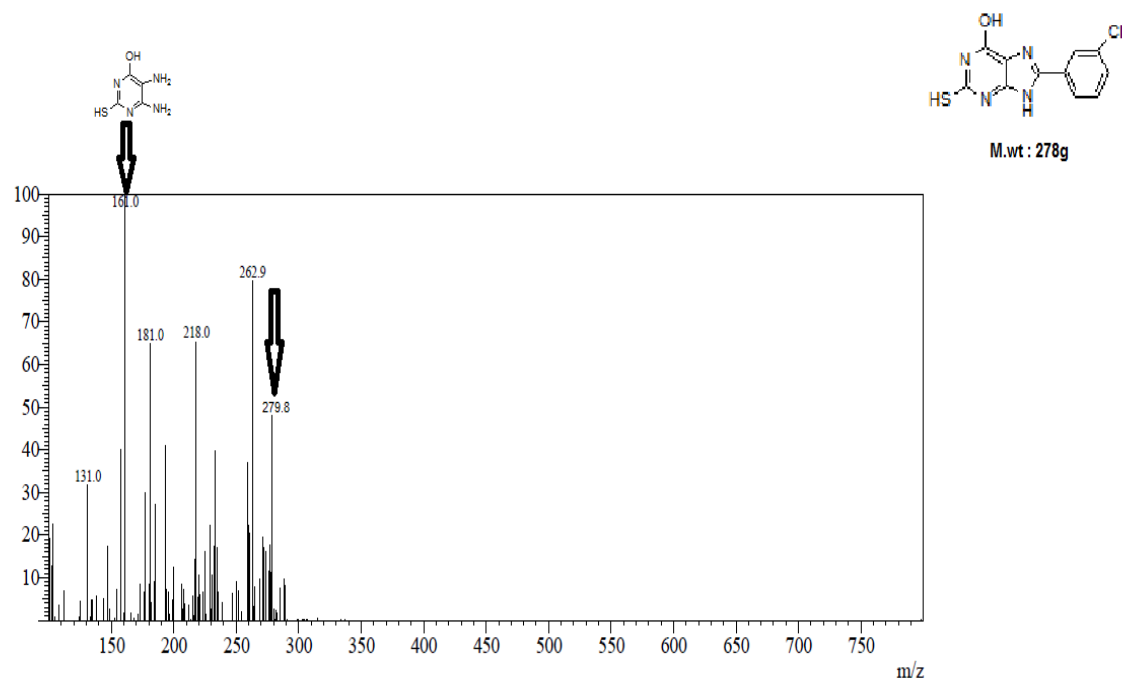
8.6.2.3 ¹H NMR Spectra of Compound 66
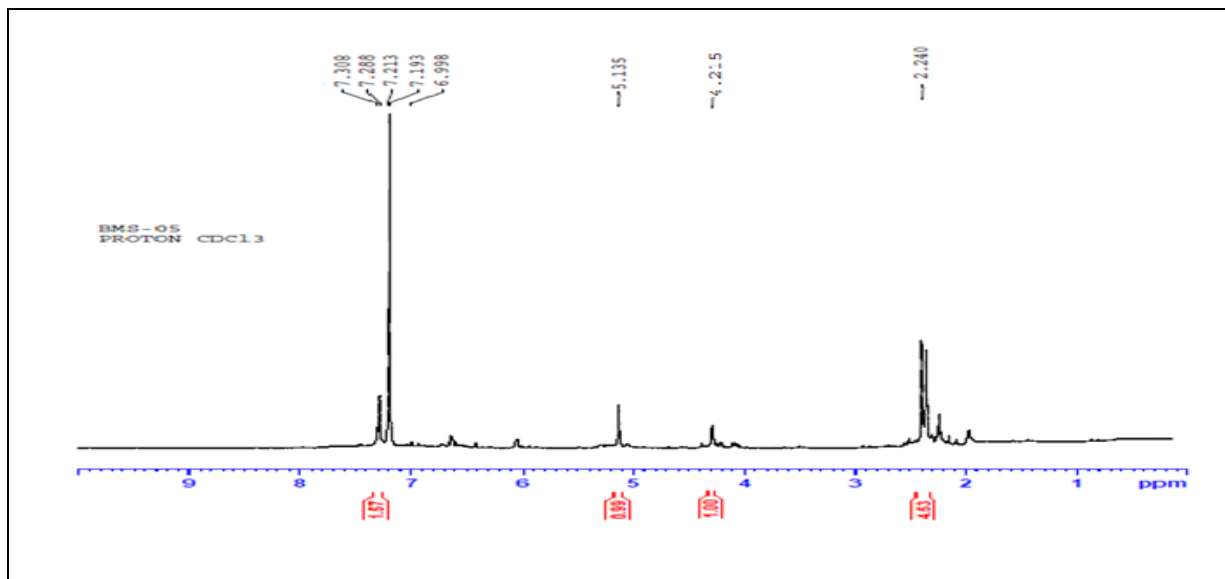
Sr. No.	Code	¹H NMR(400 MHz)	Mass
1	63	δ 6.9-7.308 (a set of signals, 4 aromatic protons), δ5.135(s, 1H) Aromatic -OH, δ4.215(s,1H) , -SH δ 2.24 (s, 1H) -NH	Molecular ion peak- 279.0 (m+1)

CHAPTER-9

EVALUATION OF BIOLOGICAL ACTIVITY

9.1 Cell lines used in *in-vitro* screening method

9.1.1 Cell line

Specific cells that can grow indefinitely given the appropriate medium and conditions i.e. living cells those are maintained *in-vitro* in artificial media of serum and nutrients for the study and growth of certain strains, experiments in controlling diseases, or study of the reaction to certain drugs or agents. (Walton, J.R *et al*., 1975) Human tumor cell line panels combined with rapid high throughput cytotoxicity testing have proven to be valuable tools for drug screening and early drug evaluation and investigation of drug resistance mechanisms.

The National Cancer Institute (NCI) pioneered the utilization of large human tumor cell line panels for drug screens, after phasing out their previously used animal models. The disease-oriented cell line panel used by NCI consists of 60 different cell lines, which consists of seven sub panels representing common solid tumors, leukemia and lymphomas. (Suggitt M *et al*., 2005) To date, more than 100,000 compounds and a large number of natural product extracts have been tested in their short-term growth inhibition assay. (Bussey KJ *et al*., 2006) Typically, compounds are applied to the cell lines in a wide concentration range, and concentrations that inhibit / kill e.g. 50 % of the cells (GI_{50}/ IC_{50}) are determined. The IC_{50} concentrations for a drug in many cell lines provide a drug specific profile, which can be compared to profiles from other drugs. This approach has successfully been used for drug mechanism classification of standard drugs, and assignment of drug action to investigational drugs and discovery of new classes of chemotherapeutic compounds.

9.1.2 Types of mammalian cell culture

a. Primary Cultures

Primary cultures are derived directly from excised, normal animal tissue and cultured either as an explant culture or following dissociation into a single cell suspension by enzyme digestion. Such cultures are initially heterogeneous but later become

dominated by fibroblasts. The preparation of primary cultures is labor intensive and they can be maintained *in-vitro* only for a limited period of time.

b. Continuous Cultures

Continuous cultures are comprised of a single cell type that can be serially propagated in culture either for a limited number of cell divisions (approximately thirty) or otherwise indefinitely. Cell lines of a finite life are usually diploid and maintain some degree of differentiation. The fact for these types of cell cultures, senescence after approximately thirty cycles of division. Means it is essential to establish a system of Master and Working banks in order to maintain such lines for long periods. Continuous cell lines that can be propagated indefinitely generally have this ability because they have been transformed into tumor cells. Tumor cell lines are often derived from actual clinical tumors, but transformation may also be induced using viral oncogenes or by chemical treatments. Transformed cell lines present the advantage of almost limitless availability, but the disadvantage of having retained very little of the original *in-vivo* characteristics.

9.1.3 Isolation of cells

Cells can be isolated from tissues for *ex-vivo* culture in several ways. Cells can be easily purified from blood; however only the white cells are capable of growth in culture. Mononuclear cells can be released from soft tissues by *enzymatic digestion* with enzymes such as collagenase, trypsin, or pronase, which break down the extracellular matrix. Alternatively, pieces of tissue can be placed in growth media, and the cells that grow out are available for culture. This method is known as *explant culture.*Cells that are cultured directly from a subject are known as *primary cells*. With the exception of some derived from tumors, most primary cell cultures have limited lifespan.After a certain number of population doublings cells undergo the process of senescence and stop dividing, while generally retaining viability.

An established or immortalized cell line acquire the ability to proliferate indefinitely either through random mutation or deliberate modification, such as artificial expression of the telomerase gene. There are numerous well established cell lines representative of

particular cell types.

9.1.4 Maintenance of cells in culture

Cells are grown and maintained at an appropriate temperature and gas mixture (typically, 37°C, 5 % CO2 and 95 % Relative Humidity) in a cell incubator. Culture conditions vary widely for each cell type and variation of conditions for a particular cell type can result in different phenotypes being expressed.

Aside from temperature and gas mixture, the most commonly varied factor in culture system is the growth medium. Recipes for growth media can vary in pH, glucose concentration, growth factors, and the presence of other nutrient components. The growth factors used to supplement media are often derived from animal blood, such as calf serum. These blood-derived ingredients pose the potential for contamination of derived pharmaceutical products with viruses or prions. Current practice is to minimize or eliminate the use of these ingredients where possible**.**

Some cells naturally live without attaching to a surface, such as cells that exist in the blood-stream. Others require a surface, such as most cells derived from solid tissues. Cells grown unattached to a surface are referred to as *suspension cultures* for example, HL60 etc. Other *adherent cultures* cells can be grown on tissue culture plastic, which may be coated with extracellular matrix components (e.g. collagen or fibronectin) to increase its adhesion properties and provide other signals needed for growth. Examples of adherent cell lines are NCI-H23, HEK-293T, MCF-7 etc.

9.1.5 Manipulation of cultured cells

As cells generally continue to divide in culture, they generally grow to fill the available area or volume. This can generate several issues:

·   Nutrient depletion in the growth media.

·   Accumulation of apoptotic/necrotic (dead) cells.

·   Cell-to-cell contact can stimulate cell cycle arrest, causing cells to stop dividing known as contact inhibition.

·   Cell-to-cell contact can stimulate promiscuous and unwanted cellular

differentiation.

These issues can be dealt with using tissue culture methods that rely on sterile technique. These methods aim to avoid contamination with bacteria or yeast that will compete with mammalian cells for nutrients and/or cause cell infection and cell death. Manipulations are typically carried out in a biosafety hood or laminar flow cabinet to exclude contaminating micro-organisms. Antibiotics can also be added to the growth media.

Amongst the common manipulations carried out on culture cells are media changes, passaging cells, and transfecting cells

a. Media changes

The purpose of media changes is to replenish nutrients and avoid the build up of potentially harmful metabolic byproducts and dead cells. In the case of suspension cultures, cells can be separated from the media by centrifugation and re-suspended in fresh media. In the case of adherent cultures, the media can be removed directly by aspiration and replaced. (MacLeod RAF *et al*., 1999)

b. Passaging cells

Passaging or sub-culturing cell culture involves transferring a small number of cells into a new vessel. Cells can be cultured for a longer time if they are split regularly, as it avoids the senescence associated with prolonged high cell density. Suspension culture are easily passaged with a small amount of culture containing a few cells diluted in a larger volume of fresh media. For adherent cultures, cells first need to be detached; this was historically done with a mixture of trypsin-EDTA; however other enzyme mixes are now available for this purpose. A small number of detached cells can then be used to seed a new culture.

9.2 Description of cell lines used in the cytotoxicity study

9.2.1 HCT-15 Cell line
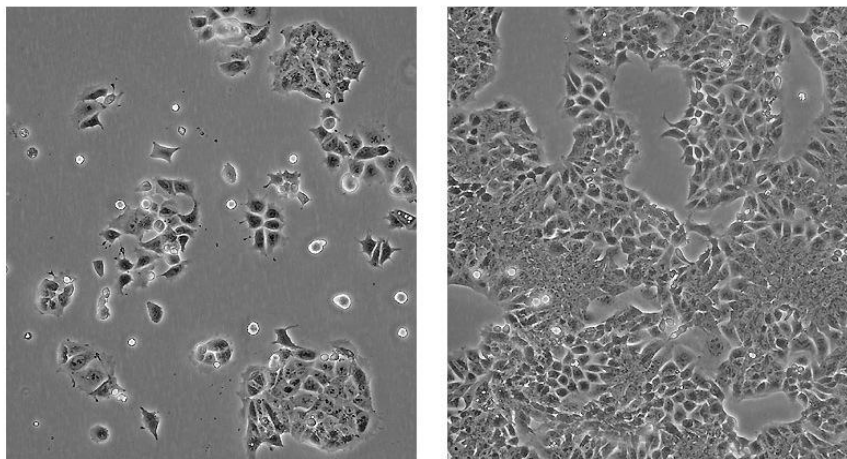
Figure 9.1. HCT-15 cell line

Organism: *Homo sapiens* (Human)

Tissue: Colon

Morphology: epithelial

Growth properties: adherent

Medium

1. Culture Medium: RPMI-1640 Medium, 10% fetal bovine serum (FBS).

Freeze Medium: RPMI-1640 Medium, 10% FBS, 5%V/V DMSO.(Link 25) HCT-15 is a human colorectal adenocarcinoma that has a mutated p53 tumor suppressor gene and overexpresses P-glycoprotein. P-glycoprotein acts as an efflux pump resulting in decreased intracellular accumulation of certain drugs contributing to drug resistance.

9.2.2. MCF-7 Cell line
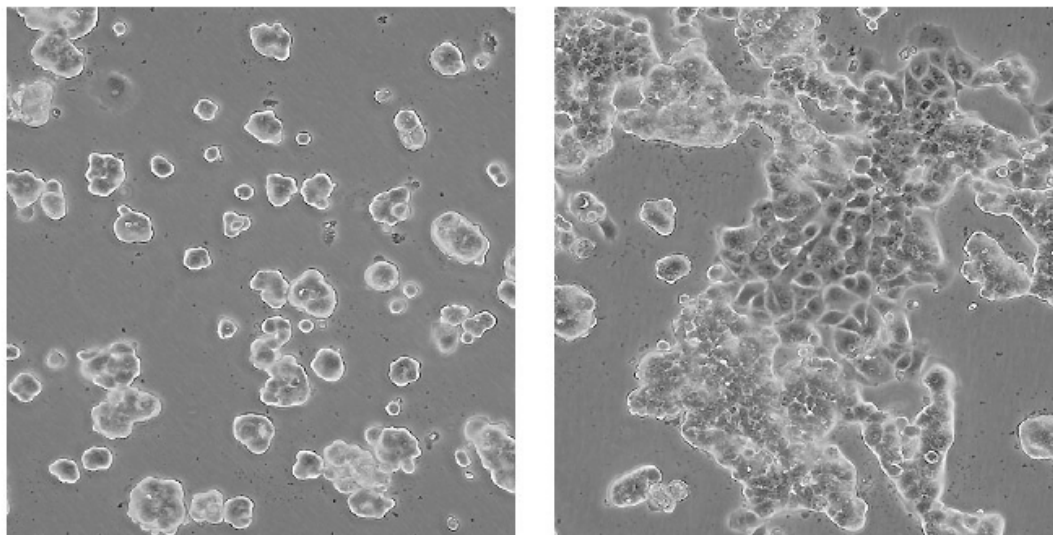
Figure 9.2. MCF-7 cell line

Organism: *Homo sapiens* (human)

Tissue: mammary gland; breast Adenocarcinoma; derived from metastatic site: pleural effusion

Morphology: epithelial

Growth Properties: adherent

Medium

1. Culture medium : Eagle's Minimum Essential Medium, 0.01mg/ml bovine insulin, fetal bovine serum to a final concentration of 10% .

2. Freeze medium :Eagle's Minimum Essential Medium, 0.01mg/ml bovine insulin, fetal bovine serum to a final concentration of 10%, 5% V/V DMSO

The MCF7 line retains several characteristics of differentiated mammary epithelium including ability to process estradiol via cytoplasmic estrogen receptors and the capability of forming domes. Growth of MCF7 cells is inhibited by tumor necrosis factor

alpha (TNF alpha). Secretion of IGFBP's can be modulated by treatment with antiestrogens)

MCF-7 was isolated in 1970 from a 69-year-old Caucasian woman. MCF-7 is the acronym of Michigan Cancer Foundation - 7, referring to the institute in Detroit where the cell line was established in 1973 by Herbert Soule and co-workers (Soule, HD *et al.,*1973). Prior to MCF-7, it was not possible for cancer researchers to obtain a mammary cell line that was capable of living longer than a few months (Glodek, Cass., 1990). The patient, whose name is unknown to the vast majority of cancer researchers, died in 1970. Her cells were the source of much of current knowledge about breast cancer (Soule, HD *et al.,* 1973). Her name was Frances Mallon and, at the time of sampling, she was a nun in the convent of the Immaculate Heart of Mary (Monroe, Michigan) under the name of Sister Catherine Frances.

9.2.3 A-375 Cell line

Organism: Homo sapiens (human)

Tissue: skin; malignant melanoma

Morphology: epithelial

Growth properties: adherent

Medium

1. Culture Medium: DMEM (high glucose), 10% fetal bovine serum (FBS).

2. Freeze Medium: 70% DMEM, 10% FBS, 5%V/V DMSO.

The growth of A375 cells is inhibited by IL1-alpha or IL1-beta at concentrations of 10-30 pg/mL, which cause growth arrest in phase G0/G1 of the cell cycle. Accordingly, A375 cells have been used in research on cytokines for bioassays of these factors. The assay is not influenced by prostaglandin E2, plant lectins, bacterial endotoxins and cytokines such as IL2, TNF, interferons or colony stimulating factors. A375 cells can be used also to assay bovine IL1. normal A375 cells exclusively express the ET (endothelins) receptor type B, The differentiation of A375 melanoma cells is induced by treatment with bromodeoxyuridine leads to phenotypical changes that are accompanied also by induction of endothelin receptor type A expression. The A375 cells also express large numbers of high-affinity receptors for bombesin and GRP (Gastrin releasing peptide). Cell extracts from A375 cells have been shown to contain catalase, which is identical with Erythrocyte-derived growth promoting factor.

Treatment of the cell extracts with an irreversible catalase inhibitor, aminotriazole, abolishes both the catalase and growth-promoting activities.
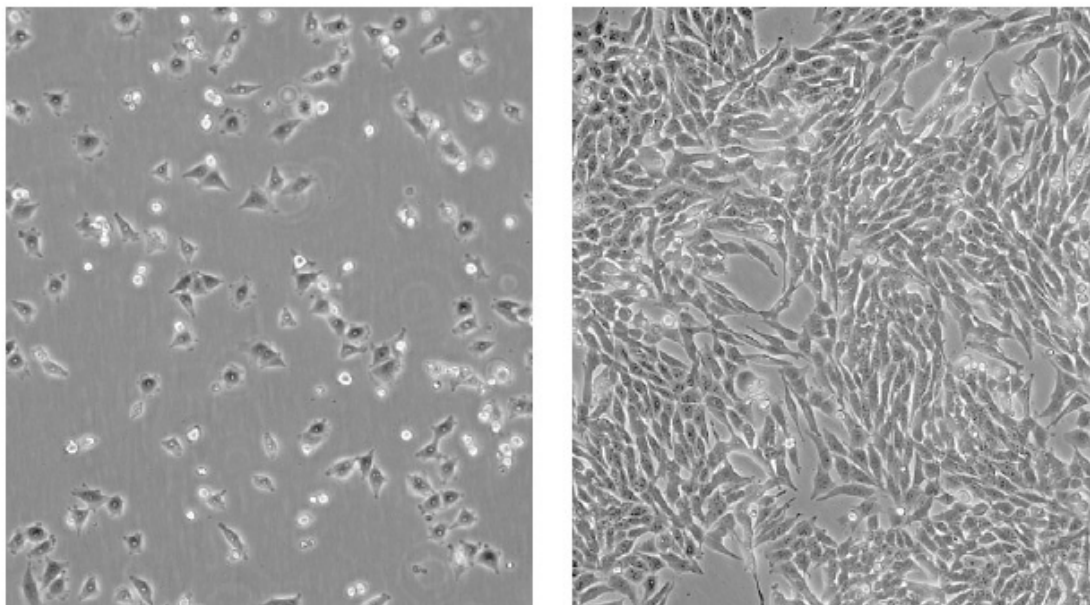
Figure 9.3: A-375 cell line

9.3 *In-vitro* cytotoxicity assays

To study cytotoxic activity of a compound, cytotoxic assays are carried out. It is now well-documented that apoptosis or Programmed cell death is the key mechanism by which Chemotherapeutic agents exert their cytotoxicity.

These assays are principally of two types:

I. **Radioactive and non-radioactive assays** that measure increases in plasma membrane permeability, since dying cells become leaky.

II. **Colorimetric assays** that measure reduction in the metabolic activity of mitochondria; mitochondria in dead cells cannot metabolize dyes, while mitochondria in live cells can metabolize it and so are distinguished.

Depending on the knowledge of physiological events occurring in cell cycle and death, assay type is chosen and used. A number of methods have now been developed to study apoptosis in cell populations. Cytotoxicity tests measure the concentration of

the substance that damages components, structures or cellular biochemical pathways, and they also allow direct extrapolation of quantitative data to similar *in-vivo* situations. (Freshney IR 5th ed., 2001) This refers to the *in-vitro* assessment of material to determine whether or not it releases toxic chemicals in sufficient quantities to kill cells either directly or indirectly through the inhibition of cell metabolic pathways.

a. Common Basic Steps of *in-vitro* Assays

Although the techniques for testing drug sensitivities of tumor cells differ, each employ four common basic steps:

i.   Isolation of cells,

ii.   Incubation of cells with drugs,

iii.   Assessment of cell survival, and

iv.   Interpretation of the result.

b. Ideal characteristics of *in-vitro* methods

· An ideal *in-vitro* screening method should be simple economical, reproducible, rapid and sensitive.

· The assay should be applicable to large number of tumor types and test compounds.

· The choice of cell lines should be representative of clinical situation as close as possible.

· The range of drug concentration used *in-vitro* should be comparable to that expected for *in-vivo* treatments.

· The assay should be able to process a large number of samples quickly and in automated fashion.

· Data acquisition should be simple, easily interpreted and applied.

c. Advantages of *in-vitro* methods:

The development of *in-vitro* cytotoxicity assays has been driven by the need

· To rapidly evaluate the potential toxicity of large numbers of compounds,

· To limit animal experimentation whenever possible, and

· To carry out tests with small quantities of compound.

· Most cost effective and easier to manage.

· The most promising advantage of *in-vitro* methods over in-vivo method is, here culture can be cultivated under a controlled environment (pH, temperature, humidity, oxygen carbon-dioxide balance etc.) resulting in homogeneous batches of cells and thus minimizing experimental errors.

d. Limitation of *in-vitro* methods:

They often furnish false positive results (compounds show no activity *in-vivo*) and false negative results (compounds show no activity *in-vitro* but show activity *in-vivo* as they need to be bio-transformed *in-vivo* to pharmacologically active compounds).

A second pitfall is that role of pharmacokinetic in determining drug effects cannot be evaluated *in-vitro*.

Geometry of solid tumors *in-vivo* is very different from that of cells growing *in-vitro* in suspension or monolayer culture.

Table 12 : *In-vitro* cytotoxicity assays and theirs principle

Sr. no.	Category of viability assay	Type of assay	Principles
1.	Membrane integrity assay	1. Trypan blue dye exclusion assay 2. Fluorescent dyes assay 3.LDH leakage assay	The determination of membrane integrity via dye exclusion from live cells.
2.	Functional assay	1. MTT, XTT assay 2. Crystal violet /Acid phosphatase (AP) assay 3. Alamar Blue oxidation reduction assay 4. Neutral red assay 5. [3H]-thymidin / BrdU Incorporation	Examining metabolic components that are necessary for cell growth.
3.	Protein assay	1. SRB assay	Based on measurement of

			total protein content.
4.	DNA labeling assay	1. Fluorescent conjugates	Simultaneous cell selection and viability assay
5.	Morphological Assay	1. Microscopic observation	Determination of morphological change
6.	Reproductive assay	1. Colony formation assay	Determination of growth rate

9.4 MTT assay

It is a laboratory test and a standard colorimetric assay for measuring cellular growth. It can also be used to determine cytotoxicity of potential medicinal agents and other toxic materials.

This assay is a sensitive, quantitative and reliable colorimetric assay that measures viability, proliferation and activation of cells. The assay is based on the capacity of mitochondrial dehydrogenase enzymes in living cells to convert the yellow water-soluble substrate 3-(4,5-dimethylthiazol-2-yl)-2,5-diphenyl tetrazolium bromide (MTT) into a dark blue formazan product which is insoluble in water. The amount of formazan produced is directly proportional to the cell number in range of cell lines. (Cory AH *et al*., 1991)

| MTT | formazan |
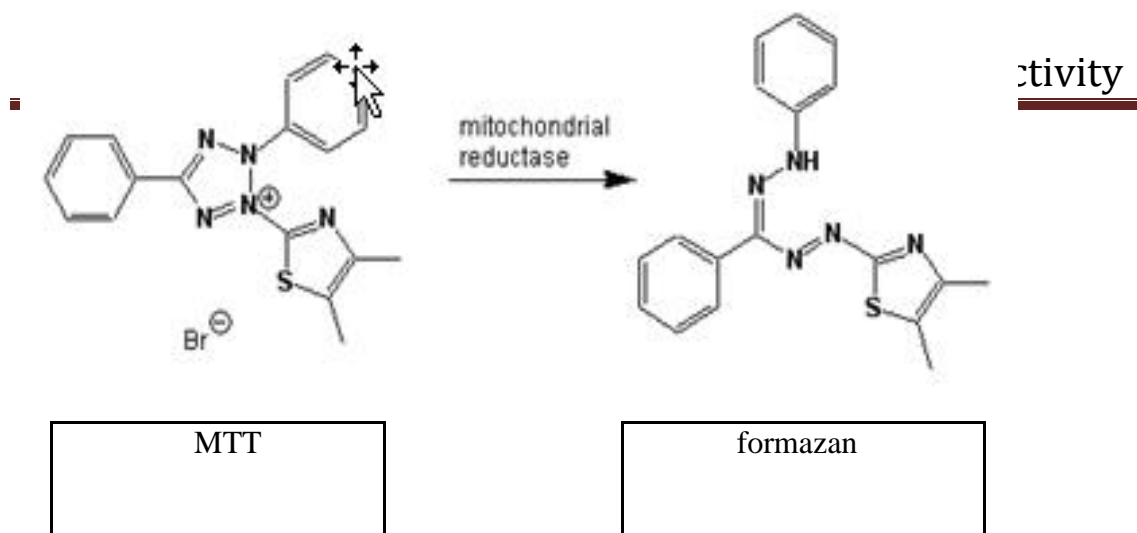
Figure 9.4 : Principle of MTT assay

a. Applications

MTT used for the non-radioactive, spectrophotometric quantification of cell proliferation and viability in cell populations using the 96-well-plate format. It can be used for:

· Measurement of cell proliferation in response to growth factors, cytokines, mitogens, and nutrients.

· Analysis of cytotoxic and cytostatic compounds, such as anti-cancer drugs and other pharmaceutical compounds.

· Assessment of growth-inhibitory antibodies and physiological mediators.

· **Advantages**

Rapid, versatile, quantitative and highly reproducible

Adaptable to large-scale screening; relevant for most cells

MTT reduction correlates to indices of cellular protein and earlier cell number

More sensitive and earlier predictor of toxicity than classical LDH or neutral red measurements

Disadvantages

Production of the MTT product is dependent on the MTT concentration in the medium. The kinetics and degree of saturation are dependent on cell type.

Assay is less effective in the absence of cell proliferation.

MTT cannot distinguish between cytostatic and cytocidal effect.

Individual cell numbers are not quantitated and results are expressed as a percentage of control absorbance.

Test is less effective if cells have been cultured in the same media that has supported growth for a few days, which leads to under estimation of control and untreated samples.

To summarize, the design of a screening assay is an array of multiple choices, all of which have significant impacts on the outcome of the overall drug discovery process. Most importantly, the correct selection of the target and assay format, detailed optimization and miniaturization as well as the choice of appropriate detection technology for each individual assay can lead to savings in time, money and labor along with improved data quality in all stages of the drug discovery process.

The following materials were procured for the project work and were maintained at appropriate temperature as recommended by the manufacturer.

9.5.1 Material & Methods:

a. Reagents

1. Trypan blue Dye (Hyclone, Lot No: 029K2358, 100 ml)
2. Triton X100 (MP Biomedicals, Lot No: 8009H, 100 ml)
3. DMSO cell culture grade (Bioworld, Lot No: 1388B230, 500 ml)
4. Sodium bicarbonate (Bioworld, Lot No: 1775B29)
5. Amphotericin B (Himedia, Lot No: 1397893, 100 ml)
6. Penicillin and Streptomycin solution stabilized (Sigma, Lot No: 1208029, 100 ml)

7. EDTA (MP Biomedicals, Lot No: YY02022B207Y)

8. DPBS / modified 1X (Dulbecoo's phosphate buffer saline without Ca^+ and Mg^+) (Himedia, Lot No: LW537, 100 ml)

9. Trypsin 1X Gamma irradiated (SAFC Bioscience, Lot No: 8NO535, 500 ml)

10. Methotrexate (MP Biomedicals, Cat no. 102299, Lot no. R27204)

11. Triton – X 100 (Bioworld, Cat no. 730208, Lot no. 1 8278075)

12. Iso Propanol (Finar Chemicals, Cat no. 11390, Lot no. 19075330)

b. Media:

1. DMEM (Dulbecoos Modified Eagels medium, low glucose with glutamine) (MP Biomedical, Lot No: C1478),

2. FBS (Fetal Bovine Serum, South American origin, 500 ml) (Quaditive, Lot No: 103128, 500 ml),

3. Tryptone Soya broth (TSB) (Himedia, Lot No: YH031).

c. Glass wares and plastic wares

1. 96-well microtiter plate (Flat Bottom, U Bottom, V Bottom),

2. Tissue culture flasks (75 cm^2 T Flask vented and 150 cm^2 T Flask vented),

3. Falcon tubes (15 ml, 50 ml), Cryotubes (2ml), Cell scrapper,

5. Reagent bottles (100 ml, 250 ml, 500 ml, 1000 ml),

6. Haemocytometer cell counting chamber.

d. Equipments

1. Fluorescence inverted microscope (Leica DM IL, Germany),

2. Biosafety cabinet classII (Esco, Singapore),

3. Cytotoxic safety cabinet (Esco, Singapore),

4. CO_2 incubator (RS Biotech, mini galaxy A, Scotland),

5. Deep freezer (Dairei, Denmark),

6. ELISA plate reader (Thermo, USA),

7. Micropipettes (Eppendorff, Germany),

8. RO water system (Millipore, USA),

9. Electronic water bath (Genei, India).

e. Cell proliferation kit

f.

1. MTT Dye Powder (Serva Electrophoresis, Cat no. 20395)

9.5.2 Methods

Preparation of compound dilution

Stock solutions of compounds were prepared in 2% DMSO at concentration of 100μM and culture medium with various concentration of samples were used in the assay. The final concentration of DMSO(2%) used does not interfere cell viability (Li-Jun Yang et al., 2009).

Table 13 : **Stock Solution of Compounds**

Compounds	MW	1M=xmg/ml	1 mM soln. (mg/5ml)
BMS04	258	258	1.29
BMS03	260	260	1.3
BMS02	259	259	1.295
BMS09	270	270	1.35

100 µM of 1mM conc. of test compounds was added in to 900 µl of culture media and as a result 100 µM conc. of test compound was obtained.

Than 1:3 dilution of test compound was done as shown in table. It was done by mixing 50 µl of test compound with 100 µl of complete media. For this initially 100 µl of complete media was added into well no. 1-9. Well no. 10 contained 150 µl test substance only, from that 50 µl was pipette out and added into well 9 which already contain 100 µl of complete midia, which lead to 1:3 dilution of test compound. Same procedure was repeated 9 times in order to get final conc. of test compounds upto 0.005 µM.

Table 14 : (1:3) dilution of test compound used in the assay

Well no. 1-9 contain complete media 100µl										
Well No.	**1**	**2**	**3**	**4**	**5**	**6**	**7**	**8**	**9**	**10**
Compound dilution	50 µl mixture from well 2	50 µl mixture from well 3	50 µl mixture from well 4	50 µl mixture from well 5	50 µl mixture from well 6	50 µl mixture from well 7	50 µl mixture from well 8	50 µl mixture from well 9	50 µl T.C. from well 10	150 µl T.C.
Final con. (µM)	0.005	0.015	0.045	0.13	0.41	1.23	3.7	11.1	33.3	100

Where, T.C.= Test compound

PLATE ASSIGNMENT

	1	2	3	4	5	6	7	8	9	10	11	12	
A	0.005 µg/ml	0.01 µg/ml	0.04 µg/ml	0.13 µg/ml	0.41 µg/ml	1.23 µg/ml	3.7 µg/ml	11.11 µg/ml	33.33 µg/ml	100 µg/ml	NC	PC	Sample 1
B	0.005 µg/ml	0.01 µg/ml	0.04 µg/ml	0.13 µg/ml	0.41 µg/ml	1.23 µg/ml	3.7 µg/ml	11.11 µg/ml	33.33 µg/ml	100 µg/ml	NC	PC	
C	0.005 µg/ml	0.01 µg/ml	0.04 µg/ml	0.13 µg/ml	0.41 µg/ml	1.23 µg/ml	3.7 µg/ml	11.11 µg/ml	33.33 µg/ml	100 µg/ml	NC	PC	Sample 2
D	0.005 µg/ml	0.01 µg/ml	0.04 µg/ml	0.13 µg/ml	0.41 µg/ml	1.23 µg/ml	3.7 µg/ml	11.11 µg/ml	33.33 µg/ml	100 µg/ml	NC	PC	
E	0.005 µg/ml	0.01 µg/ml	0.04 µg/ml	0.13 µg/ml	0.41 µg/ml	1.23 µg/ml	3.7 µg/ml	11.11 µg/ml	33.33 µg/ml	100 µg/ml	NC	PC	Sample 3
F	0.005 µg/ml	0.01 µg/ml	0.04 µg/ml	0.13 µg/ml	0.41 µg/ml	1.23 µg/ml	3.7 µg/ml	11.11 µg/ml	33.33 µg/ml	100 µg/ml	NC	PC	
G	0.005 µg/ml	0.01 µg/ml	0.04 µg/ml	0.13 µg/ml	0.41 µg/ml	1.23 µg/ml	3.7 µg/ml	11.11 µg/ml	33.33 µg/ml	100 µg/ml	NC	PC	Sample 4
H	0.005 µg/ml	0.01 µg/ml	0.04 µg/ml	0.13 µg/ml	0.41 µg/ml	1.23 µg/ml	3.7 µg/ml	11.11 µg/ml	33.33 µg/ml	100 µg/ml	NC	PC	

Where, NC-Negative control-Only Media

PC-Positive control-Media+Cell+DMSO (without test compound)

Reference substances:

Doxorubicin, a cytotoxic anticancer substance used in antineoplastic therapy also allowing us to classify the thiazole derivatives according to their relative toxicity. MW of doxorubicin is 545.3 stock solution of it was prepared with 1 ml of DMSO, which produces stock solution of doxorubicin of 10mM conc. Stock solution was further diluted for 10 times using DMSO to obtain 1mM solution.

Characterization of cell lines and culture media

Characterization is essential not only when deriving new lines, but also when a cell line is obtained from a cell bank or other laboratory. Cultures were examined under an inverted phase microscope before start of experiments and frequent assessments are made of the viability of the cell population throughout the experimental periods.

Testing for Microbial Contamination

The two methods generally used by us in our laboratory to check for bacterial and fungal contamination. Detection carried out using special media like Fluid thiogycolate media (TGM) and Tryptone Soya broth (TSB) and direct observation using Grams stain.

Contamination by bacteria, yeast or fungi was detected by an increase in turbidity of the medium and/or a decrease in pH (yellow in media containing phenol red as a pH indicator). Cells were inspected daily for presence or absence of microbial growth.

9.5.3 Protocol: (Freshney IR, 5th ed., 2005 and Sigma)

· Cell lines were cultured in the absence of antibiotics prior to testing using 25 cm^2 non-vented T-flask.

· In case of adherent cell line, attached cells were bringing in to into suspension using a cell scraper. Suspension cell lines were tested directly.

· 1.5 ml test sample (Cells) were Inoculated in to two separate test tubes of each containing Thioglycollate Medium (TGM) and Tryptone Soya broth (TSB).

· 0.1 ml *E. Coli,* 0.1 ml *B. Subtilis and* 0.1 ml *C. Sporogenes* inoculated in to separate test tubes (duplicate) containing (TGM) and (TSB). These were act as positive controls where as two separate test tubes of each containing (TGM) and

(TSB) un-inoculated as negative controls.

Broths were incubated as follows:

· For TSB, one broth of each pair were incubated at 32 ºC the other at 22 ºC for 4 days.

· For TGM, one broth of each pair were incubated at 32 ºC the other at 22 ºC for

4 days.

· For the TGM inoculated with *C. Sporogenes* incubate at 32 ℃ for 4 days.

Note: Test and Control broths were examined for turbidity after 4 days.

Criteria for a Validity of results: If control broths show evidence of bacteria and fungi within 4 days of incubation in all positive control broths and the negative control broths show no evidence of bacteria and fungi.

Criteria for a Positive Result: Test broths containing bacteria or fungi show turbidity.

Criteria for a Negative Result: Test broths should be clear and show no evidence of turbidity.

9.5.4. Preparation of media

Preparation of DMEM:

9.0 gms of DMEM powder was added in 1litre of distilled water and then it was stir continuously until clear solution formed. To this, $NaHCO_3$ was added to maintain pH 7.0 – 7.2 and then solution was filtered using memb rane filtration assembly. It was sterile in Autoclave and Stored in reservoir bottle in refrigerator at 4^oC.

Preparation of the Trypsin dilution:

5 ml of Trypsin solution was pipette out in to 50 ml falcon centrifuge tube containing 45 ml of PBS using 10 ml pipette.

9.5.5 Determination of cell viability, density and population doubling time

The quantification of cellular growth, including proliferation and viability, has become an essential tool for working on cell-based studies.

a. Cell viability by Trypan Blue Dye Exclusion Method

The viability of cells was determined by the Trypan Blue dye exclusion method. It takes advantage of the ability of healthy cells with uncompromised cytoplasmic membrane integrity to exclude dyes such as trypan blue. (Freshney IR., 5th ed., 2005)

1. Haemocytometer Cell Counts

1. Hemocytometer and cover slip were cleaned and wiped with 70% alcohol. Then cover slip were placed on haemocytometer.
2. In separate 2 ml centrifuge tube, cell suspension (cells in culture media) was added. Than two fold dilution of reaction mixture was prepared by mixing aliquot of 0.1 ml cell suspensions with 0.1 ml trypan blue.
3. Afterwards 0.1 ml of Cell suspension was than placed in to chamber of haemocytometer.
4. By using a Lieca inverted microscope, numbers of cells were counted in 1 mm^2 area with use of 10X objective.
5. Viable and non-viable cells were counted in both halves of the chamber.

2. Calculations

Total number of viable cells = A $\times$ B $\times$ C $\times$4

(1) 10

(2) Total dead cell count = A $\times$ B $\times$ D $\times$ 10^4 Where,

      A = Vol. Of cell solution (ml)

      B = Dilution factor in trypan blue

      C = Mean number of unstained cells

D = Mean number of dead/stained cells

10^4 = Conversion of 0.1 mm^3 to ml

Total cell count = Viable cell count + dead cell count

% viability = (Viable cell count / Total cell count) $\times$ 100

Note: Cell quantification, module 4B:1, Hemocytometer cell counts and viability studies, 1.1 – 1.5 used as reference in counting of cells

3. Cell density: cells/cm^2

It was particularly important in case of adherent cell line like MCF – 7. It was calculated by following equation:

[No. of cells / well or flask] / [surface area of well or flask]

4. Population doubling time (PDT)

It is the time expressed in hours, taken for cell No. to double and is reciprocal of the multiplication rate. (1/r)

N_H = No. of cells harvested at the end of growth period that is t_2

N_I = No. of cells inoculated at time t_1 = 0

n = 3.32 (log N_H — log N_I)

PDT = total time elapsed / no. of generations = 1/r

5. Multiplication rate (r): No. of generation that occurs per unit time and is usually expressed as population doubling in 24 hours.

$r = 3.32 \, (\log N_H — \log N_I) \, / \, t_2 – t_1.$

b. Subculturing/passaging of cell lines

1. Subculturing of adherent cell lines

Adherent cell-line was subcultured as per following protocol (Freshney IR, 5th ed., 2001 and Sigma). All the reagents and cell lines were bring at room temperature before start of sub culture which include FBS, DMEM, EDTA – Trypsin solution (Trypsin – EDTA made by diluting the stock 1/10 by adding PBS only) and antibiotics. Only particular cell line was handled under cytotoxicity cabinet to prevent cross contamination of cell lines.

Protocol:

- Cells were splitted when they were approximately 80 % confluence.

- Cells were washed with 0.1 ml cm2 / flask (2.5 ml in case of 25 cm2 flask) DPBS

    – EDTA (1 mM EDTA) solution. The monolayer adhere t o flask was gently rinsed by rocking the flask back and forth.

- After 5 minutes, the excess PBS – EDTA was aspirate d from the flask.

- To the above flask, 0.1 – 0.2 ml / cm2 trypsin was added until the entire monolayer was covered than incubate it for 3 – 5 mi n. at room temperature to detach the cells from monolayer.

- Cells were dispersed into a single cell suspension by pippeting the cell solution up and down. The cells were added in to media flask (DMEM + DPBS) containing FBS in it (FBS inactivates the trypsin, which was why it had to be

rinsed off with PBS – EDTA initially)

· Cells were counted by haemocytometer and diluted to the appropriate concentration for seeding. Finally, the appropriate volume of cell suspension were added in to a new flask containing medium along with 1 % antibiotic solution and place flask in 5 % CO2 incubator at 37 oC, 75 % Relative Humidity.

· This splitting / passage was repeated every 3 – 4 d ays, so that they were not diluted too much or overgrown.

·

2. **Subculturing of suspension cell line**: (Freshney IR, 5th ed., 2005)

Method for subculturing of suspension cell line is little different than adherent cell line.

Protocol:

· Cultures were observed under an inverted microscope (Leica, DMIL) using 10X objective.

Yellow color of media indicated that cells were overgrown and than centrifuge the culture flask at 150 gm for 5 minutes. After centrifugation (minispin centrifuge, eppendrof), flask was re-seeded at a slightly higher cell density and 10 – 20% of conditioned medium (supernatant) was added to the fresh media.

· From above, small sample of the cells were taken from the cell suspension (100 – 200 µL). Cell density was calculated and the desire d numbers of cells were re-seeded into freshly prepared flasks without centrifugation just by diluting the cells. Place flask in 5 % CO_2 incubator at 37 ^{o}C, 75 % Relative Humidity.

This splitting / passage was repeated every 3 – 4 d ays, so that they were not diluted

too much or overgrown.

9.5.6 Experimental setup

Cell Lines and Culture Medium:

MCF-7, A-375 and HCT-15 cultures were used in these experiments were derived from National Centre for Cell Science (NCCS), Pune. Stock cells of these cell lines were cultured in DMEM, supplemented with 10% FBS (fetal bovine serum). Along with media cells were also supplemented with 5 % HBSS, penicillin, streptomycin and

Amphotericin – B, in a humidified atmosphere of 5 % CO_2 at 37 °C until confluence

reached. The cells were dissociated with 0.2 % trypsin, 0.02 % EDTA in phosphate buffer saline solution. The stock cultures were grown initially in 25 cm^2 tissue culture flasks, than in 75 cm^2 and finally in 150 cm^2 tissue culture flask and all cytotoxicity experiments were carried out in 96 microtitre well- plates. 2×10^4 cells/well was added in to each well of 96 well-plates. It was calculated as follow.

Calculation for number of cells in 96 well plates:

For this we need to calculate for no. of cells required for 100 wells $\approx$ 96 well, No. of cells / well $\times$ 100

$\qquad = 2 \times 10^4 \times 100$

$\qquad = 2 \times 10^6$ cells / plate

Total volume of media for 100 wells

$\qquad =$ volume of media / well $\times$ 100

$\qquad = 100 \,\mu l \times 100$
$\qquad = 10 \,ml$

Therefore, we need a total of 2×10^{6} cells in 10 ml of medium, then aliquot the required volume of cell suspension in to each wells.

8.5.6 Design of experiment:

Cell lines in exponential growth phase were washed, trypsinized and re-suspended in complete culture media. Cells were seeded at 2×10^{4} cells / well in 96 well microtitre plate and incubated for 24 hrs during which a partial monolayer forms. The cells were then exposed to various concentrations of the test compounds (as indicated in plate assignment) and standard doxorubicin. Control wells were received only maintenance medium. The plates were incubated at 37 °C in a hum idified incubator with 5 % CO_2, 75 % Relative Humidity for a period of 24 hrs. Morphological changes of drug treated cells were examined using an inverted microscope at different time intervals and compared with the cells serving as control. At the end of 24 hrs, cellular viability was determined using MTT assay.

Screening of test compound by MTT assay

Protocol

· Cells were preincubated at a concentration of 1×10^{6} cells / ml in culture medium for 3 hrs at 37°C and 6.5 % CO2, 75 % Relative Humidity .

· Cells were seeded at a concentration of 5×10^{4} cells / well in 100 µl culture medium and various amounts of compound (final concentration e.g. 100 µM/ml – 0.05 µM/ml) were added into microplates (tissue culture grade, 96 wells, flat bottom).

· Cell cultures were incubated for 24 hrs at 37 °C and 6.5% CO2.

· 10 µl MTT labeling mixture was added and incubate for 4 hrs at 37 °C and 6.5 % CO2, 75 % Relative Humidity.

· 100 µl of solubilization solution was added to each well and incubate for overnight.

· Absorbance of the samples was measured using a microplate (ELISA) reader. The wavelength to measure absorbance of the formazan product is between 540 and 600 nm according to the filters available for the ELISA reader, used. (The reference wavelength should be more than 650 nm).

Data Interpretation

Absorbance values that are lower than the control cells indicate a reduction in the rate of cell proliferation. Conversely a higher absorbance rate indicates an increase in cell proliferation. Rarely, an increase in proliferation may be offset by cell death; evidence of cell death may be inferred from morphological changes.

After 24 hrs, the cytotoxicity data was evaluated by determining absorbance and calculating the correspondent chemical concentrations. Linear regression analysis with 95 % confidence limit and R^2 were used to define dose-response curves and to compute the concentration of chemical agents needed to reduce absorbance of the formazan by 50 % (IC_{50}).

Percentage cell growth inhibition or percentage cytotoxicity was calculated by following formula:

% viability = $(A_T – A_B) / (A_C – A_B) \times 100$ … … … (1)

Where,

A_T = Absorbance of treated cells (drug)

A_B = Absorbance of blank (only media)

A_C = Absorbance of control (untreated)

There by,

% cytotoxicity = 100 – % cell survival … … … (2)

Determination of IC$_{50}$ value

According to the FDA, IC$_{50}$ represents the concentration of a drug that is required for 50 % inhibition *in-vitro*. In our study, IC$_{50}$ is a concentration of drug at which 50 % of cell population die. For primary screening, we use a threshold of 50 % cell growth inhibition as a cut off for compound toxicity against cell lines. IC$_{50}$ determined from plot of Dose Response curve between log of compound concentration and percentage growth inhibition. IC$_{50}$ value has been derived using curve fitting methods with *GraphPad Prism* as statical software (Ver. 5.02).

IC$_{50}$ values were calculated using the nonlinear regression program Origin The average of two (duplicates manner) were taken in determination.

Graph was plotted by keeping log concentration of drug on X axis and % cell growth inhibition or % cytotoxicity Y axis. IC$_{50}$ was estimated as a concentration of drug at 50 % position on Y axis.

The relationship should be sigmoidal, log drug concentration on the X axis and 'response / measurement' of the Y axis. The prism web site has some good guides for this

9.6 Result and discussion

Characterization of cell lines and culture media

Characterization of cell lines was performed for detection of microbial and cross contamination. Cell lines used in our experiments were free from any kind of microbial or fungal contamination (Table No.), which in essential in order to continue our screening experiments.

Table 15 : Results for Characterization of cell lines

Cell line	%viability		PDT(hrs)	microbial contamination	cross contamination	pH
	stock	after		no contamination	no	7
A-375	64.54	71.91	27.9	no contamination	no	7.5
MCF-7	67.46	85.30	19.50	no contamination	no	7
HCT-15	62.96	92.17	30.10	no contamination	no	7

Culture media were also tested for microbial contaminations. To prevent microbial contamination, 2.5 % Amphotericin B (µg/ml) was supplemented to media which act as working concentration. Bacterial contamination was prevented by addition of 1 % of

Antibiotic, 100 X (10000 U/ml Penicillin G, 10000 µ g/ml Streptomycin) into culture medial. All subculturing activities were done under class – II Biosafety cabinet. (Esco,

Singapore)

Cross contamination of cell line was tested by direct observation of particular cell line under inverted microscope. PDT for specific cell line was determined. From viability studies and PDT, we have concluded that the cell lines derived from ATCC were initially free from cross contamination.

To prevent the cross contamination of cell lines during our experiments work, separate pipettes and plastic tips were used for individual cell line. Along with that, particular cell line was used at the time under Class – II Bio safety cabinet. These were proving to be valid steps to prevent cross contamination of cell lines throughout the experiment.

.

Table 16: Concentration of compounds and % cell inhibition MCF-7 cell line (Breast Cancer)

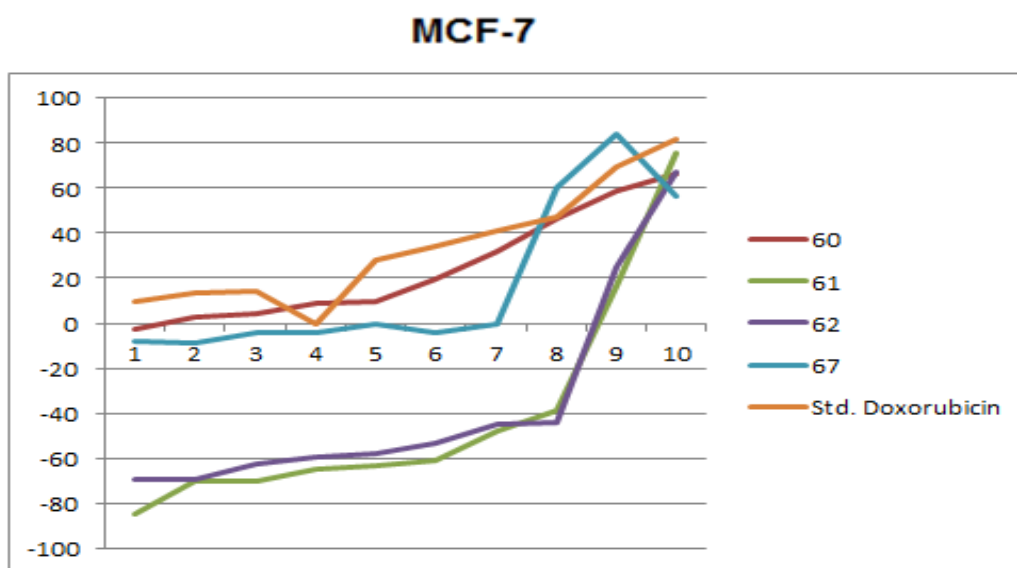| Conc. µg/ml	Log con.	% Cell Inhibition				
		60	61	62	67	Std. Doxorubicin
0.01	-2.29	-2.350	-85.06	-69.860	-8.2700	9.23
0.02	-1.82	2.354	-70.01	-69.860	-9.0600	13.53
0.05	-1.34	4.280	-70.01	-62.930	-4.2600	14.30
0.14	-0.86	8.890	-65.17	-59.340	-4.2600	18. 32
0.41	-0.39	9.645	-63.12	-57.750	0.0000	28.08
1.23	0.09	19.640	-61.22	-53.510	-4.2600	33.91
3.70	0.57	32.160	-48.08	-45.190	0.0000	41.25
11.11	1.05	46.390	-38.48	-44.340	60.0600	47.02
33.33	1.52	59.130	16.44	24.760	83.7600	69.32
100.00	2.00	66.170	75.96	67.120	56.3100	82.01
IC_{50} (µM/ml)		**4.323**	**56.00**	**52.72**	**7.408**	**56.00**

Figure 9.5 : Log concentration Vs % cell Inhibition in comparison of standard drug

Table 17: Show concentration of compounds and % cell inhibition of A-375 cell line (Human Melanoma, Skin cancer)

Conc. µg/ml	Log con.	% Cell Inhibition				
		60	61	62	67	Std. Doxorubicin
0.01	-2.29	-2.325	26.170	12.040	-9.2000	-40.87519
0.02	-1.82	7.652	31.780	14.510	-6.4300	-32.81318
0.05	-1.34	11.325	29.300	42.540	-2.7200	-29.69561
0.14	-0.86	18.365	26.570	37.510	-0.3400	-17.63049
0.41	-0.39	22.463	23.030	24.600	12.8800	-14.34109
1.23	0.09	31.342	42.870	14.280	18.7700	-12.55814
3.70	0.57	46.896	40.640	37.980	32.0700	11.25600
11.11	1.05	66.120	43.390	42.510	21.9900	48.35625
33.33	1.52	77.852	46.230	55.340	28.1300	71.32783
100.00	2.00	84.321	68.490	64.930	47.1800	86.69251
IC$_{50}$ (µM/ml)		**3.059**	**24.53**	**19.53**	**4.096**	**6.801**

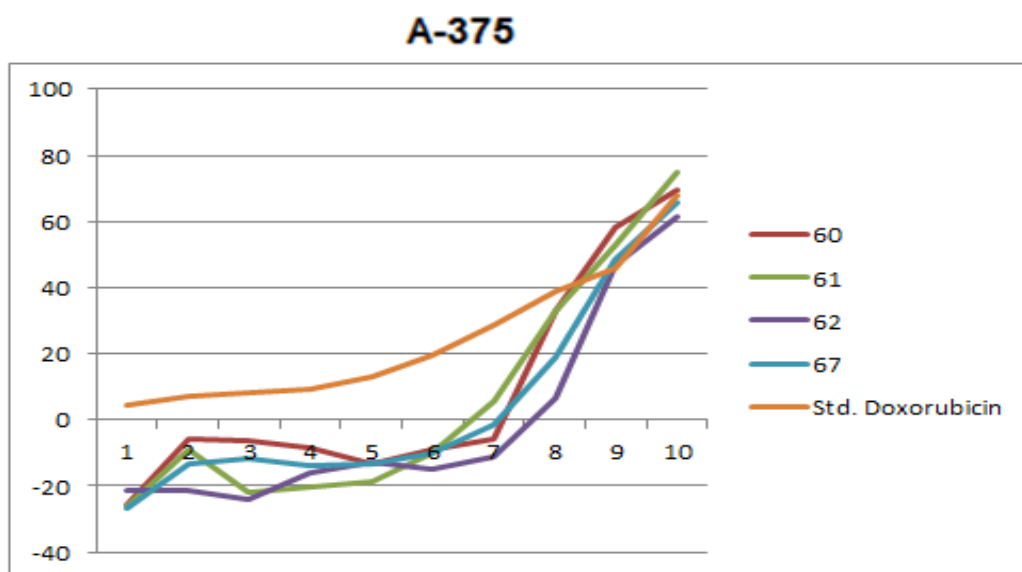**Figure 9.6 :Log concentration Vs % cell Inhibition in comparison of standard drug**

Table 18: Concentration of compounds and % cell inhibition of HCT-15 cell line (Human Colon cancer)

Conc. µg/ml	Log con.	% Cell Inhibition				
		60	61	62	67	Std. Doxorubicin
0.01	-2.29	-25.690	-26.340	-21.390	-26.8100	4.37000
0.02	-1.82	-5.950	-9.120	-21.590	-13.0800	7.34000
0.05	-1.34	-6.470	-21.810	-23.910	-11.7400	7.98000
0.14	-0.86	-8.650	-20.040	-15.740	-13.9700	9.04000
0.41	-0.39	-13.380	-18.490	-12.520	-13.0400	13.31000
1.23	0.09	-9.030	-9.870	-15.050	-9.9400	19.70000
3.70	0.57	-5.900	5.700	-11.040	-1.2700	28.88000
11.11	1.05	32.950	33.220	6.820	19.0400	38.95000
33.33	1.52	58.270	53.080	46.900	48.5300	45.88000
100.00	2.00	69.580	75.110	61.440	65.6600	67.99000
IC_{50} (µM/ml)		**15.56**	**11.59**	**26.03**	**18.86**	**9.415**

Figure 9.7 Log concentration Vs % cell Inhibition in comparison of standard drug
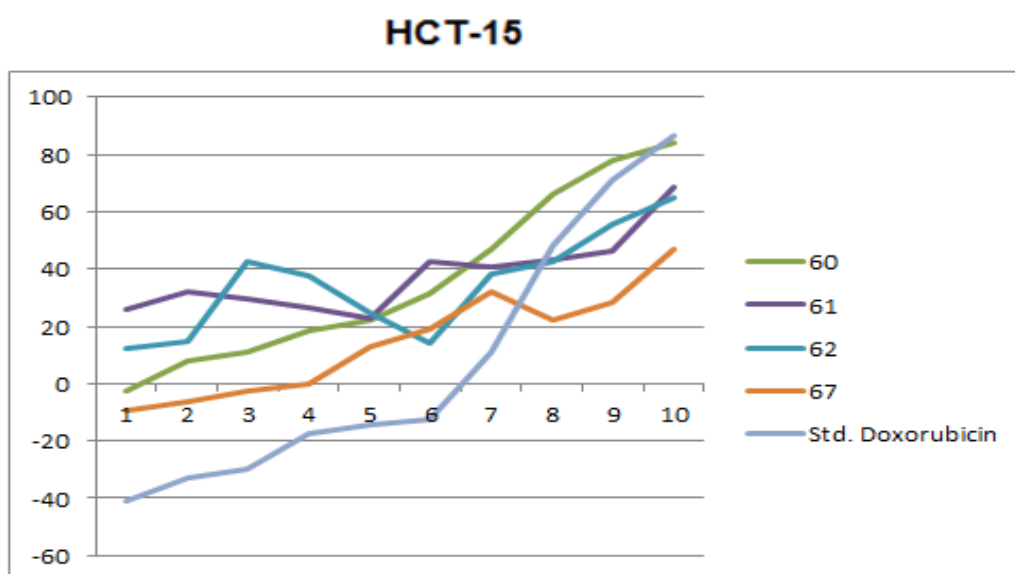
HCT-15

Table 19: Compounds and IC$_{50}$ value

S.N.	Compound No.	IC$_{50}$(µM/ml)		
		MCF-7 cell line	A-375 cell line	HCT-15 cell line
1	BMS-4	4.323	3.059	15.76
2	BMS-3	56.00	24.53	11.59
3	BMS-2	52.72	19.53	26.03
4	BMS-9	7.408	4.096	18,86
6	Doxorubicin	**10.33**	**6.801**	**9.415**

Figure 9.8 Effect of Compounds on Cell Line in MTT assay
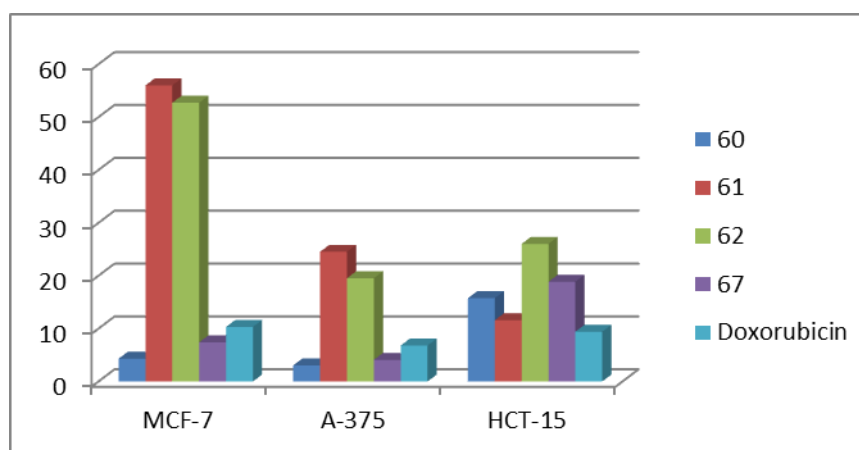
In the present investigation, all the extracts were evaluated against various cell lines named MCF-7, MDA-MB-468 and normal cell line Vero for each tested compound as well as Std. anticancer drug Colchicin, Dose Response Curve (DRC) against all cell lines was plotted with 10 analysis point i.e. with 10 different drug concentrations. The concentration causing 50% cell growth inhibition (IC$_{50}$) was determined from DRC using *GraphPad Prism* software (Ver. 5.04) (GraphPad Software, Inc., USA) and Micorsoft Excel 2007 (Microsoft Corporation, USA) application.

Compounds 60 and 67 are showing more potent cytotoxic activity on MCF-7 and A-375 cell line as compare to standard (Doxorubacin). All compounds are showing comparative score on cell line HCT-15 cell line.